Automation of Electrospark Deposition of TiC$_p$/Ni on RSW Copper Electrodes

by

Murtasim Syed

A thesis

presented to the University of Waterloo

in fulfillment of the

thesis requirement for the degree of

Master of Applied Science

in

Mechanical Engineering

Waterloo, Ontario, Canada, 2010

AUTHOR'S DECLARATION

I hereby declare that I am the sole author of this thesis. This is a true copy of the thesis, including any required final revisions, as accepted by my examiners.

I understand that my thesis may be made electronically available to the public.

Abstract

Electrospark Deposition (ESD) is a specialized micro-bonding process which is used to coat a base material, known as the substrate, with a stronger, tougher, and more durable top layer, the electrode. Short durations of electrical pulses ranging from milliseconds to microseconds are used to deposit the electrode onto the substrate. This process can be used to repair damaged parts, tools or equipment, or to improve and extend tool and equipment life.

The objective of this study is to develop a better understanding of the TiC_p/Ni Metal Matrix Compound (MMC) coating process on RSW electrodes for the purpose of automation. Key aspects of the process are identified to aid in developing a method and approach for process automation.

In order to test the effects of automating this ESD process three automation solutions were considered and tested. The first was a Manual-Automated Hybrid setup which involved the use of a manual vibrating TiC_p/Ni electrode applicator which was mounted on a CNC lathe. The second solution was the novel Actively Controlled Rotating and Reciprocating mechanism which replaced the vibration of the manual applicator with an actively controlled reciprocating mechanism and added rotational control of the TiC_p/Ni electrode. The third solution was the novel Actively Controlled Rotating and Vibrating mechanism which used the rotational portion of the Actively Controlled Rotating and Reciprocating mechanism but replaced the reciprocating mechanism with a vibrational one.

Observations of initial tests lead to an understanding of how the TiC_p/Ni electrode wears during the process while using a manual applicator as opposed one of the novel mechanisms and helped to solidify a method to ensure even wearing of the TiC_p/Ni electrode for automation.

Further testing of the Actively Controlled Rotating and Reciprocating mechanism provided information about the electrical characteristics of the process and the effects of these results on the process. These test results were used to develop a constraint on the contact duration between the TiC_p/Ni electrode and the RSW Copper electrode.

Force measurements of the manual operators at Huys Industries Ltd, the Actively Controlled Rotating and Reciprocating mechanism, and the Actively Controlled Rotating and Vibrating mechanism were used to identify differences in the process results based on the mechanism used. With the use of this data an upper limit for the contact force for this process was specified in order to ensure damage free coatings.

The Actively Controlled Rotating and Vibrating mechanism was used to specify a minimum travel speed for the TiC_p/Ni electrode along with a minimum number of passes required to ensure gapless coatings.

The Actively Controlled Rotating and Vibrating mechanism produced relatively decent coatings of TiC_p/Ni on the RSW Copper electrodes and serves as a proof of concept and basis for automation of this process.

Acknowledgements

I would like to thank Professor Jan Huissoon for his guidance and support as my academic supervisor. His knowledge and experience were invaluable assets to my understanding and progress of this thesis and his encouragement helped me to cross any hurdles I encountered throughout my research.

I would like to thank Nigel Scotchmer, Kevin Chan, and Dominic Leung from Huys Industries Ltd. for their assistance in helping me understand the ESD process and for allowing me to use their facilities for gathering data.

I would also like to thank Siu Kei Tang for helping me in further understanding of the ESD process as well as understanding test results and coming up with possible solutions to problems which were encountered along the way.

Finally, I thank my family for supporting, encouraging, and motivating me during my studies.

Dedication

I dedicate this thesis to my family who have always supported and encouraged me to achieve all of my ambitions and aspirations in life.

Table of Contents

List of Figures

List of Tables

Chapter 1
Introduction

1.1 Background

Electrospark Deposition (ESD) is a specialized micro-bonding process which is used to coat a base material, known as the substrate, with a stronger, tougher, and more durable top layer, the electrode. This process may also be referred to as Electrospark Alloying (ESA) [1] or Pulse Electrode Surfacing (PES) [2].The electrode is continuously moved with respect to the substrate via vibrations or rotation about the it's longitudinal axis [3]. Capacitors are used to energize the consumable electrode as it creates a short circuit with the substrate. The short circuit is followed by an arc which carries particles of the electrode onto the base material [4; 5]. This process may be used for the purpose of repairing damaged parts, tools or equipment, or to improve and extend tool and equipment lifespan [6]. ESD can be used on a wide range of metals with different characteristics such as Steel, Aluminum, or Copper.

There are several advantages to ESD of which one of the most significant is that it is a low heat input process due to duty cycles as low as 1% [4; 6; 7]. The micro-bonding can occur in as little as a few microseconds allowing the base material to cool between arc pulses [3]. This allows the substrate to remain unaffected by thermal distortion or changes in metallurgical structures [7]. Another benefit of ESD is that it produces metallurgical bonds which make it more durable and resistant to damage than mechanical bonds [7]. These metallurgical bonds can also be created between dissimilar metals such as Copper and Titanium Carbide (TiC) despite their different mechanical characteristics, due to the low heat input from the process [4]. In addition, the ESD process does not require any special surface preparation or environmental conditions and does not produce any hazardous waste or fumes, eliminating the need for expensive equipment such as vacuum systems, chambers, chemicals, or spray booths [4].

One process which can benefit from the use of ESD is Resistance Spot Welding (RSW). This is a process used for joining sheet metal and is extensively used in the automotive industry but may also be used for the fabrication of furniture, appliances, and other lighter

applications [8]. A spot weld is produced by clamping two pieces of sheet metal between two copper electrodes and conducting electrical current through the joint. The resistance of the sheets to the flow of current causes them to heat, melt, and form a weld [9]. Although the copper electrodes are not consumed in this process they often exhibit significant wear due the high clamping force and heat generation [5]. This has lead to the need for modifications to the electrodes to enhance electrode durability and life.

ESD has been used by Huys Industries Ltd. to develop a patented Titanium Carbide (TiC_p/Ni) metal matrix composite (MMC) coating on RSW copper electrodes [5; 10]. A study conducted by Chan et al. [11] has shown that coated electrodes can have up to double the life of uncoated electrodes when welding hot-dip-galvanized high strength low alloy (HSLA) steel. The current process for coating these copper electrodes employs a manual coating application which is inconsistent, resulting in cracking and delamination of the coating as can be seen in Figure 1.1 [12]. The manual process is also expensive and time consuming and together these problems lead to a need for an automated solution to provide a more efficient, repeatable, and reliable method for this coating process.
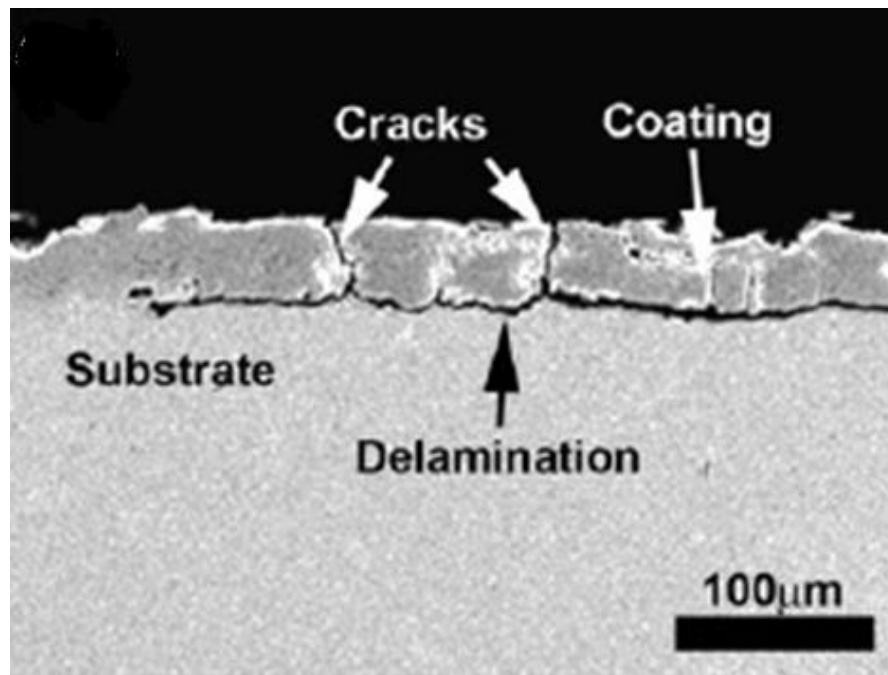
Figure 1.1: SEM cross-section image of monolithic TiCp/Ni coating [12]

2

1.2 Objective

The objective of this thesis is to identify the key parameters required for the automation of the TiCp/Ni MMC coating process on RSW copper electrodes and to identify a method and approach for process automation.

1.3 Thesis Outline

This thesis will consist of 6 chapters. The second chapter will present a literature review outlining the ESD process in further detail along with prior work on ESD automation. Chapter 3 will explore several possible methods for automation for coating RSW electrodes with TiC_p/Ni MMC. Chapter 4 will explain the experimental setup and testing procedures for each of the automation solutions considered. Chapter 5 will summarize the results of the experiments and testing. Chapter 6 will provide conclusions found throughout the research and will propose future work.

Chapter 2
Literature Review

This section will provide a detailed background of the ESD process and prior work conducted on this process, outlining specific findings relating to the general approach and methodology employed for ESD.

2.1 ESD Equipment

The basic concept of the ESD process is very simple and does not require any high-tech or advanced equipment. Only two main components are required for the ESD process; the power source and the electrode holder or torch as seen in Figure 2.1 [5; 6; 13]. The electrode holder may also be referred to as the applicator.
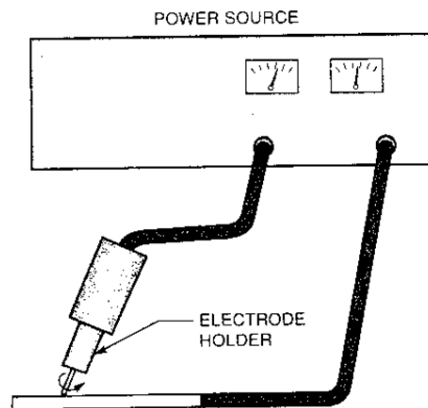
Figure 2.1: Basic Elements of Electrospark Deposition Equipment [13]

The power source generally consists of a Direct Current (DC) rectifier and discharge circuit [5; 13] while the electrode holder usually provides electrode motion [13]. The DC rectifier circuit converts Alternating Current (AC) to DC which is then used to charge a series of capacitors [5]. Two simple ESD power supply circuits can be seen in Figure 2.2. The electrode motion is usually in the form of either rotation or vibration [14], however oscillation may also be considered a subset of vibration [5]. In order to provide power to the moving electrode either a rotary contactor may be used or a braided wire may be wrapped around the shaft of the electrode holder [6; 7; 13]. The electrode holder is generally covered

4

in a non-conductive outer material to minimize the risk of electrical shock and has a metallic lining to provide mechanical stability [13].
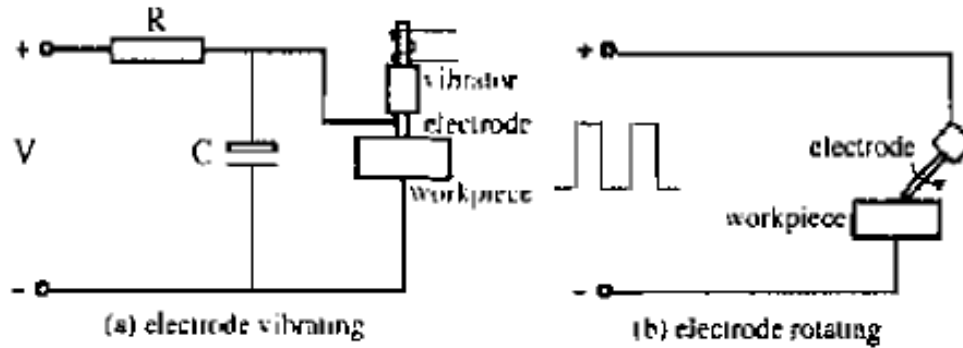
Figure 2.2: Simple ESD Power Supplies [14]

Other additions may also be used along with the basic elements mentioned above to enhance the ESD process. The electrode holder may provide shielding gases in some cases if the specific materials or environment require it [5; 13]. A gas nozzle similar to the one used for gas tungsten arc welding (GTAW) can be attached to the end of the electrode [5; 13]. Advanced power supplies may also be used with control over the Voltage, Current, Discharge Rate, etc [5; 13; 14]. An example of an advanced accelerated ESD power supply used by Wang et al can be seen in Figure 2.3.
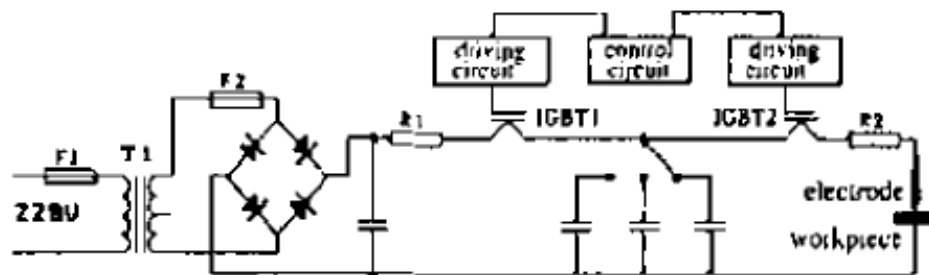
Figure 2.3: Advanced Accelerated ESD Power Supply [14]

For the purpose of coating TiC_p/Ni on RSW copper electrodes two additional elements are added to the ESD system; a specialized holder is used to mount the RSW electrode along with a motor which rotates the RSW electrode. The complete RSW electrode coating setup

5

can be seen in Figure 2.4. The hand-held applicator is the TiC_p/Ni electrode holder and uses an eccentric mass to vibrate the electrode.
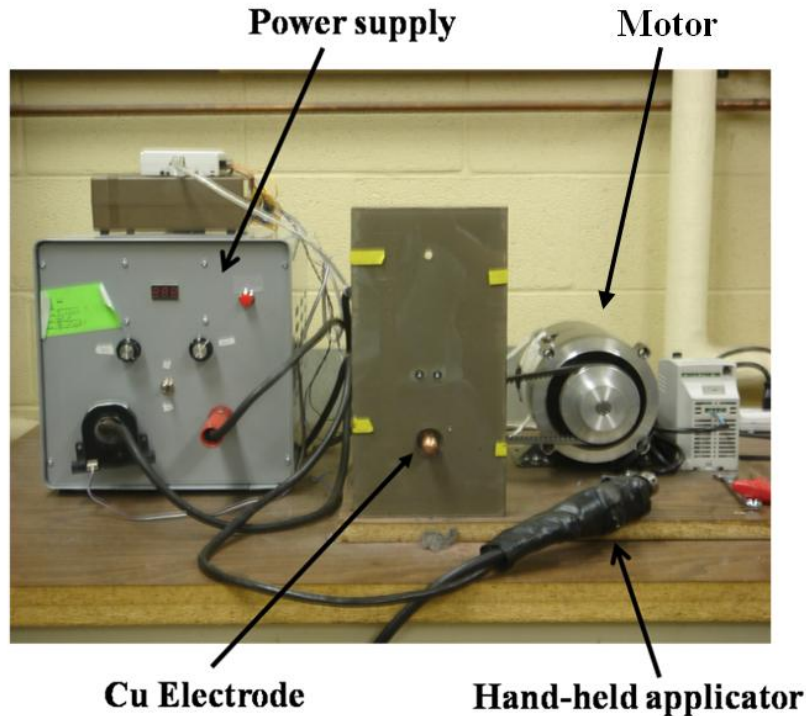
Figure 2.4: ESD Equipment for RSW Electrode Coating [5]

2.2 ESD Process

The ESD process mainly consists of two elements; the materials for the substrate and electrode, and the process parameters such as Voltage, Current, Spark Frequency, etc. The following sub-sections will discuss these elements of the process, how they are currently used for manual ESD applications, and the pros and cons of the process.

2.2.1 Materials of Coatings and Substrates

Since ESD is a low heat input, short duration, high current process it may be used on a wide variety of base or substrate materials. Nearly any electrically conductive material can employ ESD for coating and nearly any electrically conductive metal, alloy, or cermet that can be melted in an electric arc can be deposited on metal substrates [4; 5; 7; 11; 13]. Table 2.1 and

Table 2.2 provide a list of various coatings and substrate materials to have been successfully used in the ESD process as observed by Johnson et al. to date [4]. It should be noted that not all combinations of substrates and coatings are readily compatible; however the ESD process permits a much wider range of non-compatible materials to bond than other welding processes [4; 5]. This wide range of material compatibility is believed to be the result of the rapid solidification of the coating on the substrate [5]. For example, it has been observed by Banovic et al. that iron and aluminum cannot be welded without cracks with aluminum content above 10 wt% [15], however Johnson et al have found that crack-free deposits of 35 wt% aluminum have been made by ESD on stainless steels[4; 16].

Table 2.1: ESD Coatings Applied to Date [4]

Wear Resistance Coatings	Corrosion Resistance Coatings	Build-up or Special Surface Modification
Hard carbides[a] of: W, Cr, Ti, Ta, Hf, Mo, Zr, V, Nb	Stainless steels, Hastelloys[b], Inconels[b], Monels[b]	Ni-base and Co-base super alloys
Hardfacing alloys: Stellites[b], Tribaloys[b], Colmonoys[b], etc.	Aluminides of: Fe, Ni, and Ti	Refractory Alloys (W, Ta, Mo, Nb, Re, Hf)
Borides of: Cr, Ti, Zr, and Ta	FeCrAlY, NiCrAlY, CoCrAlY	Noble metals (Au, Pt, Ag, Pd, Ir)
Intermetallics and Cermets	Al and Al Bronze Alloys	Other Alloys (Fe, Ni, Cr, Co, Al, Cu, Ti, V, Sn, Er, Zr, Zn)
[a] With metal binders, usually 5-15% Ni or Co [b] Trademarks: Hastelloy – Haynes International, Kokomo, IN Inconel & Monel – International Nickel Co, Huntington, WV Stellite & Tribaloy – Deloro-Stellite Co., Goshen, IN Colmonoy – Wall Colmonoy Corp., Detroit, MI		

Table 2.2: Substrate Alloys Coated by ESD to Date [4]

High and Low Alloy Steels	Nickel and Cobalt Alloys	Refractory Metals (W, Re, Ta, Mo, Nb)
Stainless Steels	Titanium Alloys	Chromium
Tool Steels	Aluminum Alloys	Uranium
Zirconium Alloys	Copper Alloys	Erbium

7

The two materials of particular interest to this study are Copper (Cu) and Titanium Carbide (TiC_p/Ni), where the Copper will be the substrate and the Titanium Carbide will be the coating. Figure 2.5 shows a picture of the TiC_p/Ni electrode and Figure 2.6 shows an SEM cross-sectional view of the TiC_p/Ni composition. Figure 2.7 also shows some commonly used RSW Copper electrodes.

Figure 2.5: Sintered TiCp/Ni Electrode
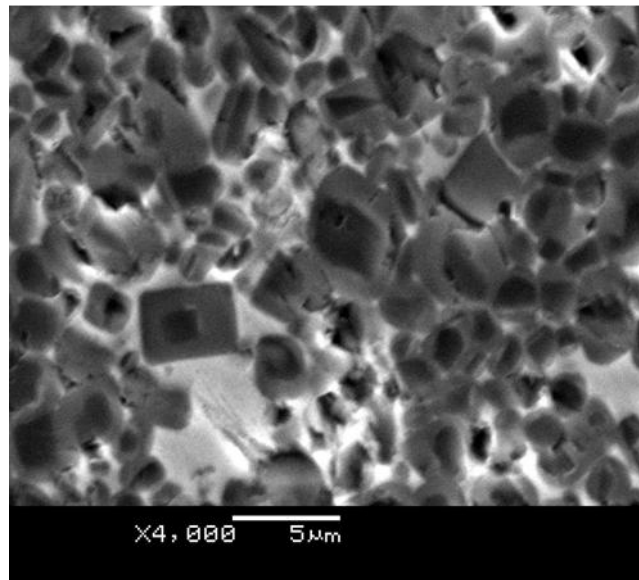
Figure 2.6: Sintered TiCp/Ni Electrode SEM Cross-Sectional View [5]

8

Figure 2.7: Some Commonly Used RSW Copper Electrodes [17]

Titanium Carbide and Copper are very different materials based on their mechanical and thermal properties [18; 19; 20; 21]. Some of the main properties of these two materials are highlighted in Table 2.3. Copper is a relatively soft metal while TiC is relatively hard which makes the TiC an excellent choice for coating; however the differences in their properties can cause many difficulties when attempting to coat Copper with TiC. For example, TiC has a much higher melting point than Copper, 3140 °C vs. 1084 °C respectively [18; 19; 20; 21]. The coefficient of thermal expansion is more than twice as high for Copper as it is for TiC. These differences create complications when attempting to coat Copper with TiC such as cracking and delamination as observed by Chen et al [22] and as seen in Figure 1.1.

Table 2.3: Properties of Copper (Cu) and Titanium Carbide (TiC) [18; 19; 20; 21; 23]

Property	Copper (Cu)	Titanium Carbide (TiC)
Density (g/cm³)	8.93	4.9
Thermal Conductivity (W/m·K)	398	35
Coefficient of Thermal Expansion (μm/m·°C)	16.5	8
Tensile Strength MPa (ksi)	221-455 (33-66)	896 (130)
Poisson's Ratio	0.308	0.19
Melting Point (°C)	1084	3140

9

2.2.2 ESD Parameters

There are several parameters used in the ESD process which may affect the coating characteristics. As mentioned in the previous section the material of the substrate and electrode may affect the process due to incompatible material characteristics. Many other factors must be considered in the ESD process of which the main categories include the Electrode, Substrate, Environment, and Electrical characteristics [5; 7]. A list of these process parameters and their respective variables can be seen in Table 2.4.

Table 2.4: ESD Process Parameters [5; 7]

Electrode	Substrate	Protective Environment	Electrical	Other
Material	Material	Shielding Gas Type	Power Input	System Efficiency
Geometry	Surface Finish	Flow Rate	Voltage	Number of Passes
Motion	Cleanliness	Temperature	Capacitance	Overlap of Passes
Speed	Temperature	Flow Geometry	Spark Rate	Spark Duration
Contact Pressure	Geometry			
Orientation				
Application Direction				

It is believed that the electrical characteristics of the ESD process have the greatest influence on the deposition quality and deposition rate [5; 6]. An increase in spark energy results in an increased deposition rate [5]; the spark energy is defined as:

$$E_p = \int_0^{t_p} V(t) \cdot I(t) dt$$

where V(t) is a function of voltage during discharge, I(t) is a function of current during discharge, and t_p is the pulse duration [5]. The spark energy may be controlled by adjusting the capacitance, charging voltage, inductance, or resistivity of the power supply [5; 6].

The ESD process usually has spark durations ranging from a few microseconds to a few milliseconds, which are about three orders of magnitude shorter than other pulsed welding processes [5]. Deposition frequencies can range from 60 Hz to 4 kHz [4; 5; 6; 7; 13] with a duty cycle as low as 1% [5]. This low duty cycle is one of the key factors which make ESD a low heat input process and permits the substrate to remain at or near ambient temperature [5]. This can greatly eliminate or reduce the heat affected zone, metallurgical change and dimensional change of the substrate [5].

2.2.3 Materials Transfer Mechanism

The ESD process is a specialized micro-bonding process in which the electrode (positive pole) continuously moves with respect to the substrate (negative pole) creating short durations of high frequency electrical pulses [12]. The electrode is energized through a series of capacitors which discharge as the electrode short circuits with the substrate, causing the electrode and substrate to melt and small particles of the electrode are accelerated through the resulting arc, impacted against the substrate, and solidified rapidly [4; 5; 12]. Lie et al [24] have developed a physical model of the ESD process and have broken it down into four main stages as can be seen in Figure 2.8. In the first stage the electrode makes contact with the substrate causing electrical discharge and heat input due to the localised electrical energy. In the second stage the electrode and substrate begin to melt from the heat input and a spark is generated through which the melted particles of the electrode travel. In the third stage the melted electrode particles splash onto the substrate and begin to bond to the substrate and solidify. In the final stage the electrode particles solidify on the substrate and the electrode contacts the substrate again to repeat the next discharge cycle.
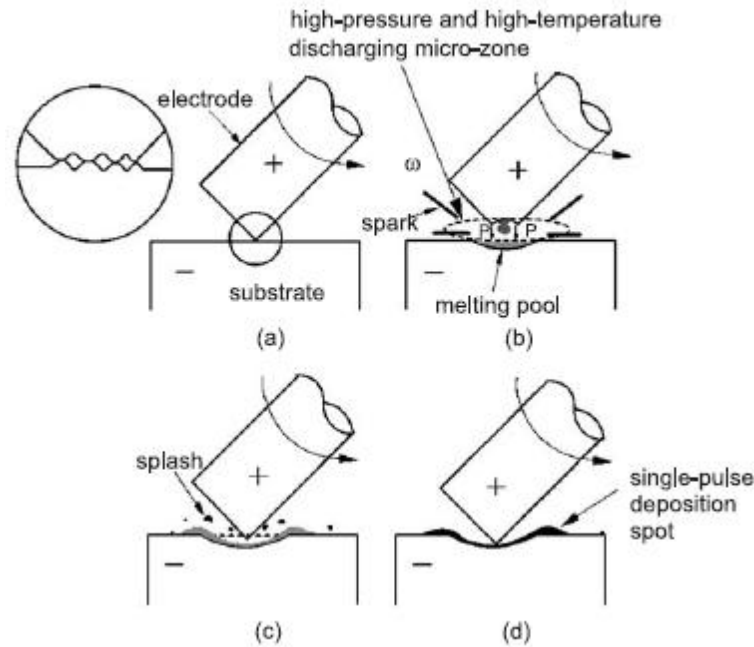
Figure 2.8: The physical model of the formation of a single-pulse deposition [5; 24]

2.2.4 Manual Process

The ESD process often consists of an electrode holder which is designed for manual operation [13]. The electrode holder is generally covered in a non-conductive outer material to minimize the risk of electrical shock and has a metallic lining to provide mechanical stability [13]. The current electrode holder used by Huys industries for the purpose of coating TiC on RSW Copper electrodes can be seen in Figure 2.9. This electrode holder vibrates the electrode with the use of a rotating eccentric mass and a compliant electrode mount. As the rotating eccentric mass rotates it causes the compliant electrode mount to oscillate at a frequency corresponding to the rotational speed of the eccentric mass. This oscillation is the primary method to make and break electrical contact between the TiC_p/Ni electrode and the Copper substrate.

The operator holds the electrode holder in their hand and guides the TiC_p/Ni electrode over the contour of the RSW Copper electrode while it rotates as discussed previously. The rotation of the RSW Copper electrode also aids in the process of making and breaking

electrical contact as well as ensuring an even and complete coat across the entire surface of the RSW Copper electrode. The resulting coating can be seen in Figure 2.10. Figure 2.11 also shows an SEM image of a manually coated RSW Copper electrode tip with TiC_p/Ni.

A simple power supply may be used which would be a fixed voltage power supply in which no parameters can be changed. A more advanced power supply would allow the operator to change parameters such as Voltage, Maximum Current, Charge Rate, Discharge Rate, etc. The complete manual setup can be seen in Figure 2.4.

Figure 2.9: Manual ESD Applicator for RSW Electrode Coating

Figure 2.10: TiCp/Ni MMC Coated RSW Cu Electrode by Manual ESD [5]
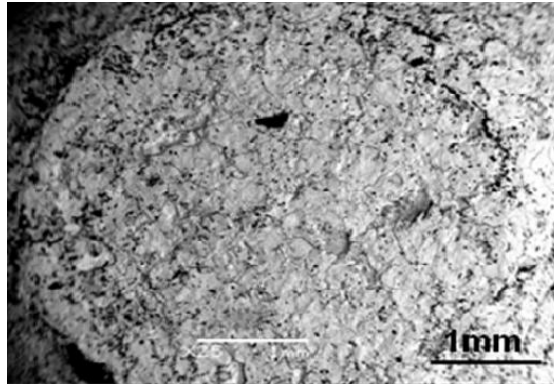
Figure 2.11: SEM Image of a Manually Coated RSW Cu Electrode Surface with TiCp/Ni [5]

2.2.5 Pros and Cons

The ESD process may be used for the purpose of repairing damaged parts, tools or equipment, or to improve and extend tool and equipment lifespan [6] by coating the substrate with a stronger, tougher, and more durable coating. The ESD process provides many advantages over other welding processes, some of which have already been discussed; however the process also has its limitation and disadvantages. Some of the main pros and cons of the ESD process have been outlined in Table 2.5.

As has been indicated earlier, one of the greatest advantages of the ESD process is that it is a low heat input, low duty cycle process [4; 6; 7]. The micro-bonding can occur in as little as a few microseconds allowing the base material to cool between arc pulses [3] which allows the substrate to remain unaffected by thermal distortion or changes in metallurgical structures [7]. Another benefit of ESD is that it produces metallurgical bonds which make it more durable and resistant to damage than mechanical bonds [7]. These metallurgical bonds can also be created between dissimilar metals such as Copper and Titanium Carbide (TiC) despite their differences in mechanical characteristics due to the low heat input from the process [4]. Aside from this, no special environment or preparation is needed for ESD. Due to this, no hazardous waste or fumes are generated, eliminating the need for expensive equipment such as vacuum systems, chambers, chemicals, or spray booths [4]. These factors all contribute to the successful application of TiC_p/Ni on RSW Copper electrodes as a coating.

Despite all these advantages, ESD still suffers from being limited to thin coatings and cracking and delamination of the coating between certain materials [5; 7]. The ESD process is also slower than many other welding processes [5; 6]. When attempting to coat RSW Copper electrodes with TiC_p/Ni it can be particularly difficult since these two materials are generally incompatible and special care must be taken when setting process parameters in order to ensure good quality coatings. Furthermore, due to the continuous consumption of the electrode in the ESD process, the contact geometry is irregular in the discharge zone and prevents reproducibility of coating properties [25]. Such irregular contacts may also generate harmful transient arcs, which are characterized by high energy transfer, spot localization, electrode overheating [25]. All these effects are not desirable for an efficient and regular deposition resulting in coating discontinuity, high surface roughness, spatter layers and crater erosion [25].

Table 2.5: Summary of Advantages and Limitations of the ESD Process [5; 7]

Advantages	Limitations
Metallurgically bonded coating	Maximum coating thickness of currently 50 to 250 µm, depending on material
Low heat input, eliminates distortion or metallurgical changes in substrate	Stress relief cracking inherent in some materials
Nano-structured or amorphous layers possible through rapid solidification	Both substrate and coating material must be electrically conductive
Little or no substrate preparation or post-coating surface finishing required	Maximum effective coating rate of $20cm^2$/min
Reproducible process, easily automated	Extensive optimization of coating parameters may be required for some application
Operators easily trained	
Portable equipment and process	
Applicable to complex shapes	
Can apply nearly all metals and cermets	

2.3 Automation of ESD

Since the basic principles of the ESD process are simple it would seem to be relatively easy to automate the process; however due to the many process parameters, it can become more difficult than may first appear [4]. The main requirement for automation is that the electrode must remain in constant motion with respect to the substrate so as not to allow a continuous short circuit [4]. An advanced power supply as discussed earlier is also useful for automation since it allows for greater control over process parameters and provides better repeatability [14]. A general automated ESD applicator can be seen in Figure 2.12. Attempts have also been made by Frangini et al [25] to develop a spring loaded electrode as a simple means to produce smooth coatings under force-controlled spark discharges [25].

Although ESD has been successfully automated, a specific application for RSW Copper electrode coatings using TiC_p/Ni has not been developed. Standard equipment such as that shown in Figure 2.12 is not feasible for this purpose because it is designed for simple surface geometries and for coating similar and compatible materials. Coating RSW Copper electrodes with TiC_p/Ni is very sensitive to process parameters and requires a specialized automated application.
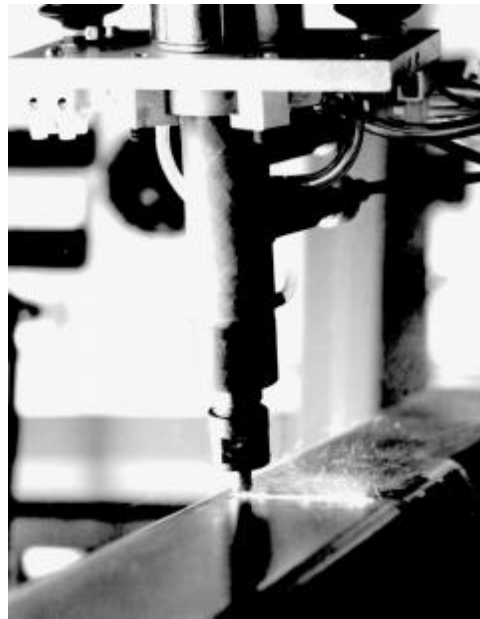
Figure 2.12: A General Automated ESD Applicator with Rotating Electrode [4]

2.4 Summary

ESD is a relatively simple and effective method of applying strong and durable coatings on substrates for the purpose of repairing damaged parts, tools or equipment, or to improve and extend tool and equipment lifespan [6]. Nearly any electrically conductive material can be coated with nearly any electrically conductive metal, alloy, or cermet [4; 5; 7; 11; 13]. Table 2.1 and Table 2.2 provide some substrates and coatings applied to date [4]. ESD is unique compared to other welding processes because of its inherent low heat input which allows it to bond dissimilar metals such. This aspect of ESD makes it a perfect choice for coating RSW Copper electrodes with TiC_p/Ni.

Despite the aforementioned qualities, ESD is not easily automated when coating RSW Copper electrodes with TiC_p/Ni. There is a great deal of incompatibility due to the differences in properties between these two materials as outlined in Table 2.3, which requires special attention to process parameters. Currently available automation solutions for ESD are scarce and only provide automation for simple surface geometries or for specialized cases and nothing has been developed for the special case of RSW Copper electrode coating with TiC_p/Ni. ESD also generally suffers from irregular electrode geometry and contact and on top of this RSW Copper electrodes have complex and varying surface geometries as seen in Figure 2.7. These aspects pose a problem when attempting to use existing automation solutions for RSW Copper electrode coatings and create a need to identify key process parameters along with a method and approach for automation for this specialized case of ESD.

Chapter 3
Possible Automation Solutions

3.1 Existing Automation

Currently existing automation solutions for ESD have been designed for simple applications such as flat surface coatings as seen in Figure 2.12 or more complex and specific application like gun barrel repairs as researched and developed by Advanced Surfaces and Processes Inc (ASAP) [26]. A picture of this system can be seen in Figure 3.1.

Figure 3.1: ESD Automation of Gun Barrel Repair [26]

Although the aforementioned methods work well for the specific cases they were designed for, they do not port over well for coating TiC_p/Ni on RSW Copper electrodes. The soft nature of Copper and the differences in properties between Copper and TiC_p/Ni make it exceptionally difficult to automate this process. The complicated surface geometries of the RSW Copper electrodes also increase the difficulty of automation. Special care must be taken with the process parameters and specialized equipment must be designed for this particular case.

3.2 Novel Methods

A few novel methods for automation were explored during this research, each one having specific capabilities which were tested to identify the most important process parameters and design methodology.

3.2.1 Preliminary Designs

Preliminary conceptual designs were first created to consider the possible pros and cons of each design and which method would be best suited for this application and had the most promising prospective.

3.2.1.1 Preliminary Design 1

The first design to be considered was to attach the existing manual applicator to a CNC lathe as seen in Figure 3.2. The CNC lathe would provide two degrees of freedom in the X and Z axes allowing the electrode to follow to contour of the RSW Copper electrode for complete coating coverage. The manual applicator would provide vibration to the TiC_p/Ni electrode for the making and breaking of electrical contact while the RSW Copper electrode will be rotated on the lathe chuck.
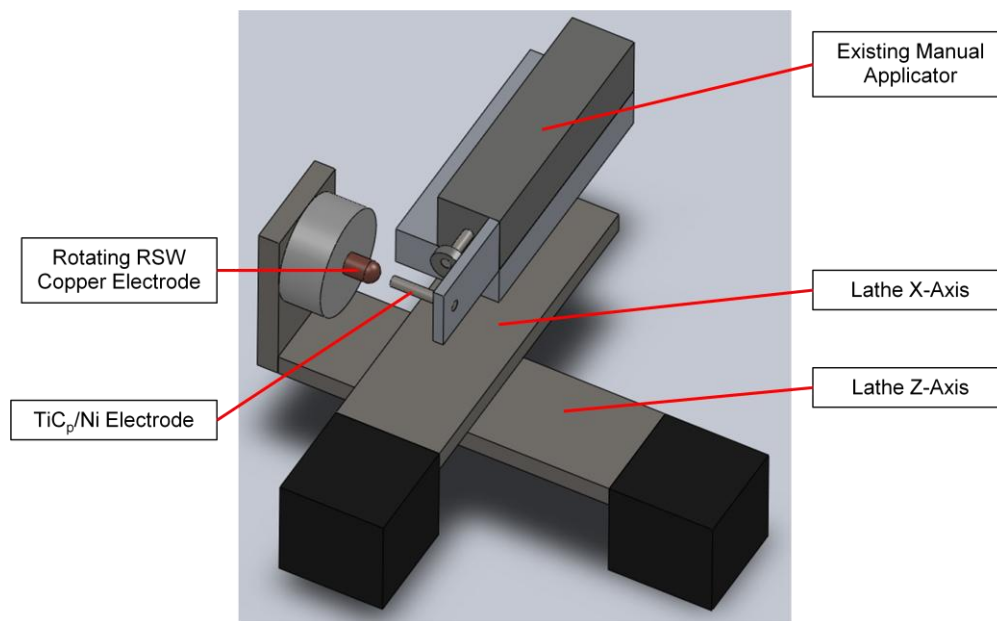
Figure 3.2: CNC Lathe Mounted with Existing Manual Electrode Applicator

3.2.1.2 Preliminary Design 2

The second design incorporates most of the features of the first design but replaces the manual applicator with an electromagnet as can be seen in Figure 3.3. With this design the CNC lathe provides X and Z axis movements of the TiC_p/Ni electrode while an electromagnet provides reciprocation of the TiC_p/Ni electrode for making and breaking of electrical contact. This electromagnet allows for active control of the frequency of reciprocation. The RSW Copper electrode is rotated by the lathe chuck.
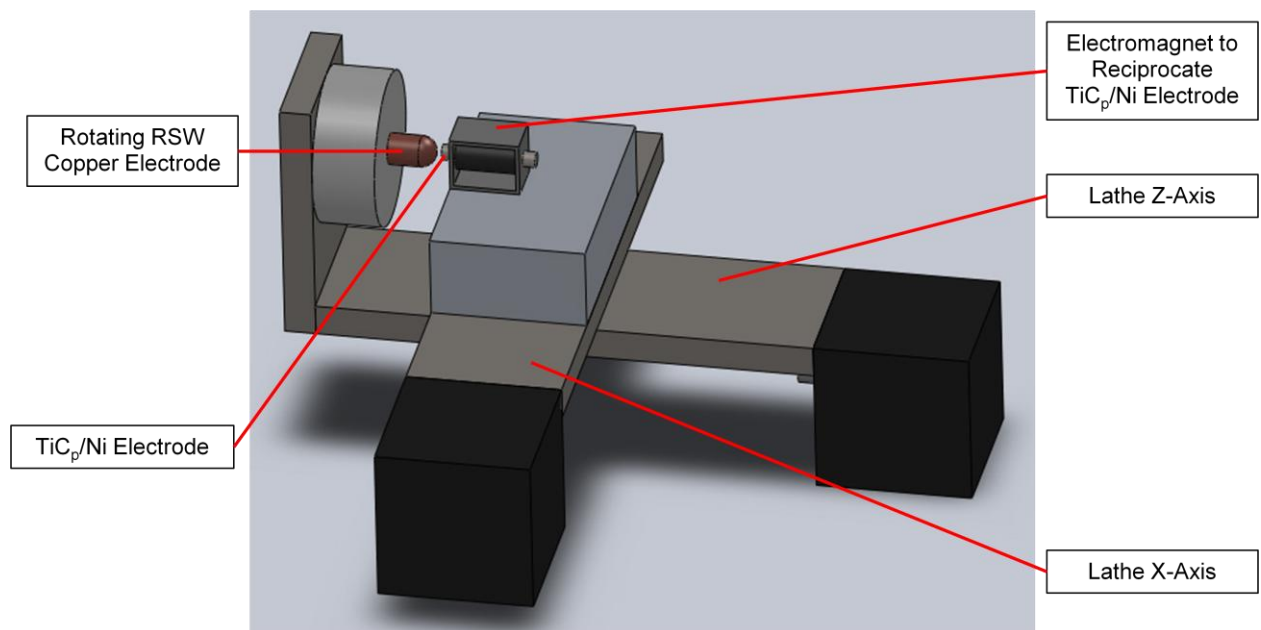
Figure 3.3: CNC Lathe with Reciprocating TiCp/Ni Electrode

3.2.1.3 Preliminary Design 3

The third design uses all the concepts of the second design and adds rotation to the TiC_p/Ni electrode as well. This addition is made with the use of a motor which provides rotational motion and connects the TiC_p/Ni through linking arms. The mechanism can be seen in Figure 3.4. With this setup the reciprocation will provide making and breaking of the electrical contact while the rotation of the TiC_p/Ni electrode will permit consistent and uniform wearing of the electrode; inconsistent wearing of the electrode generates irregular contact

geometry as discussed earlier and is a problem with ESD [25]. The RSW Copper electrode is rotated by the lathe chuck.
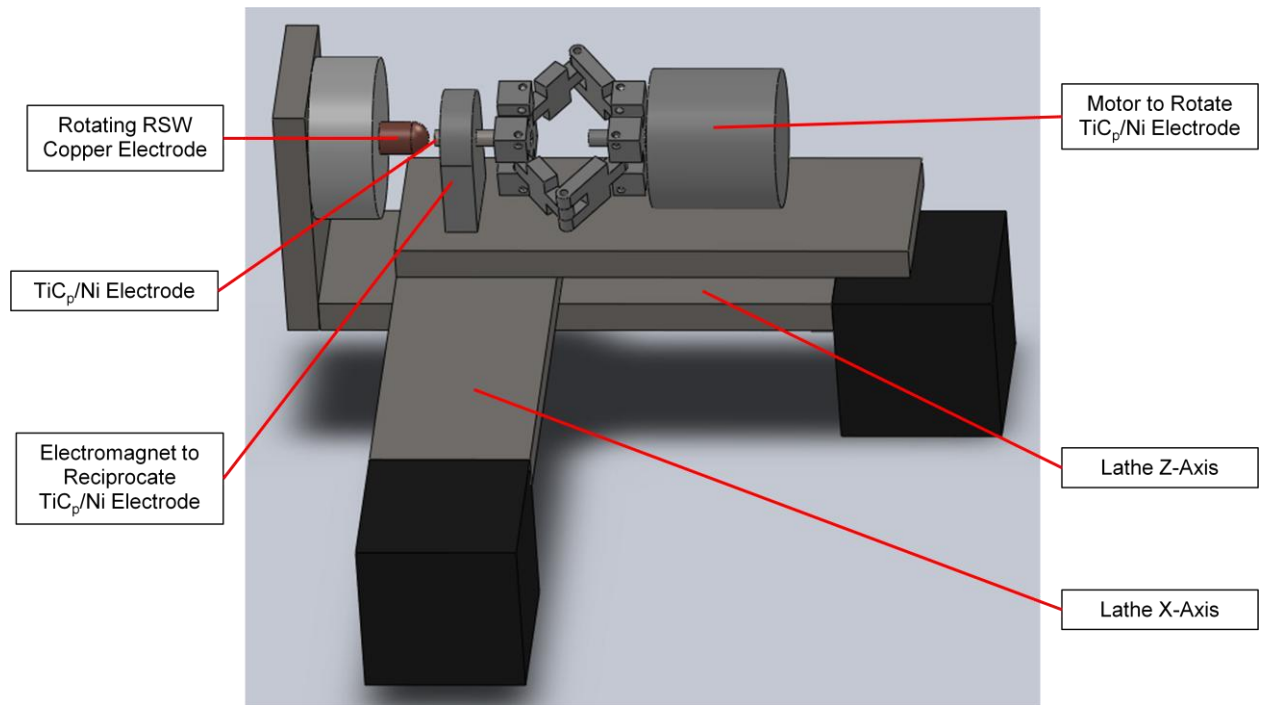
Figure 3.4: Lathe with Rotating and Reciprocating TiCp/Ni Electrode

3.2.2 Manual-Automated Hybrid Design

The initial approach taken to automate this process was to mount the existing manual applicator to a CNC lathe as can be seen in Figure 3.5. This was the simplest and quickest approach to take and is a direct application of the Preliminary Design 1 discussed in the previous section. As mentioned above, the lathe would provide motion in the X and Z axes of the lathe permitting the TiC_p/Ni electrode to move across the entire face of the RSW Copper electrode while the manual applicator provides vibration of the TiC_p/Ni electrode. The RSW copper electrode was mounted to the rotating lathe chuck as seen in Figure 3.6. Electrical contact was made with the RSW Copper electrode via a contact brush also be seen in Figure 3.6 and a simple fixed 36 volt power supply was used to provide power. The RSW Copper electrode was mounted in the same manner for all subsequent designs and will not be discussed again in later sections. The complete setup can be seen in Figure 3.7.
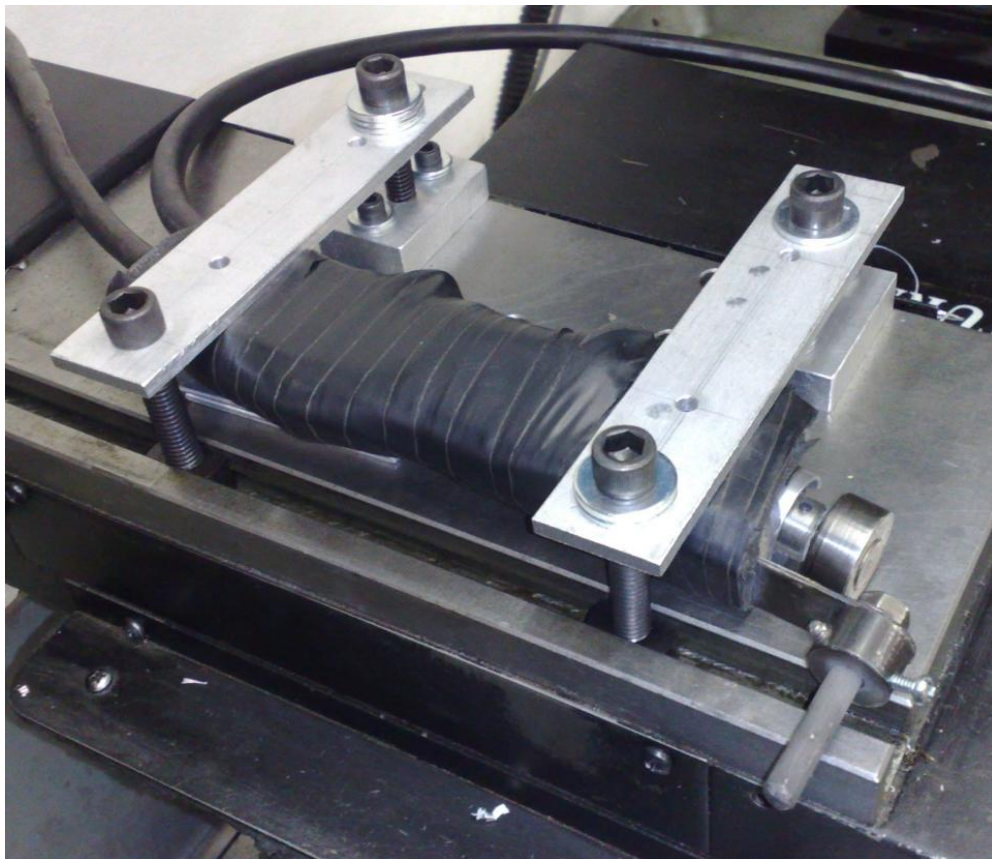
Figure 3.5: Manual Applicator Mounted to Lathe Table
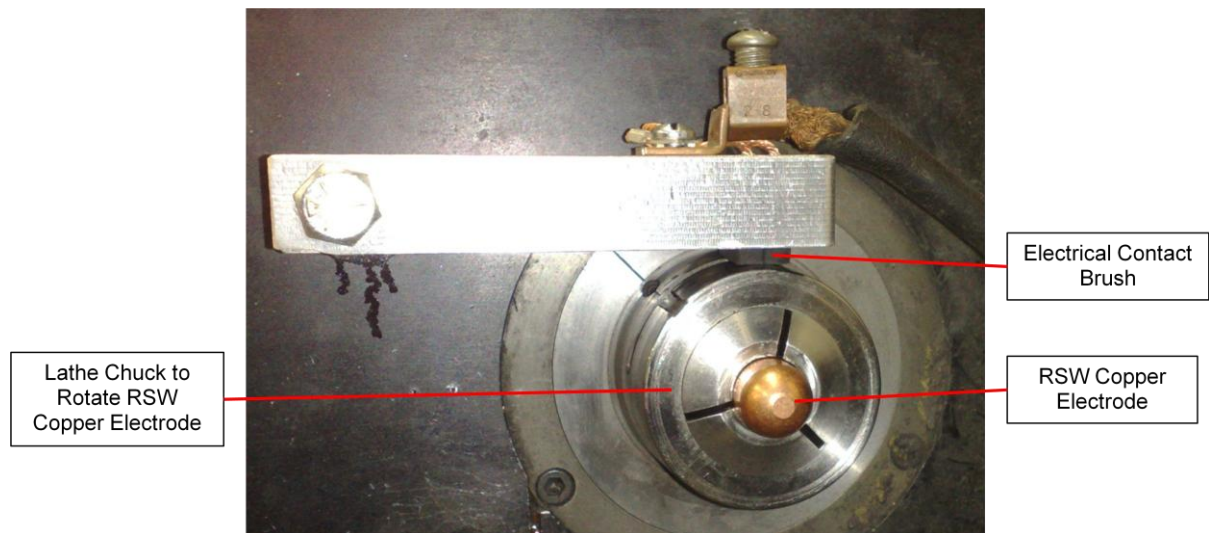
Figure 3.6: RSW Copper Electrode in Lathe Chuck
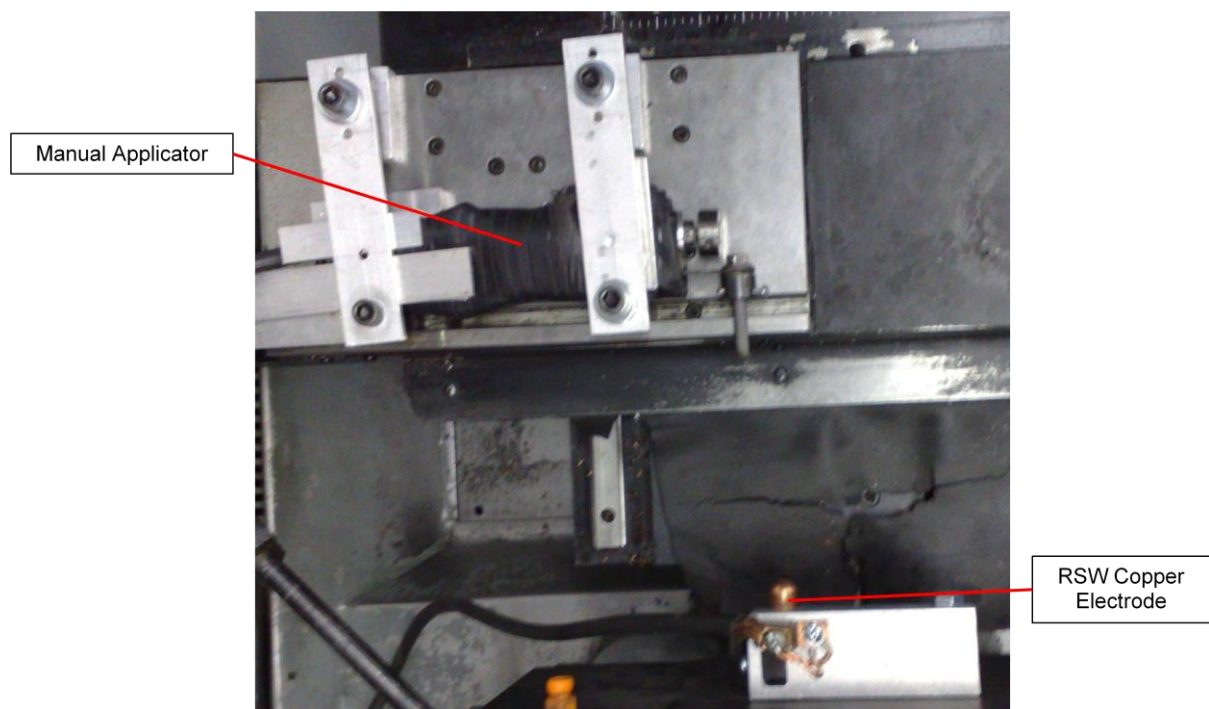
Figure 3.7: Top View of Manual-Automated Hybrid Design

3.2.2.1 Successes with the Manual-Automated Hybrid Design

The first methodology for coating the RSW Copper electrodes with the use of the existing

manual applicator with the aid of a CNC lathe proved to be successful for creating partial

coatings of TiC_p/Ni. As can be seen in Figure 3.8, when the TiC_p/Ni electrode is new and unconsumed, the first few RSW Copper electrodes to be coated show signs of a thin TiC_p/Ni layer similar to what is observed in the manual process as seen in Figure 2.10.

Figure 3.8: First Three RSW Electrodes Coated with Manual-Automated Hybrid Design with New TiCp/Ni Electrode

3.2.2.2 Problems with the Manual-Automated Hybrid Design

Although this approach was able to produce properly bonded coatings of TiC_p/Ni on the RSW Copper electrodes, this was only possible with a new TiC_p/Ni electrode. Once the TiC_p/Ni electrode began to be consumed the process became irregular and the coating became inconsistent. The result of this inconsistency can be seen in Figure 3.9.

Figure 3.9: RSW Copper Electrodes Coated with Manual-Automated Hybrid Design After Partial Wearing of TiCp/Ni Electrode

3.2.3 Actively Controlled Rotating and Reciprocating Design

The second approach to be taken was to create a completely new applicator from the ground up. This applicator required a mechanism for making and breaking electrical contact between the electrode and substrate which would replace the vibrating element of the manual applicator. This was accomplished by using two solenoids for reciprocating the TiC_p/Ni electrode which was mounted on a linear guide. One of the solenoids was for driving the electrode forward to make contact with the substrate and the other to drive the electrode in reverse to break contact.

In addition a stepper motor was also added to the mechanism to permit rotation of the electrode. This would allow the electrode to wear evenly and generate a predictable wearing pattern which could be accounted for while traversing across the face of the RSW Copper electrode. By accomplishing this even and predictable wearing pattern, it was thought that the problem observed in the previous design would be eliminated. The rotating and reciprocating mechanism can be seen in Figure 3.10 and multiple views of the mechanism can be seen in Appendix A. This mechanism is a realisation of Preliminary Design 3 discussed earlier.
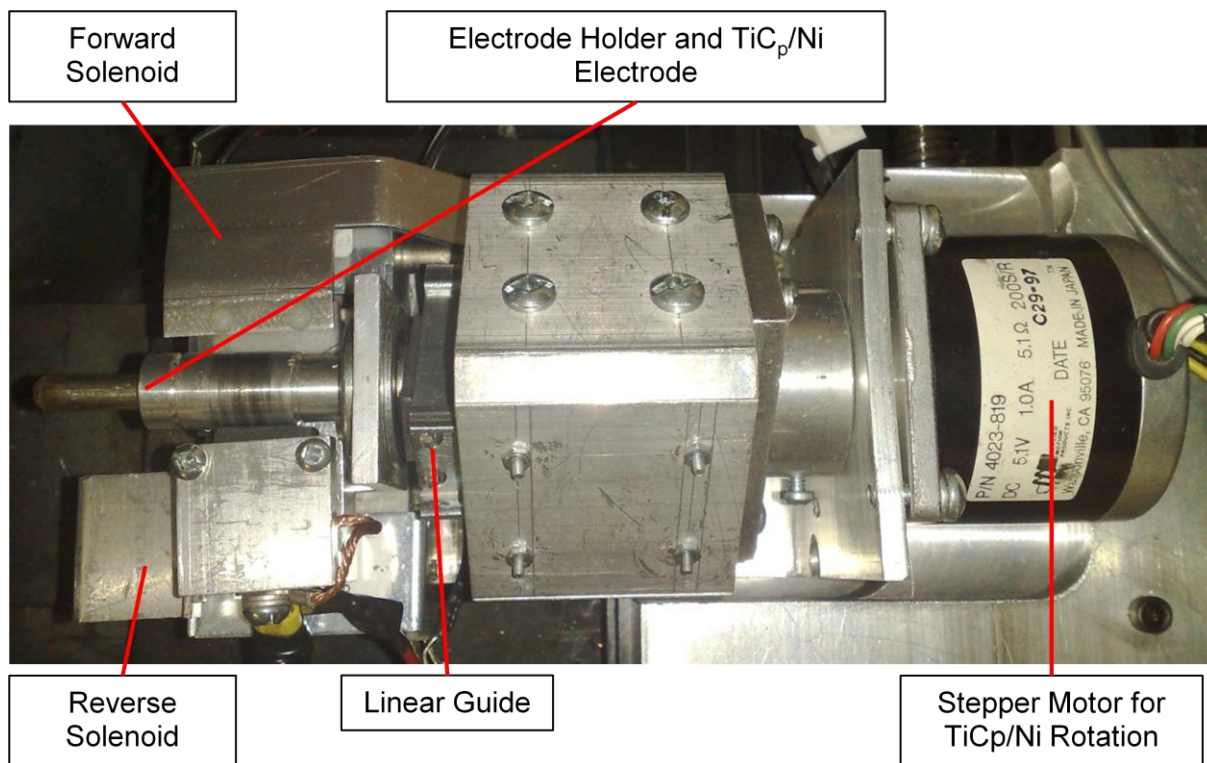
Figure 3.10: Actively Controlled Rotating and Reciprocating Mechanism

The entire mechanism was powered by a custom power supply which provided 12V for the solenoids and 5V for the stepper motor, and the system was controlled with a custom control unit as can be seen in Figure 3.11. The custom control unit controls the various parameters of the mechanism; Rotational RPM, Frequency of Reciprocation, Duty Cycle of Reciprocation, and the Force applied by the solenoid during forward travel. The inputs are set manually via potentiometer control knobs and are fed into an Arduino microcontroller. The Arduino then sends low level control signals to a custom interface board which then amplifies the low level control signals to high level outputs for the solenoids and stepper motor. The complete setup for the actively controlled rotating and reciprocating mechanism can be seen in Figure 3.12.

The main advantage of this design is that it allows a great deal of control over the four process parameters mentioned above. The solenoids also provide a relatively long travel distance (~1cm) for the TiC_p/Ni electrode in comparison to the vibration of the manual

applicator, which means that precise positioning of the mechanism with respect to the substrate is not required.

However due to design limitations there are limits to each parameter. The stepper motor can be set to a maximum of 40 RPM while the frequency can only be set to a maximum of 16 Hz. Also, setting the force of the forward driving solenoid is very complex and limits the range and ability to set the force precisely.
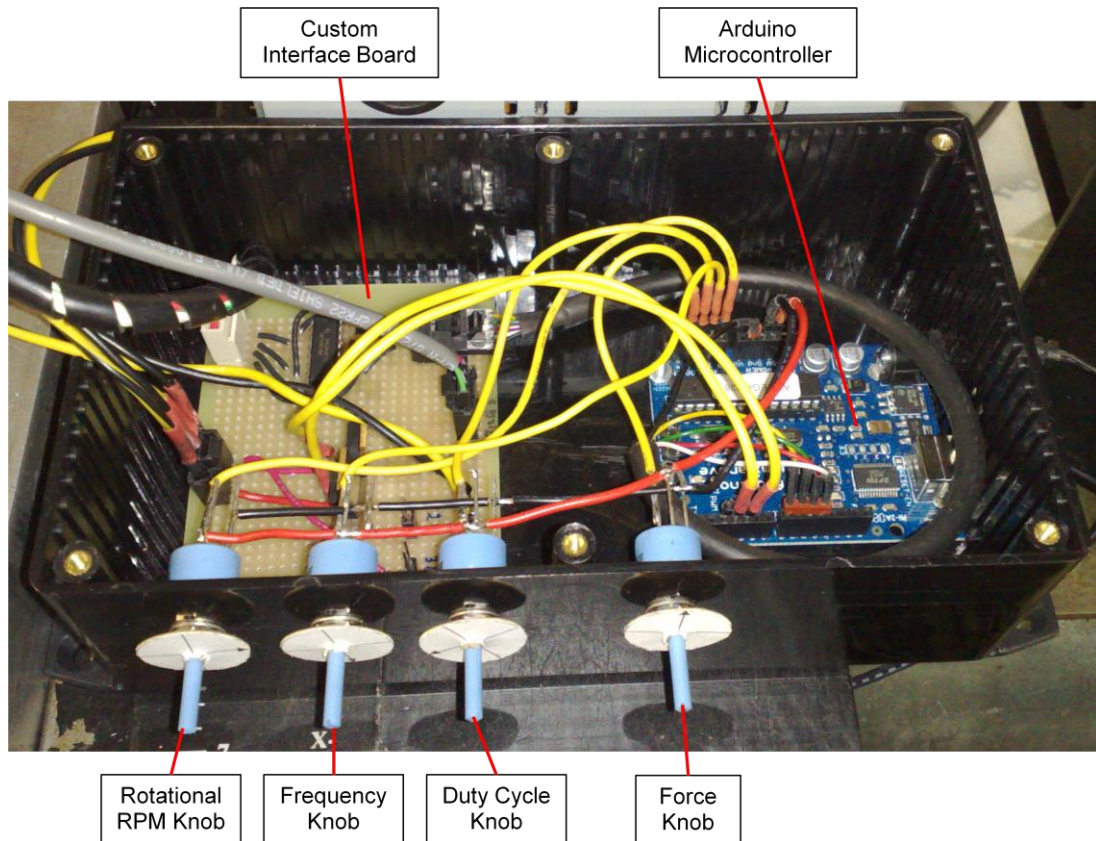
Figure 3.11: Custom Control Unit
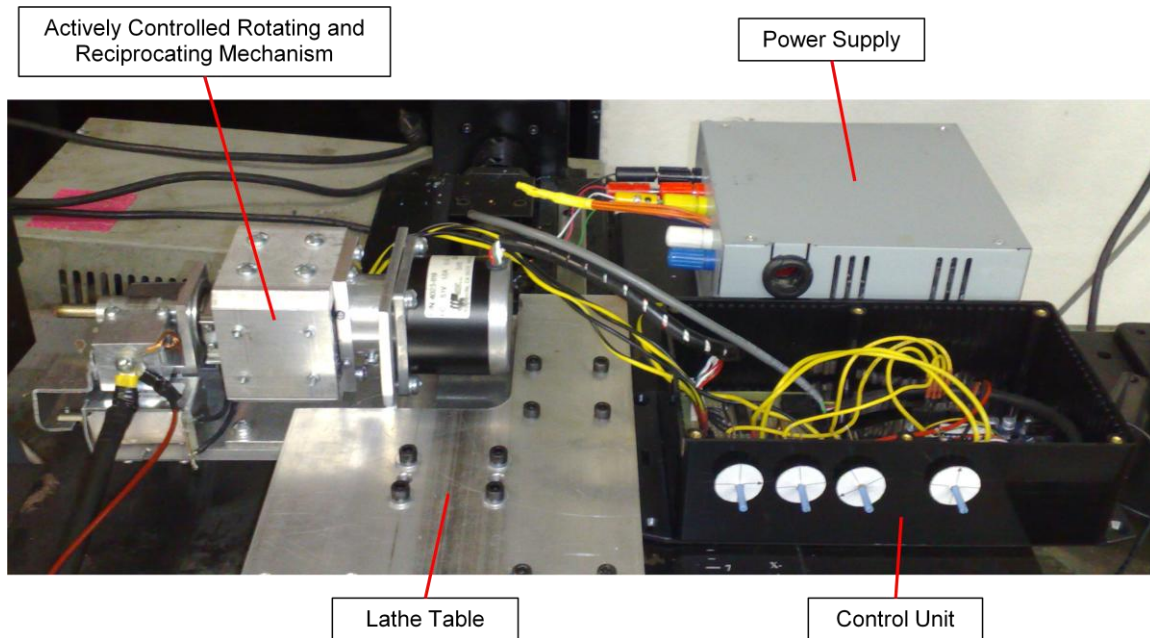
Figure 3.12: Complete Setup for the Actively Controlled Rotating and Reciprocating Mechanism

3.2.4 Actively Controlled Rotating and Vibrating Design

The final approach in the design process was to modify the actively controlled rotating and reciprocating design to make an actively controlled rotating and vibrating design. The basic concepts and principles of this design are the same as the previous design. A stepper motor is used to rotate the TiC_p/Ni electrode as in the previous design and for the same reasons: to enable even and predictable wearing of the TiC_p/Ni electrode, but the reciprocating mechanism is replaced with a vibrating mechanism as can be seen in Figure 3.13. More pictures of the actively controlled rotating and vibrating mechanism can be seen in Appendix B.

The vibrating mechanism uses a standard 12V DC motor and eccentric mass to generate vibration. The vibrating mechanism replaces the solenoids in the previous design and permits much higher frequencies; a maximum of ~300 Hz based on a maximum motor RPM of ~18000. The introduction of a vibrating mechanism eliminates the advantage of the coarse position control offered by the previous design. To alleviate this issue the linear guide was spring loaded to provide a forward bias and permit a relatively large range of linear play (~1.5cm).

The power supply remained the same as the previous design and the hardware for the custom control unit was also the same but the programming for the custom control unit was modified for this new design. The control knobs for Duty Cycle and Force as seen in Figure 3.11 were unused in this design. The complete setup for the actively controlled rotating and vibrating design can be seen in Figure 3.14.

DC Motor with Eccentric Mass for Vibration

Electrode Holder and TiC$_p$/Ni Electrode

Stepper Motor for TiCp/Ni Rotation

Spring Loaded Linear Guide
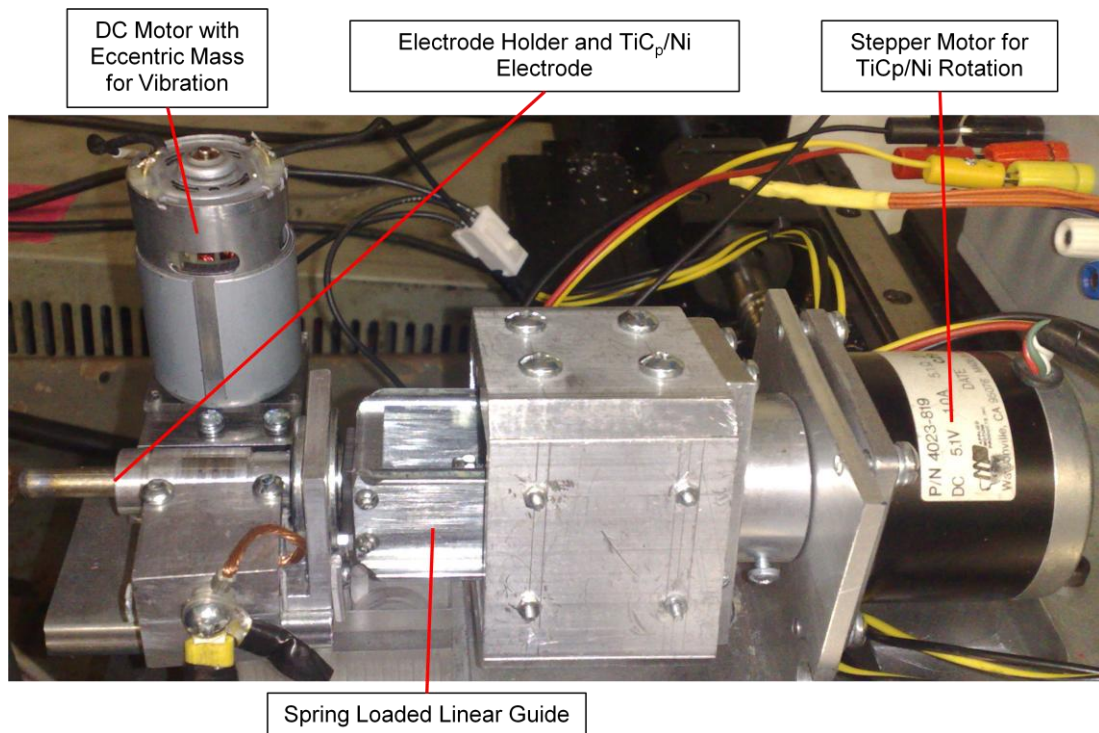
Figure 3.13: Actively Controlled Rotating and Vibrating Mechanism

Actively Controlled Rotating and Vibrating Mechanism

Power Supply

Lathe Table

Control Unit
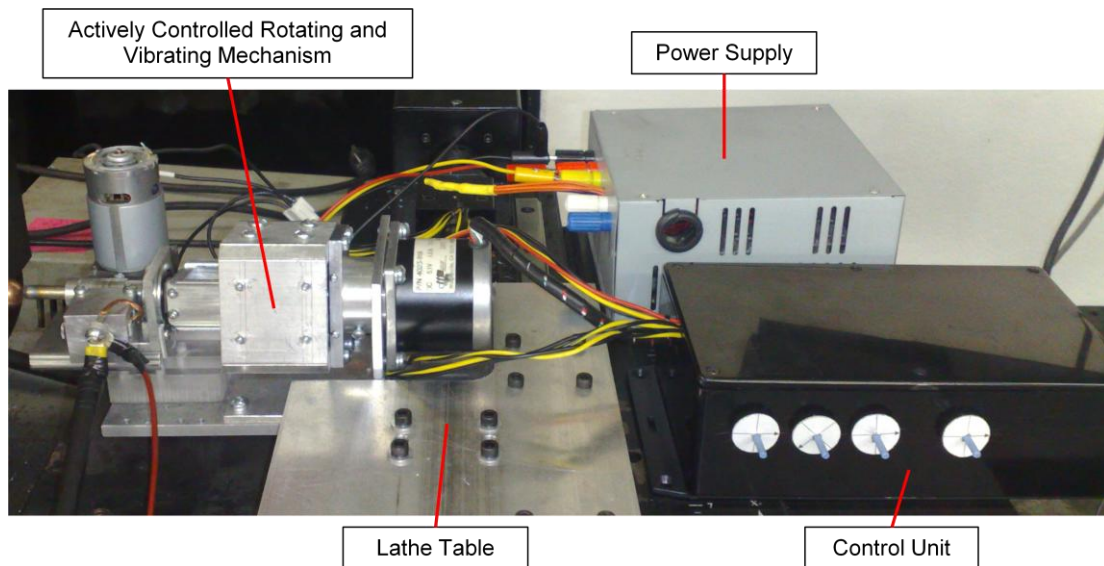
Figure 3.14: Complete Setup for the Actively Controlled Rotating and Vibrating Mechanism

Chapter 4

Experimental Test Setup and Methodology

4.1 Test Setup and Method for Manual-Automated Hybrid Setup

The Manual-Automated Hybrid setup had a fixed 36V power supply and had a similar circuit diagram to the one shown in Figure 2.2. The vibrational frequency of the manual applicator could be controlled by varying the input voltage to the applicators' motor. The vibrational frequency of the applicator was measured using a strobe light to view the rotation of the eccentric mass at varying voltages. The strobe light was also used to measure two harmonics of the actual rpm to ensure correct measurements. The rotational speed of the eccentric mass relates directly to the vibrational frequency. The results of the measurements can be seen in Table 4.1. The results were then plotted and a logarithmic equation was fitted to the graph to represent the relationship between the voltage and vibrational frequency as seen in Figure 4.1. When used normally with a 120V outlet the manual applicator has a frequency of nearly 300 Hz.

Table 4.1: Rotational Speed and Frequency vs. Voltage of Manual Applicator

Volts (V)	RPM	RPM/2	RPM/3	Vibrational Frequency (Hz)
30	3770	1890	1280	63
40	8000	4020	2680	133
50	10000	5040	3540	167
60	12000	6200	4100	200
70	13500	6900	4700	225
80	14800	7500	5000	247
90	15600	7900	5350	260
100	16100	8150	5500	268
110	16600	8400	5600	277
120	17200	8700	5900	287
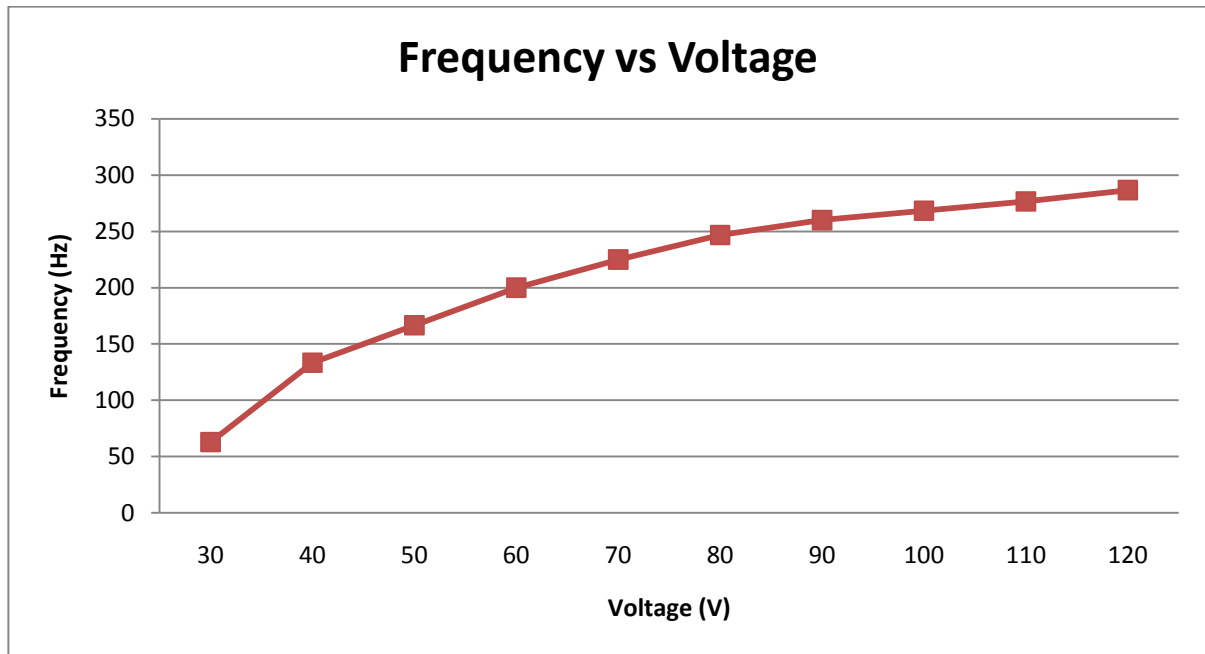
Figure 4.1: Frequency vs. Voltage of Manual Applicator

The next element of the Manual-Automated Hybrid setup was to develop the correct G-Code for the CNC lathe to ensure full coverage of the RSW Copper electrode. A basic diagram of the TiC_p/Ni electrode motion is shown in Figure 4.2. There were four main stages in the G-Code:

1. Move TiC_p/Ni electrode toward RSW Copper electrode to create contact

2. Move TiC_p/Ni in an arc along the side of the RSW Copper electrode

3. Move TiC_p/Ni electrode back away from RSW Copper electrode to completely break contact

4. Move TiC_p/Ni back to starting point

These four stages were accomplished by controlling the X and Z axes of the lathe table. These two axes provide two degrees of freedom on one plane and ensured that one side of the RSW Copper electrode would be coated. To complete coverage along the rest of the RSW Copper electrode a third degree of freedom was needed. This was provided by the lathe chuck which rotated the RSW Copper electrode as shown in Figure 4.2.

33
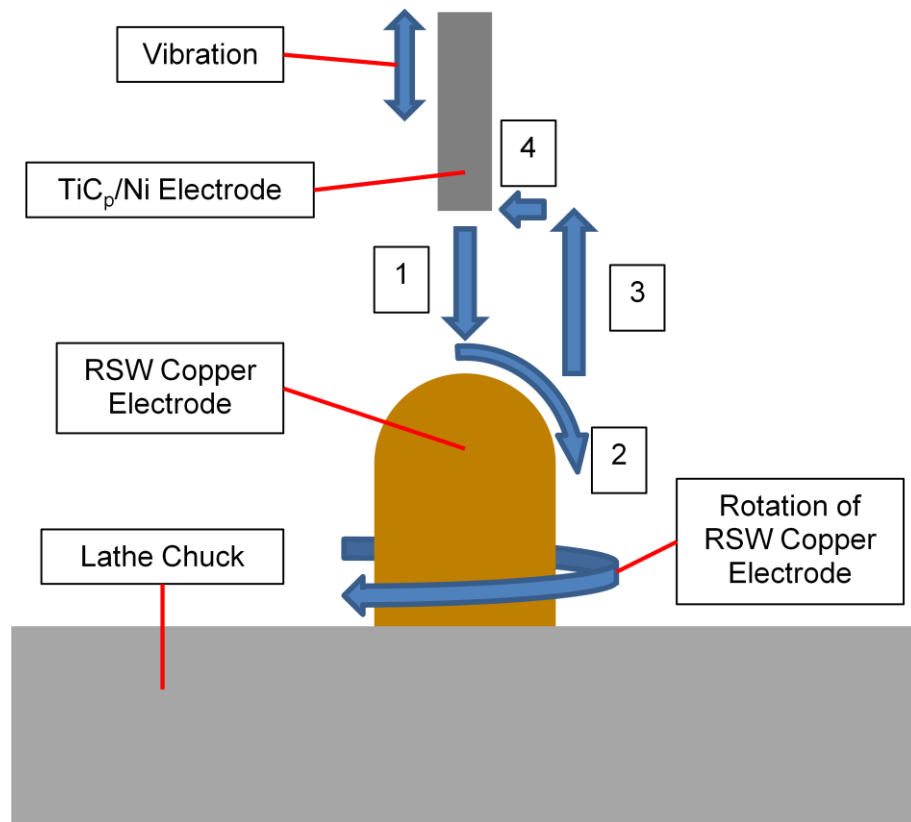
Figure 4.2: TiCp/Ni Electrode Motion for Full Coverage of RSW Copper Electrode

The TiC_p/Ni electrode needed to be zeroed before running the G-Code due to the small positional tolerance provided by the manual applicator and to provide varying degrees of force for the contact between the TiC_p/Ni electrode and the RSW Copper electrode. In order to zero the TiC_p/Ni electrode it was moved forward until contact was made with the RSW Copper electrode. This would represent a point of near-zero force contact. The vibration of the manual applicator would provide the necessary making and breaking of contact for the ESD process. To generate larger forces for the coating process the electrode was moved further forward by a small distance and zeroed. By doing this when the G-Code was run the TiC_p/Ni electrode would move beyond the point of initial contact and make the compliant material of the manual applicator bend causing it to apply a larger force.

The last parameter to control in this process was the feed rate of the TiC_p/Ni electrode. The feed rate was set in inches per minute (IPM) and determined how fast the TiC_p/Ni electrode

34

would traverse across the face of the RSW Copper electrode for stage 2 in Figure 4.2. This value was set in the G-Code and varied between tests.

The results of the tests were based on a visual inspection of the resulting coatings on the RSW Copper electrodes and the wearing characteristic of the TiC_p/Ni electrode as multiple coats were applied.

4.1.1 Problems with Manual-Automated Hybrid Setup

As discussed earlier the main problem with the Manual-Automated Hybrid setup was that the coatings produced by this setup were inconsistent due to wearing of the TiC_p/Ni electrode as it was consumed in the process. This would result in varying coating characteristics for the same process parameters.

4.2 Test Setup and Method for Actively Controlled Rotating and Reciprocating Setup

Similar to the Manual-Automated Hybrid setup, the Actively Controlled Rotating and Reciprocating setup used a fixed 36V, 60Hz, half-wave rectified power supply. Another newly developed power supply by Huys Industries Ltd. was also used for comparison purposes between the two power supplies. The new power supply is discussed in the next design setup. The reciprocating mechanism was discussed in section 3.2.3 and uses two solenoids to drive the TiC_p/Ni electrode forward and reverse. The solenoids were used to control the frequency of reciprocation of the TiC_p/Ni electrode. The control unit shown in Figure 3.11 was used to vary the frequency up to a maximum of 16 Hz, the mechanical limit of the mechanism. Along with the reciprocation frequency the duty cycle of the frequency could also be set via the control unit. While the reciprocation frequency controls the number of times the TiC_p/Ni electrode would come in contact with the RSW Copper electrode every second, the duty cycle would control the duration of contact for each cycle. This allows greater control over the time that the TiC_p/Ni electrode has to melt and transfer over to the substrate.

The rotation of the TiC_p/Ni was also controlled via the control unit up to a maximum of 40 RPM, the mechanical limit of the mechanism. This was used to ensure even wearing of the TiC_p/Ni electrode, however it could also be used to hold the TiC_p/Ni electrode in one orientation if needed. This could potentially add the ability to index the TiC_p/Ni electrode. The TiC_p/Ni electrode would be held in one orientation while the coating is applied for a specified duration of time, then the TiC_p/Ni electrode would be rotated a specified number of degrees and held in a new orientation. This would force consumption of different parts of the TiC_p/Ni electrode tip throughout the entire coating process but allow localised consumption during short periods within the coating process. By indexing the TiC_p/Ni electrode this mechanism could mimic the manual applicator more closely while still permitting even wearing of the TiC_p/Ni electrode. In addition, rotating the TiC_p/Ni electrode could aid in the process of breaking away of the TiC_p/Ni electrode from the RSW Copper electrode after contact is made.

The force of contact that the TiC$_p$/Ni electrode would apply to the RSW Copper electrode could also be controlled via the control unit. This was accomplished by varying the timings at which each of the two solenoids were activated. If a large contact force was desired then the forward solenoid was activated independently of the reverse solenoid. If a smaller force was desired then the reverse solenoid was activated before the forward solenoid completed its forward travel. This would cause a force in both the forward and reverse directions simultaneously causing the resultant forward force to be reduced. The sooner the reverse solenoid was activated before the completion of the forward cycle the less the contact force would be.

The G-Code used to traverse across the surface of the RSW Copper electrode was the same as the Manual-Automated Hybrid setup. The diagram of the four stages of the G-Code can be seen in Figure 4.2.

The method used to set the zero position of the TiC$_p$/Ni was different than the Manual-Automated Hybrid setup. This difference is due to the fact that the Actively Controlled Rotating and Reciprocating Mechanism has a significantly longer TiC$_p$/Ni electrode travel (~1cm). To set the zero position the TiC$_p$/Ni electrode was first pulled back to the furthest reverse position by using the reverse solenoid, then the mechanism was moved forward until contact between the TiC$_p$/Ni electrode and the RSW Copper electrode was made. Then the mechanism was moved back ~0.5cm to permit the solenoid mechanism to reciprocate freely. This position was set as the zero position. Accurate positioning of the mechanism was not necessary since the solenoid mechanism inherently has a large positional tolerance. This allows the mechanism to continue running without being reset after the TiC$_p$/Ni electrode is consumed.

The feed rate of the TiC$_p$/Ni electrode was set in the same manner as the Manual-Automated Hybrid setup and was adjusted for different tests.

Measurements of the electrical characteristics and force characteristics of the automated coating process were taken with the use of a Data Acquisition (DAQ) System. The DAQ System is discussed in section 4.4 below.

The results of the tests were based on a visual inspection of the resulting coatings on the RSW Copper electrodes and the wearing characteristic of the TiC_p/Ni electrode as multiple coats were applied.

4.2.1 Problems with Actively Controlled Rotating and Reciprocating Setup

As mentioned in section 3.2.3 there are some problems with the Actively Controlled Rotating and Reciprocating setup. One of the problems is that the there are mechanical limitations to the rotational speed and the frequency of reciprocation of the mechanism. The frequency of reciprocation is limited by nearly $1/20^{th}$ of the vibrational frequency of the manual applicator. The rotational speed is limited to 40 RPM which is much lower than what is capable with a brushed DC motor. The force applied by the solenoids has a very limited range and scope. The method employed for controlling the force makes accurate force control very difficult. If the reverse solenoid is activated too quickly then the TiC_p/Ni may not move forward at all and if the reverse solenoid is activated too late then it may not provide any reverse force.

4.3 Test Setup and Method for Actively Controlled Rotating and Vibrating Setup

The power supply used for the Actively Controlled Rotating and Vibrating setup was a newly developed variable power supply by Huys Industries Ltd. This was a 60Hz full-wave rectified power supply and allowed control of various settings; ESD Voltage, Arc Voltage, Motor Speed, Pressure, Arc Charge, Arc Discharge, ESD Charge, ESD Discharge, Arc Scale, and ESD Scale. It was recommended that only the first four settings be changed by the user as the remaining settings are system parameters specific to the power supply. Of the four user controllable parameters only two are of importance to this study, the ESD Voltage and the Arc Voltage. The ESD Voltage is considered to be one of the most important electrical parameters in the ESD process. This controls the voltage that the capacitors will be charged to before discharge can take place for the ESD process. The power supply will keep the output opened until the set voltage is reached and if the TiC_p/Ni electrode makes contact with the RSW Copper electrode before the capacitors are charged to the specified level then the power supply will prevent electrical conductance. The ESD Voltage can be set between 15V and 50V. The Arc Voltage controls the arc capacitors which boost the discharge process by adding energy once the TiC_p/Ni electrode begins to melt and forms an arc with the RSW Copper electrode. The Arc Voltage can be set between 15V and 50V; however it must remain below the value set for the ESD Voltage.

The rotation of the TiC_p/Ni electrode was controlled by the control unit in the same manner as explained for the Actively Controlled Rotating and Reciprocating setup and provided the same benefits: even wearing of the TiC_p/Ni electrode, potential for indexing, and aiding in breaking electrical contact.

Vibration control was achieved through the control unit. The code which was used to control the frequency of reciprocation was modified to control the rotational speed of the DC motor used to rotate the eccentric mass which provides vibration. The DC motor was provided with a PWM signal from 0% to 100% which set the speed of the motor from 0 RPM to ~18000 RPM (the maximum speed of the DC motor). The vibrational frequency that corresponds to this range is 0 Hz to ~300Hz.

The G-Code used for this setup was the same as in the previous setup and used the same feed rates as well. The zeroing method for the TiC_p/Ni electrode was different because this mechanism used a spring loaded forward bias mechanism as discussed in section 3.2.4. The spring loaded mechanism eliminates the need for accurate positioning and simplifies the zeroing process. The setup was moved forward until the TiC_p/Ni electrode made contact with the RSW Copper electrode, then the setup was moved forward half of the total spring extension (~0.75cm). This position was set as the zero for this setup and any positional inaccuracies would be covered by the spring. For the purpose of force control, the zero position could be changed with a forward bias to be closer to the RSW Copper electrode in order to increase the force, or it could be reverse biased to be further away from the RSW Copper electrode in order to reduce the force.

As with the Actively Controlled Rotating and Reciprocating setup, the electrical and force characteristics of this process were measured with the use of a DAQ system as discussed in section 4.4 below.

The results of the tests were based on a visual inspection of the resulting coatings on the RSW Copper electrodes and the wearing characteristic of the TiC_p/Ni electrode as multiple coats were applied.

4.3.1 Problems with Actively Controlled Rotating and Vibrating Setup

As with the Actively Controlled Rotating and Reciprocating setup, this setup has a mechanical limitation of 40 RPM for the rotational speed of the TiC_p/Ni electrode. Another problem with this setup is that the force control is not very accurate due to its dependence on two variables; the zero position of the setup and the vibration frequency of the mechanism.

4.4 Data Acquisition (DAQ) System

A Data Acquisition (DAQ) System was used to measure and record electrical and force characteristics for the automated setups. The DAQ system was a National Instruments USB-6211 M Series Multifunction DAQ with a 250kS/s Sampling rate. The software used to control the DAQ system was National Instruments LabVIEW 9.0. The DAQ system consists of a Voltage reading, a Current Sensor reading, and a Force Sensor Reading as can be seen in the schematic diagram in Figure 4.3. MATLAB was used to generate graphs from the data collected in LabVIEW.
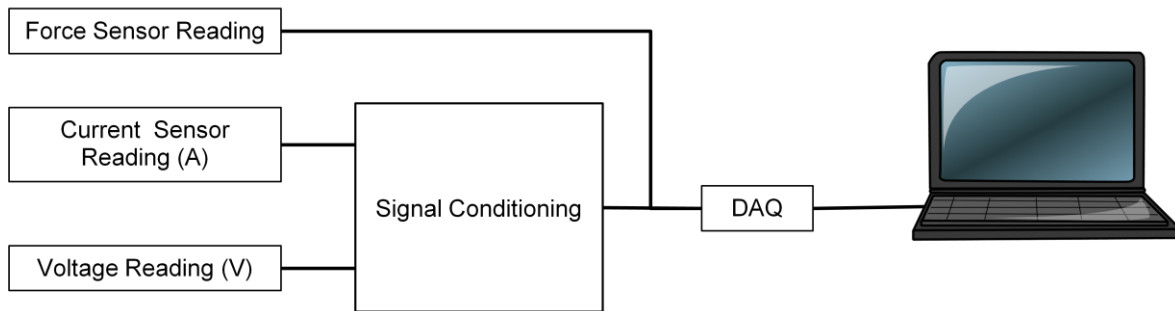
Figure 4.3: Data Acquisition (DAQ) System for ESD Parameter Readings

The Voltage reading was taken directly between the negative terminal of the ESD setup (the lathe chuck) and the positive terminal of the ESD setup (the TiC_p/Ni electrode). The Current sensor was a Hall Effect sensor which took readings at the positive terminal of the ESD power supply. The DAQ has an input limit of -10V to 10V so the Voltage and Current readings were first passed through a Signal Conditioning box in order to scale down the readings to lower values. The force sensor was a Force Sensing Resistor (FSR) as can be seen in Figure 4.4. This sensor provides a voltage between 0V and 5V based on the force applied on the FSR pad. The Voltage Divider Circuit is used to change the sensitivity of the sensor. The LabVIEW program and MATLAB script for reading and graphing the Voltage and Current measurements can be seen in Appendix C and Appendix D respectively. The LabVIEW program and MATLAB script for reading and graphing the Force measurements can be seen in Appendix E and Appendix F respectively.

Figure 4.4: Force Sensing Resistor (FSR)

The electrical characteristics of the manual applicator were taken by applying three sets of varying force to the coating process by hand, light force, medium force, and heavy force. By varying the amount of force applied by hand on the RSW Copper electrode with the TiC_p/Ni electrode a distinct change in the electrical characteristics can be see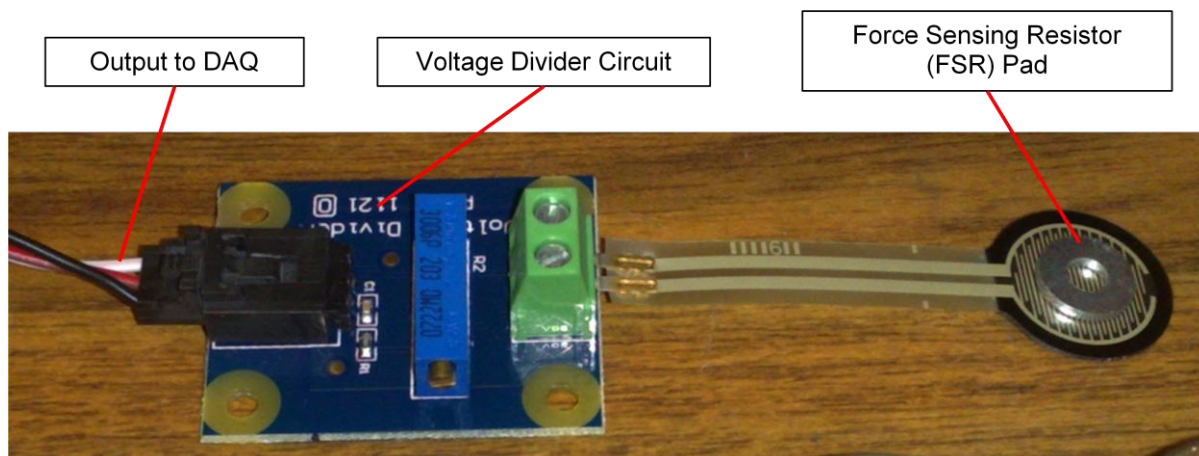n as shown in Figure 4.5, Figure 4.6, and Figure 4.7. Figure 4.5 shows the result of applying a light force by hand and produces an inconsistent and irregular electrical pattern. If the force applied is too light then the coating of the TiC_p/Ni electrode on the RSW Copper electrode is very slow, inconsistent and thin. Figure 4.7 shows the result of applying a heavy force to the manual coating process and shows that many regular low current spikes are generated without the voltage of the capacitors charging up fully. By applying too much force the vibration of the TiC_p/Ni electrode in the manual applicator is prevented from breaking contact and creates a continuous short circuit. Finally, Figure 4.6 shows the results of applying medium force with the manual applicator. The result is a regular set of four current spikes generated at 60 Hz which is consistent with the charging frequency of the power supply. The four spikes generated within each set occur at a frequency of ~300 Hz which is consistent with the vibrational frequency of the manual applicator as shown in Figure 4.1. The application of medium force produces the most consistent and successful coatings with the manual applicator. Due to the use of a basic power supply without charge control it can be seen that the voltage of the capacitors vary between each contact.
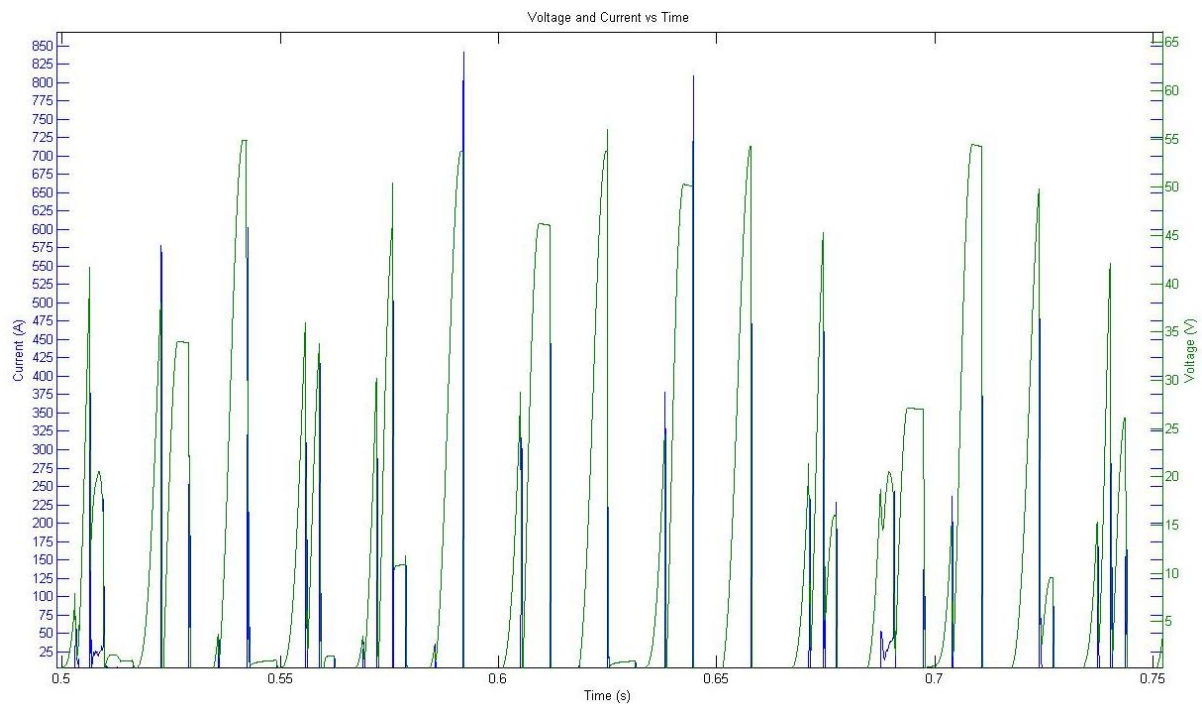
Figure 4.5: Electrical Characteristics of Light Force Manual Coating
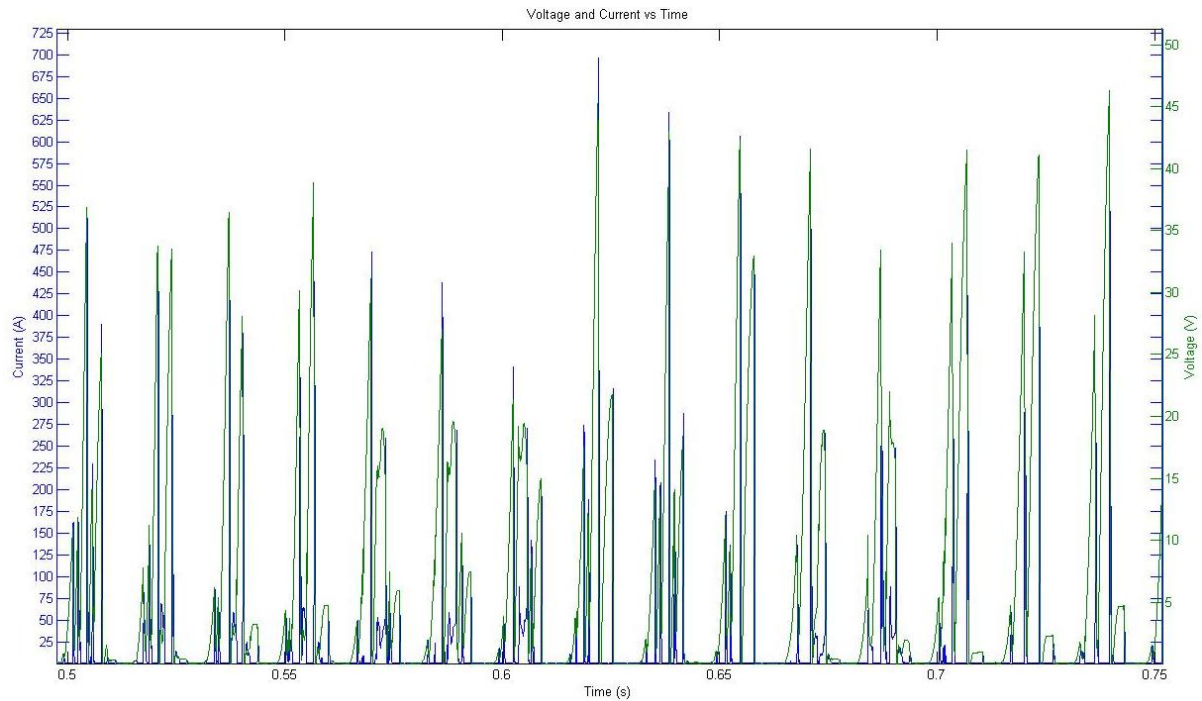
Figure 4.6: Electrical Characteristics of Medium Force Manual Coating
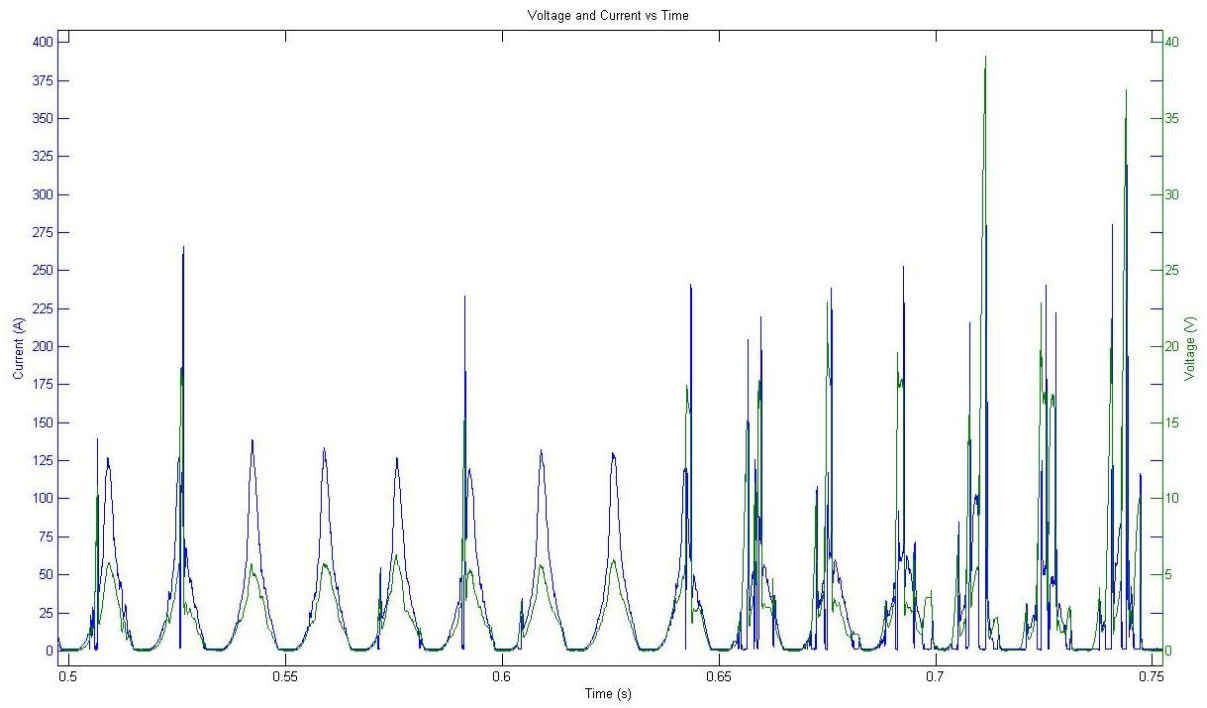
Figure 4.7: Electrical Characteristics of Heavy Force Manual Coating

4.5 Force Measurements

Force measurements were taken to correlate the voltage from the FSR to Newtons (N). The setup for the tests can be seen in Figure 4.8. The FSR was placed on top of an RSW Copper electrode with a flat surface and known masses were placed on top of the FSR. The resulting voltages associated to each mass were measured and recorded in Table 4.2. The results of Table 4.2 were then graphed as can be seen in Figure 4.9. The results show that the measured force is exponentially related to the measured voltage. The maximum output voltage of the FSR is 5V.
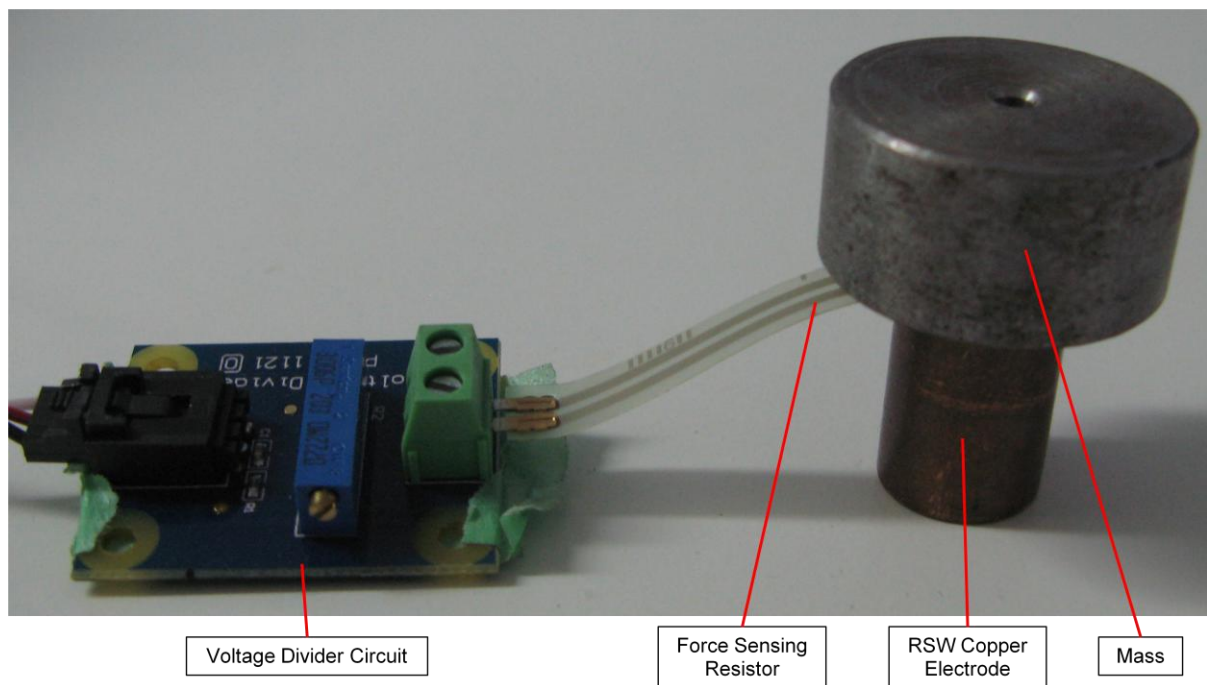
Figure 4.8: Test Setup for Force Measurements of Force Sensing Resistor

Table 4.2: Voltage and Force vs. Mass for Force Measurements of Force Sensing Resistor

Mass (Kg)	Voltage (V)	Force (N)
0.3	0.8	2.943
0.425	1.6	4.16925
1.193	2.6	11.70333
2.57	3.2	25.2117
3.183	3.4	31.22523
4.557	3.6	44.70417
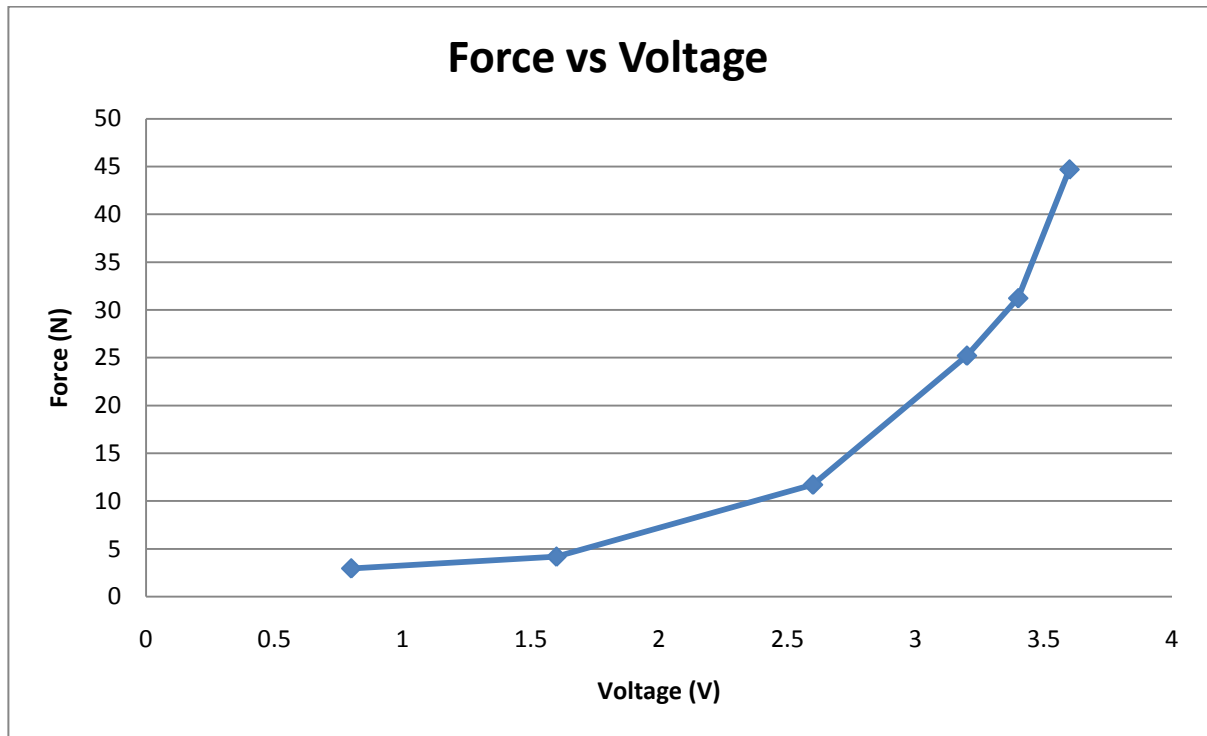
Figure 4.9: Force vs. Voltage of Force Sensing Resistor

Force data was collected from manual operators at Huys Industries Ltd for the purpose of comparing with measurements obtained with the automated setups. The FSR was placed on the RSW Copper electrode holder used for manual coatings and the operators held the manual TiC_p/Ni electrode applicator in their hands as can be seen in Figure 4.10. The operators would then move the manual applicator and the TiC_p/Ni electrode over the FSR in the same manner as they would move it for coating RSW Copper electrodes. The force applied on the FSR was then measured and graphed. An example of the measurements can be seen in Figure 4.11 and more measurements can be seen in Appendix G. It can be seen by the results of the force measurements that the manual operators normally apply a force which generates between 1.5V to 2V from the FSR. This voltage range corresponds to a force approximately between 4N to 7N.

Figure 4.10: Setup for Manual Operators for Force Measurements

Figure 4.11: Force Measurement of a Manual Operator at Huys Industries Ltd.

47

Chapter 5

Results and Discussion

5.1 Manual-Automated Hybrid Setup Results

As was discussed in section 3.2.2.1 the initial results of the Manual-Automated Hybrid setup proved to be successful producing reasonable coatings of TiC_p/Ni on the RSW Copper electrodes as shown in Figure 3.8. As the process was continued though the coatings became less consistent and the process degraded quickly as the TiC_p/Ni electrode wore out from consumption. Some result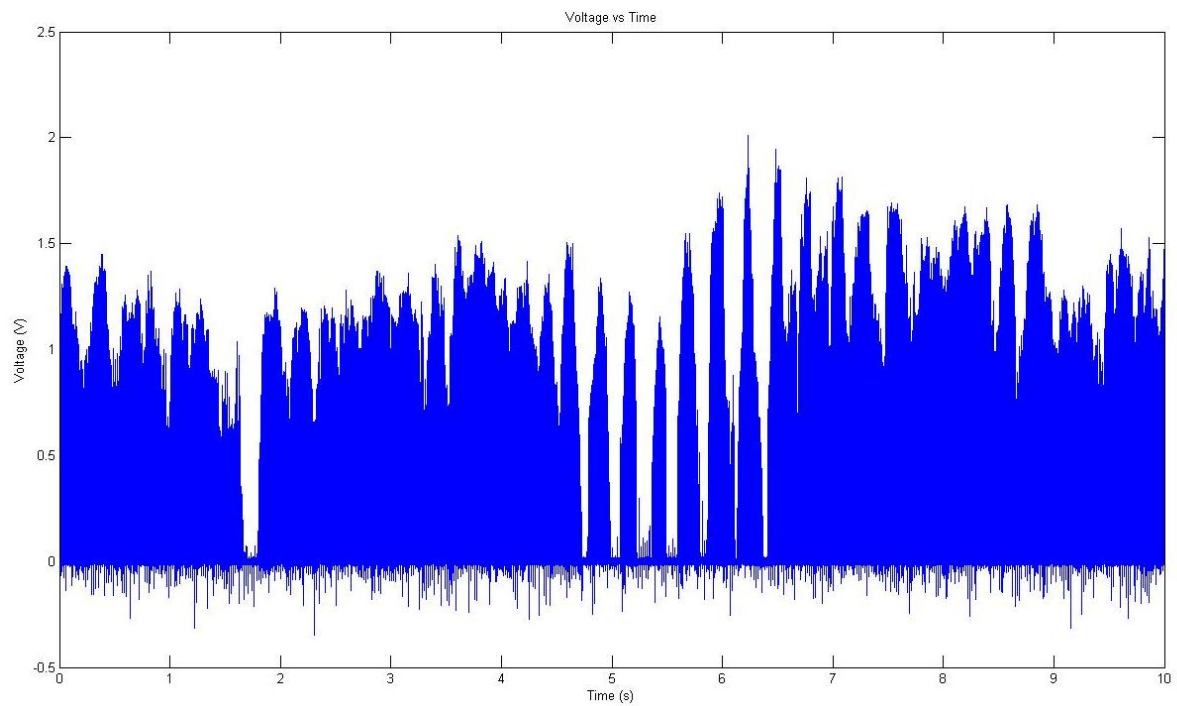s of the process after the wearing of the TiC_p/Ni electrode can be seen in Figure 3.9. A better example of the inconsistency of the process can be seen in Figure 5.1. The four coatings applied to the RSW Copper electrodes shown in Figure 5.1 were all done with the same settings; vibrational frequency of ~300Hz, 1.5 IPM, zero offset of +0.01in, and the same G-Code. The degradation of the process is shown from left to right in Figure 5.1 where the first RSW Copper electrode which was coated with these settings is seen on the far left and the last is seen on the far right. The image shows that less and less TiC_p/Ni was being transferred to the RSW Copper electrodes as the process was repeated. Portions of the latter RSW Copper electrodes were being left uncoated in the same areas where previous RSW Copper electrodes were being fully covered. Initially it was assumed that this problem could be corrected by moving the TiC_p/Ni electrode forward to account for the wearing, however this proved to be unsuccessful and did not change the results, still producing irregular and inconsistent partial coats. In order to eliminate the problem the only solution was to use a new TiC_p/Ni electrode or to turn the existing TiC_p/Ni electrode to an orientation where an unused portion of the TiC_p/Ni electrode would come in contact with the RSW Copper electrode. These observations lead to the conclusion that the problem seen here was the result of an uneven and unpredictable wearing pattern of the TiC_p/Ni electrode.

Figure 5.1: Results of Degrading Manual-Automated Hybrid Setup

The top and front view of the wearing of the TiC_p/Ni electrode can be seen in Figure 5.2 and Figure 5.3 respectively. It can be seen from the top view that the TiC_p/Ni electrode was consumed from one side: the side which was in contact with the RSW Copper electrode. The front view further illustrates that the TiC_p/Ni electrode began to create a concave-like surface near the tip. This was due to the area of contact between the TiC_p/Ni electrode and the RSW Copper electrode.
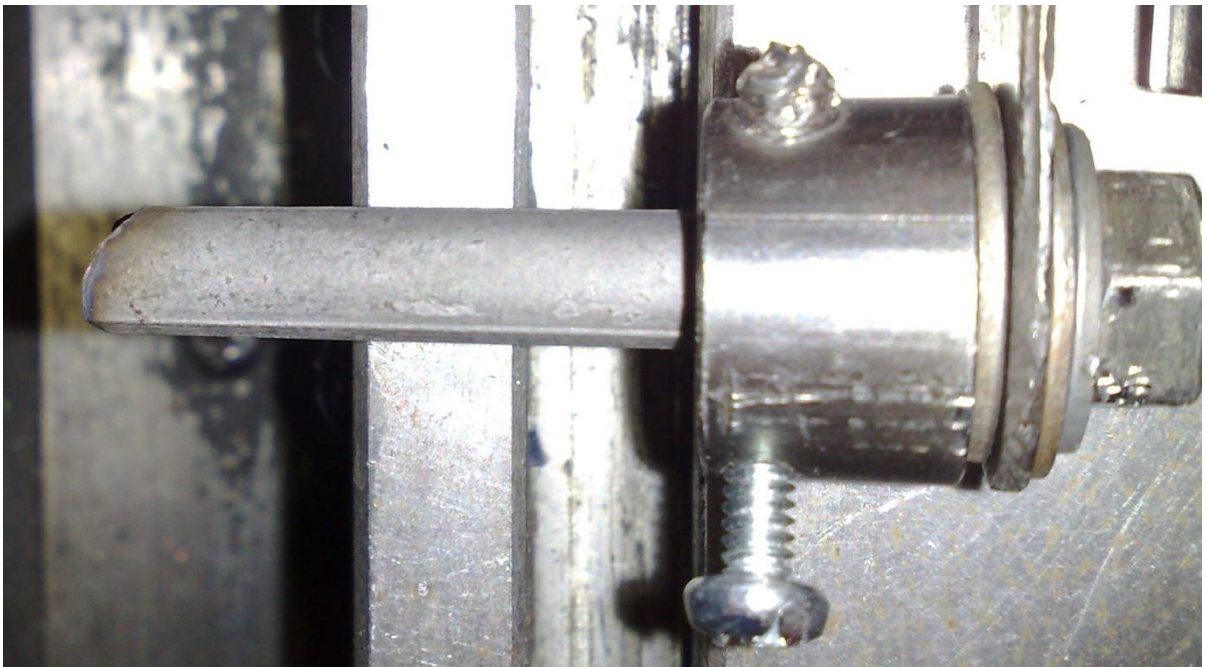

Figure 5.2: Top View of TiC_p/Ni Electrode Wearing with Manual-Automated Hybrid Setup
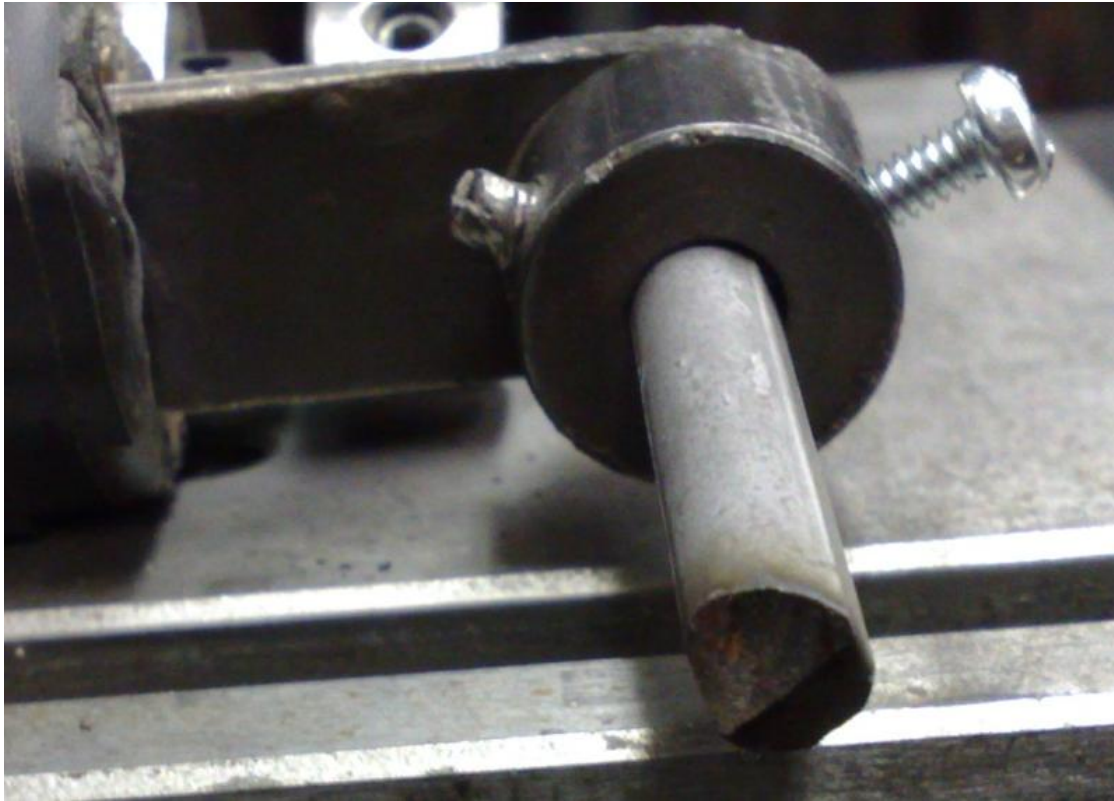
Figure 5.3: Front View of TiC$_p$/Ni Electrode Wearing with Manual-Automated Hybrid Setup

When a new TiC$_p$/Ni electrode is used it produces a single point of contact with the RSW Copper electrode at a known location. This concept is demonstrated in Figure 5.4. By knowing where the TiC$_p$/Ni electrode will contact the RSW Copper electrode it is easy to produce a G-Code which can profile the tip of the RSW Copper electrode and ensure full coverage of the surface as described in Figure 4.2. This is why the initial results of the Manual-Automated Hybrid setup produces successful coats as seen on the left of Figure 5.1. The G-Code which was created for this setup was made for use with new TiC$_p$/Ni electrodes. Once the TiC$_p$/Ni electrode began to wear as seen in Figure 5.3 the contact geometry between the TiC$_p$/Ni electrode and the RSW Copper electrode changed. The resulting interface is that of two surfaces with an unknown point of contact. This effect is shown in Figure 5.5. Since the point of contact is unknown with a worn TiC$_p$/Ni electrode a pre-set G-Code cannot be used for the coating process and there is no way to ensure that the entire RSW Copper electrode will be coated. This is what caused the gaps and incomplete coating on the RSW

50

Copper electrodes shown on the right of Figure 5.1. Since this setup utilizes the manual applicator as a part of the design there are limitations to corrective solutions for this problem. The manual applicator does not permit the TiC_p/Ni electrode to wear evenly and predictably so the only way to eliminate this problem with this setup would be to monitor the TiC_p/Ni electrode wear and adjust the G-Code to compensate for the wearing.
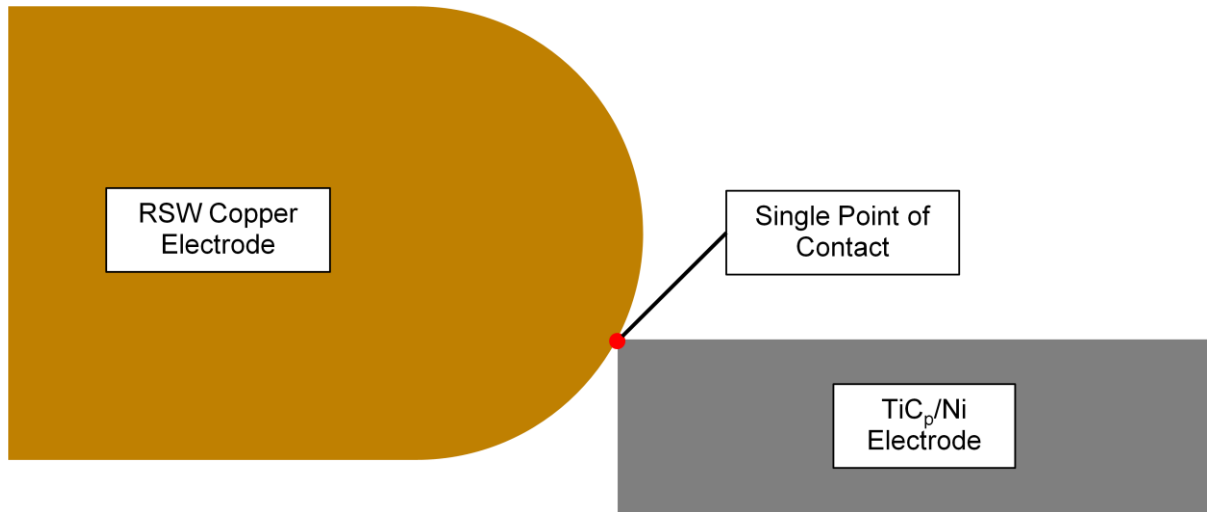
Figure 5.4: Single Point of Contact with a New TiC$_p$/Ni Electrode
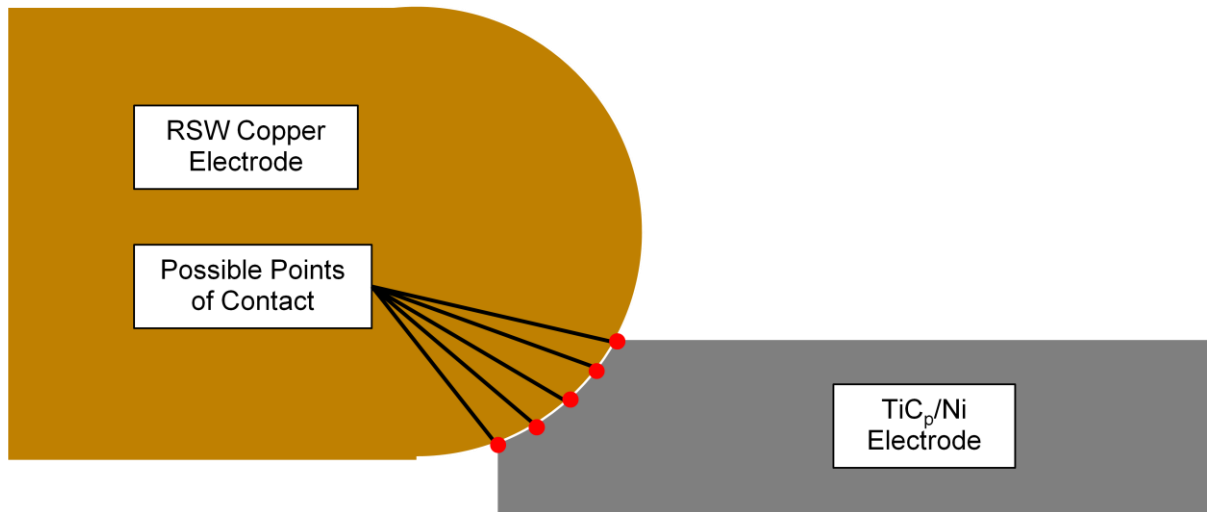
Figure 5.5: Unknown Point of Contact after Wearing of the TiC$_p$/Ni Electrode with the Manual-Automated Hybrid Setup

The Manual-Automated Hybrid setup initially provided a good solution for automating the RSW Copper electrode coating process with the use of new TiC_p/Ni electrodes. Once the TiC_p/Ni electrode began to wear though the process degraded and a full coating was no longer possible with the current setup. There is no method to modify the setup to allow for even TiC_p/Ni electrode wear which means that the only way to fix this problem is to monitor the coating process and adjust the G-Code, but this is not possible because the G-Code cannot be adjusted automatically and requires manual input. Any further study of the electrical characteristics of the Manual-Automated Hybrid setup cannot be conducted because of this problem as well and prevents any additional data acquisition. Due to these complications with this setup it is necessary to develop a new design which eliminates the problem of uneven TiC_p/Ni electrode wear.

5.2 Actively Controlled Rotating and Reciprocating Setup Results

Since the major flaw of the Manual-Automated Hybrid setup was uneven wearing of the TiC$_p$/Ni electrode the primary objective of the Actively Controlled Rotating and Reciprocating setup was to provide a method for overcoming this issue. In order to solve this problem this new design uses a rotating mechanism for the TiC$_p$/Ni electrode as discussed in section 3.2.3 and shown in Figure 3.10. Figure 5.6 shows the shape of a new TiC$_p$/Ni electrode installed on the Actively Controlled Rotating and Reciprocating setup. As can be seen from Figure 5.6 the TiC$_p$/Ni electrode starts off with a sharp edge at the tip which will make contact with the RSW Copper electrode. This setup looks identical to the single contact point model shown in Figure 5.4 and was expected to produce the similar results to the Manual-Automated Hybrid setup while the TiC$_p$/Ni electrode remained new and unconsumed.
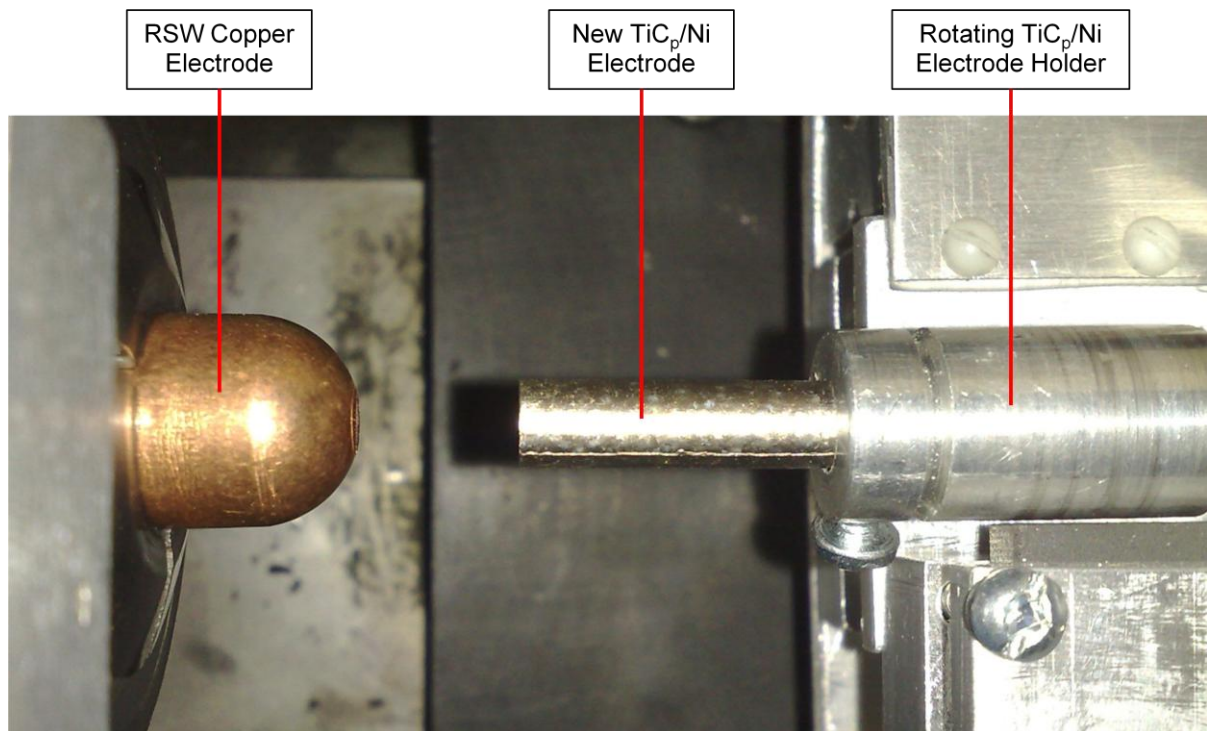

Figure 5.6: New TiC$_p$/Ni Electrode in Actively Controlled Rotating and Reciprocating Setup

The Actively Controlled Rotating and Reciprocating setup was used to coat multiple caps with the methodology discussed in section 4.2. The same G-Code which was used for the Manual-Automated Hybrid setup was used for this setup with the main difference being that the TiC_p/Ni electrode was being rotated as it moved across the surface of the RSW Copper electrode. After running the G-Code multiple times and coating a number of RSW Copper electrodes it was observed that the TiC_p/Ni electrode began to be consumed in the process and produced a semi-spherical shape at the tip as can be seen in Figure 5.7. The wearing pattern observed with this setup produced a predictable shape as was assumed and simplifies the automation process by eliminating one unknown variable. The shape produced by this process also generates a single contact point similar to the one shown in Figure 5.4 but with a different interface between the TiC_p/Ni electrode and the RSW Copper electrode. This interface is shown in Figure 5.8.
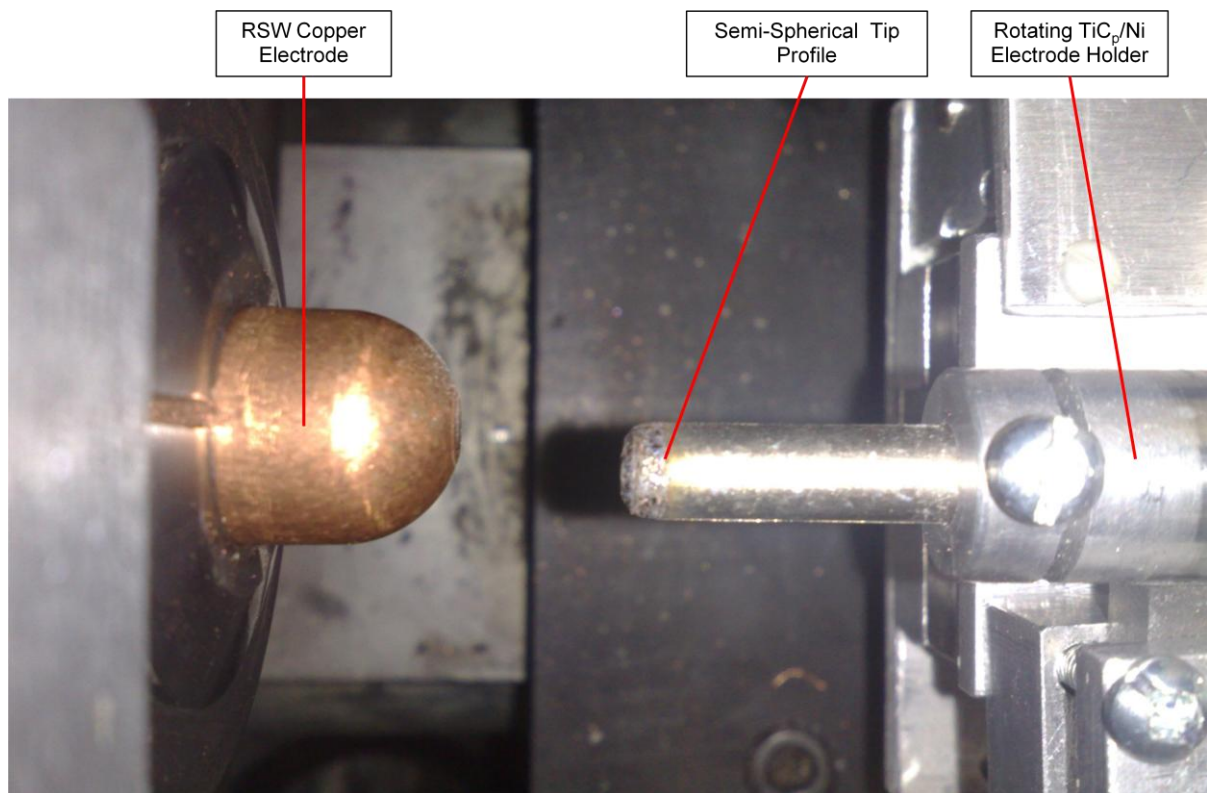

Figure 5.7: Semi-Spherical Tip Profile of TiC$_p$/Ni Electrode after Partial Consumption
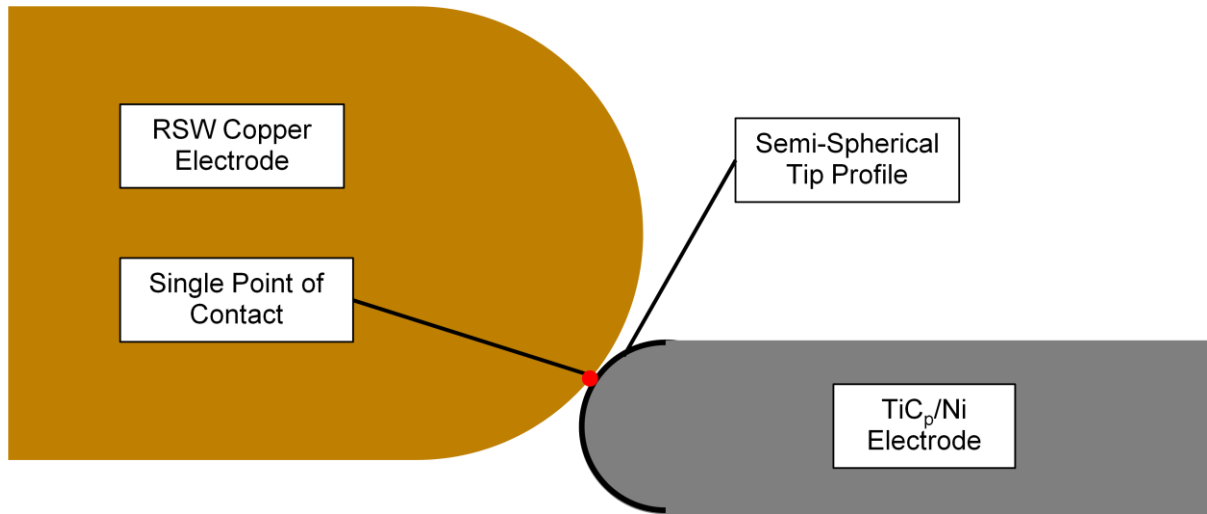
54

Figure 5.8: Single Point of Contact after Wearing of the TiC$_p$/Ni Electrode with the Actively Controlled Rotating and Reciprocating Setup

Since the TiC$_p$/Ni electrode wearing issue was resolved with the rotating mechanism, further study of the electrical characteristics of the Actively Controlled Rotating and Reciprocating setup were conducted. The process was run at various frequency settings ranging from 1Hz to 16Hz and the rotational speed of the TiC$_p$/Ni electrode was set at 40RPM. The duty cycle was initially set to 50%. An example of the resulting waveforms can be seen in Figure 5.9. The first and most obvious observation made was that the voltage level of the capacitors was inconsistent, ranging from 35V to 55V. This inconsistency was attributed to the older simple power supply which was used for this process. Figure 5.10 shows a closer look at a single deposition pulse from the process and it can be seen that the generated waveform has a very similar resemblance to the waveforms recorded by S. K. Tang [5] in his ESD single deposition study as shown in Figure 5.11. Two current peaks are observed for a single deposition, with the first peak being the greater of the two. The voltage of the capacitors drops to ~15V during the first current peak and subsequently drops to 0V during the second current peak. The total duration of the discharge process is also very similar to what is seen in Figure 5.11 at ~0.0006s. This indicates that deposition is occurring during the process as expected.
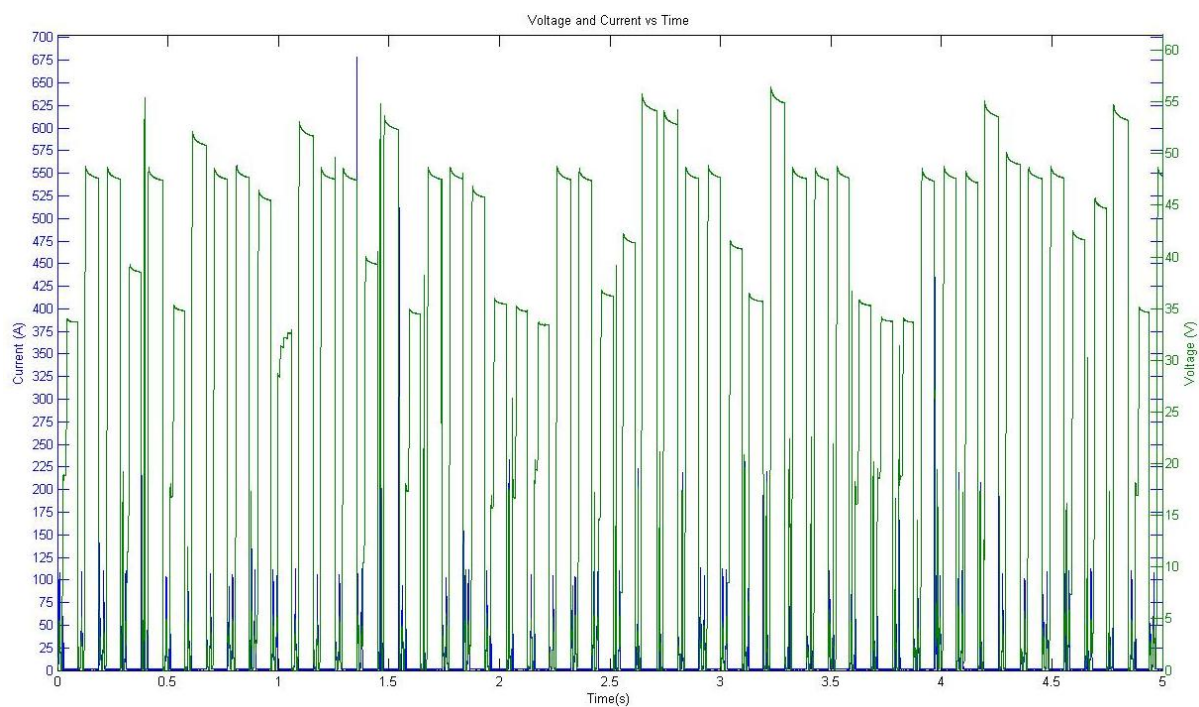
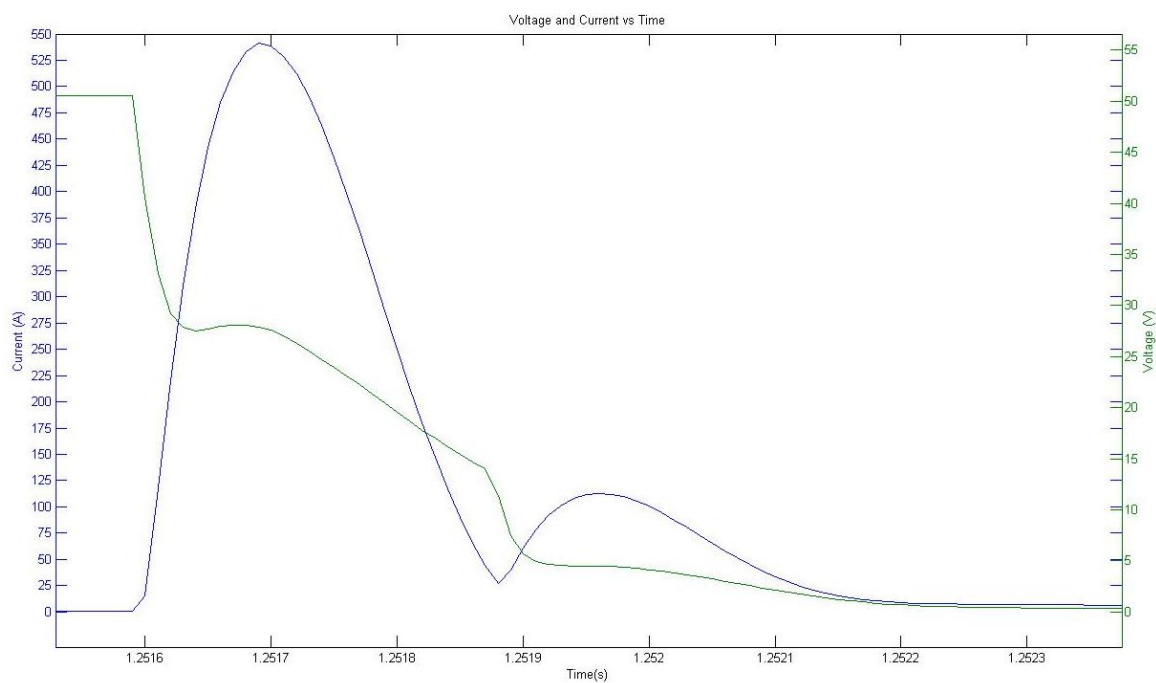**Figure 5.9: Electrical Waveform of Actively Controlled Rotating and Reciprocating setup at 10Hz**

Figure 5.10: Single Deposition of Actively Controlled Rotating and Reciprocating Setup
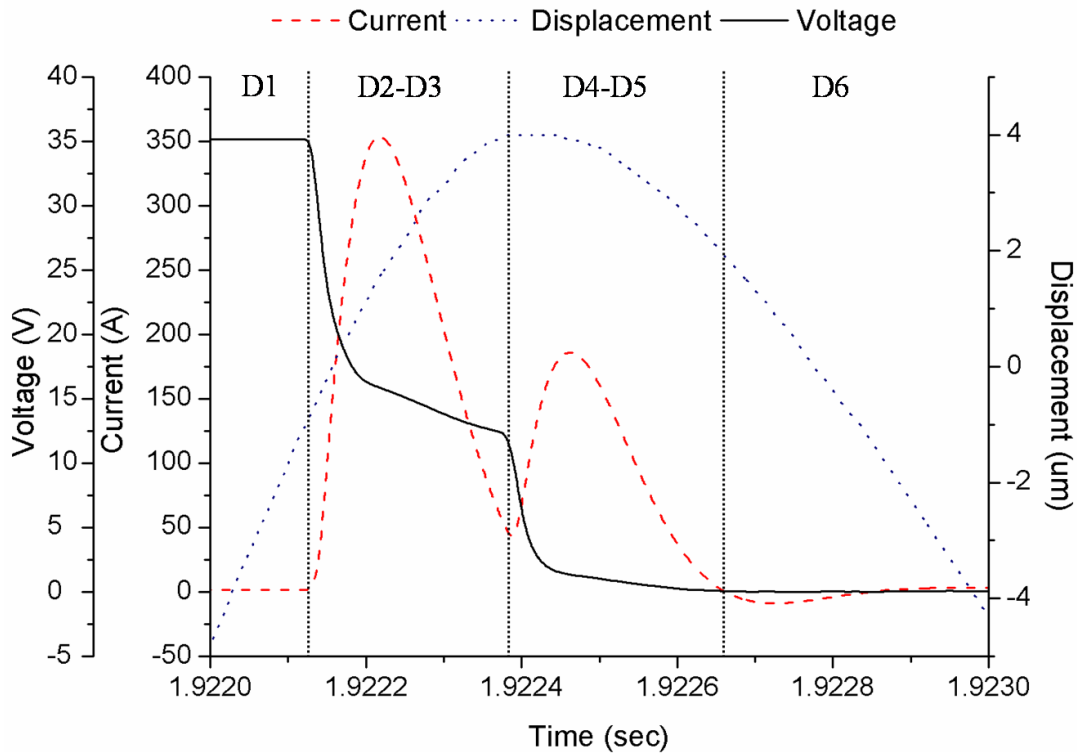
Figure 5.11: Current, Voltage, and Displacement Waveform of ESD Single Deposition in Dynamic Mode [5]

Aside from the single deposition waveform seen in Figure 5.10 another effect of the mechanism was observed between individual depositions. After a single deposition completed two more simultaneous current and voltage peaks were observed. An example of this can be seen in Figure 5.12. It can be seen from this graph that one deposition occurs at approximately 0.77s followed by two smaller peaks occur between 0.77s and 0.8s, a difference of 0.3s. The next deposition occurs at 0.87s indicating a frequency of 10Hz. Since the charging frequency of the power supply is 60Hz a single charge cycle takes ~0.017s and two charge cycles take just under 0.035s. Therefore it can be concluded that the two small peaks are actually two charge cycle of the power supply. It can also be concluded that the reason the capacitors do not fully charge is because the TiC_p/Ni electrode remains short circuited with the RSW Copper electrode after the deposition, thus causing the current to discharge from the capacitors immediately. This result is considered to have a negative impact on the coating process for three main reasons. The first problem is that the extra

current peaks last much longer than the individual deposition discharges and increase the overall duty cycle of the coating process. This will ultimately result in added heat input to the process and will eliminate one of the main advantages of the ESD process: low heat input. The second problem with this result is that it reduces the efficiency of the process since the energy is wasted in these short circuits without any deposition during this time. The third problem is that the coatings which are applied during previous deposition pulses are subject to being torn away from the grinding force generated between the TiC_p/Ni electrode and the RSW Copper electrode if they remain in continuous contact for long durations of time as observed here.
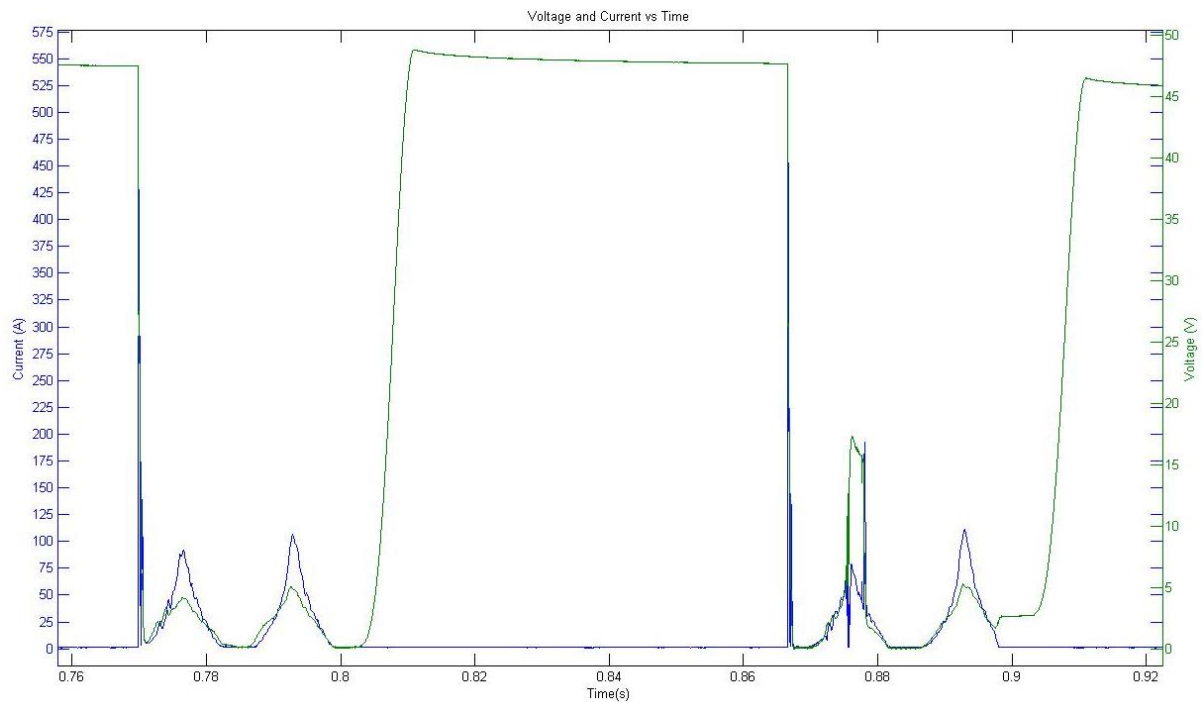
Figure 5.12: Electrical Waveform Between Individual Depositions at 10Hz, 50% Duty Cycle

A solution to the aforementioned problem was easily found by reducing the duty cycle of the reciprocating mechanism. It was desired that the TiC_p/Ni electrode pull back within the 0.017s required for one charge cycle of the power supply so that the contact duration does not exceed the time of one charge cycle. To accomplish this for a frequency of 10Hz, the duty cycle of reciprocation must be below 25%. The mechanism was set to a duty cycle of

25% and the resulting graph can be seen in Figure 5.13. It can be seen that the smaller current and voltage peaks which were observed with the 50% duty cycle have been eliminated. The main conclusion to be drawn from this portion of the study is that the contact duration of the ESD process must remain below the charge duration of a single charge cycle of the power supply in order to ensure maximum system efficiency and to reduce the risk of surface grinding damage during the process.
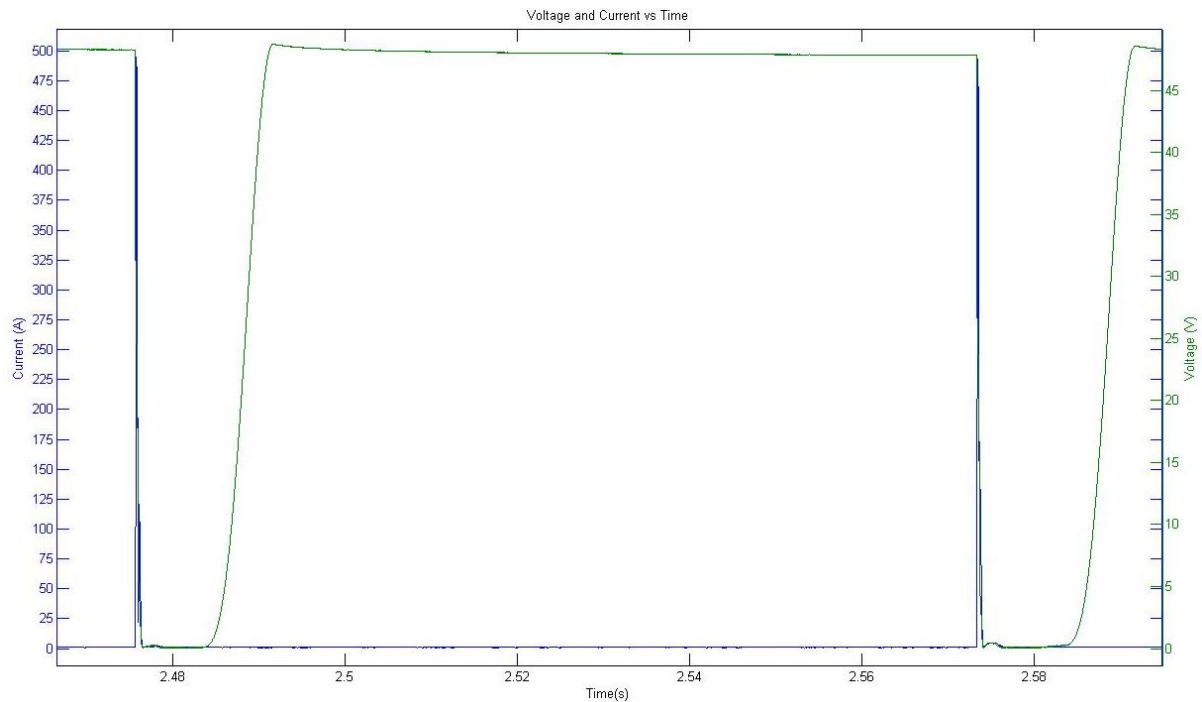
Figure 5.13: Electrical Waveform Between Individual Depositions at 10Hz, 25% Duty Cycle

It was mentioned earlier that the simple power supply generated inconsistent voltage levels. This is an undesired effect when attempting to automate the ESD process since it makes the electrical characteristics of the process unpredictable. Such fluctuations can cause the coating characteristics to change from one coating to the next making it difficult to adjust process parameters to guarantee successful coatings. The new advanced variable power supply was used to eliminate this issue since it has voltage control circuitry. The effects of the new power supply can be seen in Figure 5.14 and it is clear that the new power supply maintains a

set charge level for the capacitors. This makes the process more predictable and simplifies the automation process.
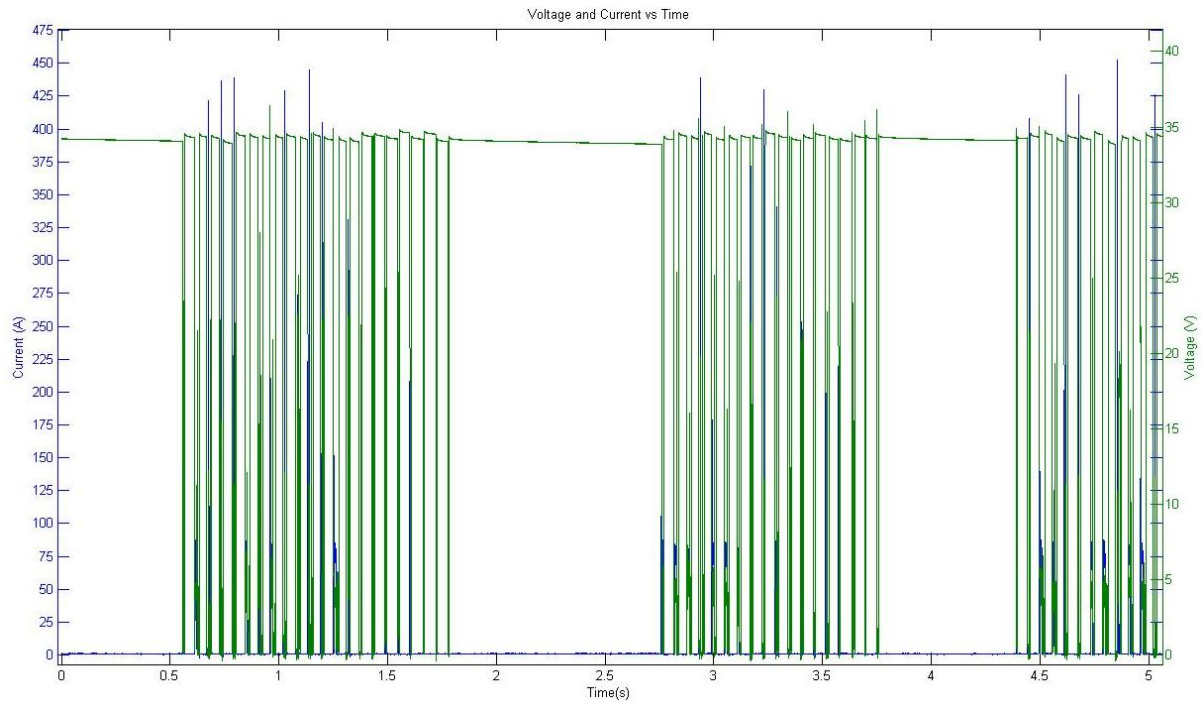
Figure 5.14: Electrical Waveform of Actively Controlled Rotating and Reciprocating setup at 10Hz with New Power Supply

Force measurements of the Actively Controlled Rotating and Reciprocating mechanism were also taken to compare with the measurements taken by the manual operators at Huys Industries Ltd. The setup for the tests can be seen in Figure 5.15. The FSR was stuck on top of a flat RSW Copper electrode which was fitted in the lathe chuck. The Actively Controlled Rotating and Reciprocating mechanism was brought in front of the FSR and was run with varying frequencies and force inputs. An example of the measured force with settings of 16Hz, 50% Duty Cycle, and 75% Force can be seen in Figure 5.16. The minimum controllable force setting was 75% due to limitations of the design. Other tests with different settings all produced higher average outputs than can be seen in Figure 5.16 and this test produced the lowest observable force with this mechanism. Figure 5.17 also shows the time duration between individual contacts as well as a close-up of the contact spikes. It can be

60

noted that the time between contacts is approximately 0.06s and the process maintains a very low contact duty cycle which is key element of the ESD process. The tests show that the Actively Controlled Rotating and Reciprocating mechanism produces much larger forced than the manual operators. The average output of this setup is observed to be between 3.5V and 4V. Based on the graph shown in Figure 4.9 this corresponds to forces greater than 40N, nearly 10 times larger than the force observed by the manual operators. As a result of this excessive force it was noted that the wearing of the TiC_p/Ni electrode was different than that what was expected. The TiC_p/Ni showed signs of Copper accumulation on the surface as well as signs of material being pushed outwardly around the edge of the TiC_p/Ni electrode. An example of this can be seen in Figure 5.18. This is an indication that the forces generated by the Actively Controlled Rotating and Reciprocating mechanism are far too great for the process. In order to ensure that the TiC_p/Ni electrode is not damaged during the coating process the force generated by the automated mechanism must be significantly reduced.
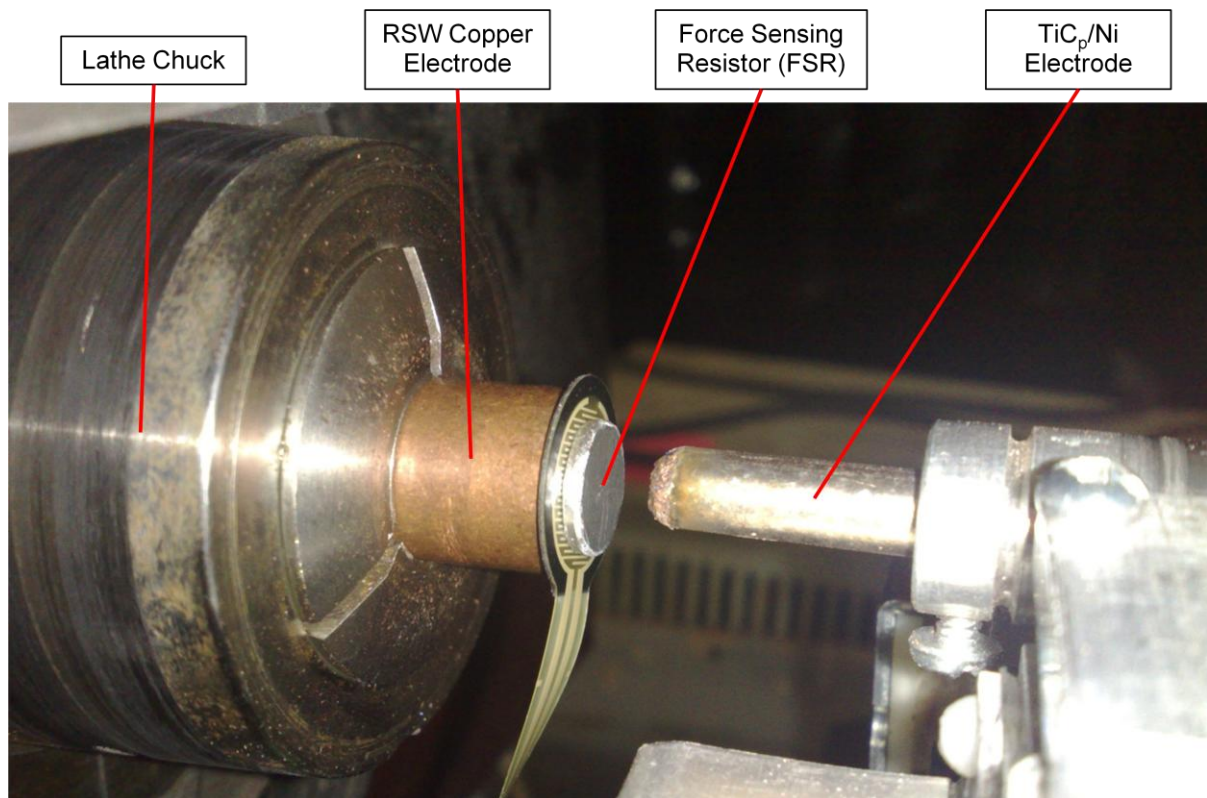

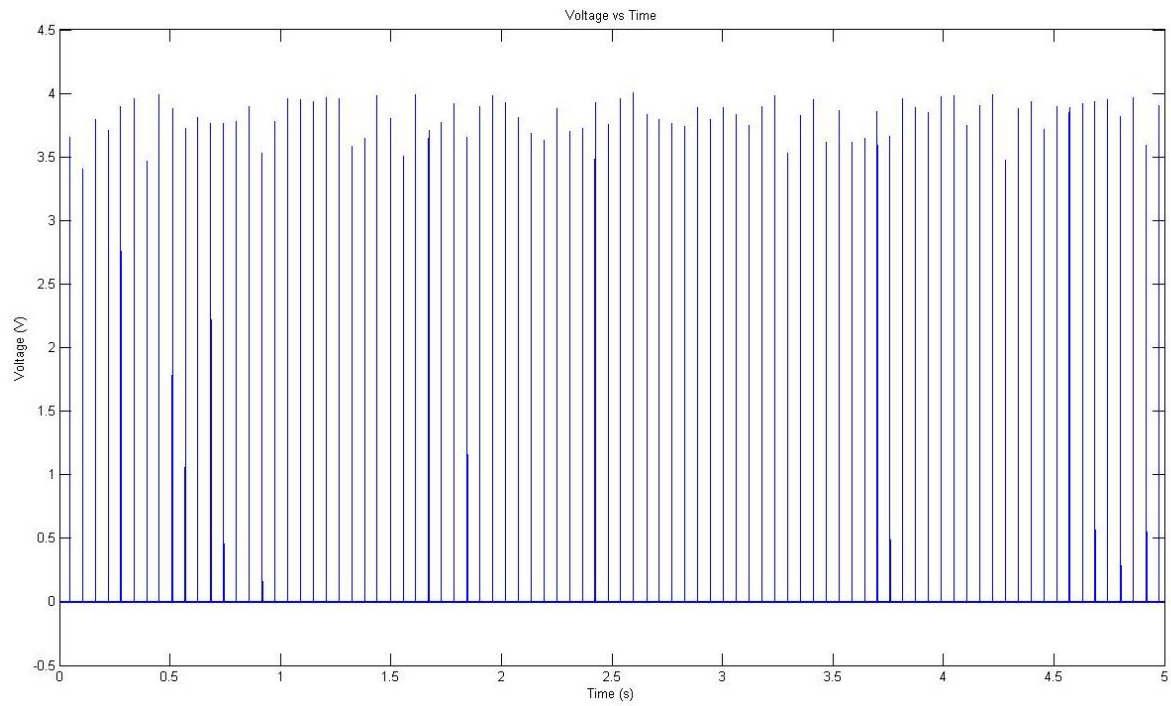**Figure 5.15: Test Setup for Force Measurements of Automated Setup**

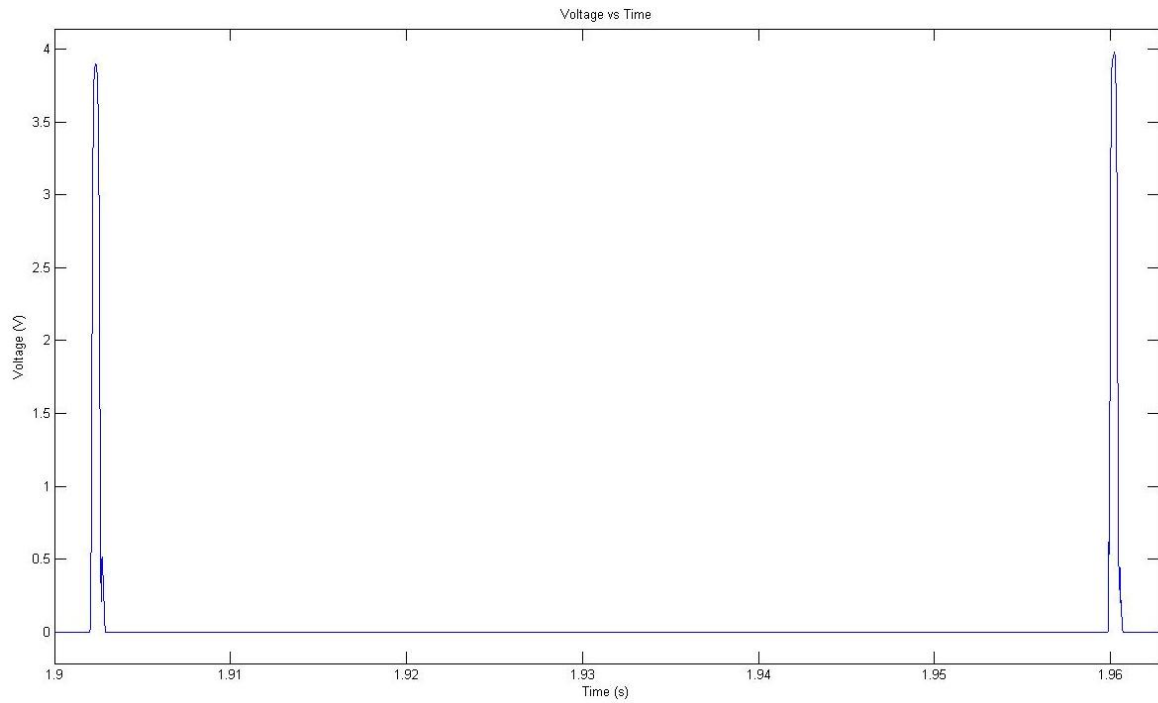**Figure 5.16: Force Measurement at 16Hz, 50% Duty Cycle, 75% Force**

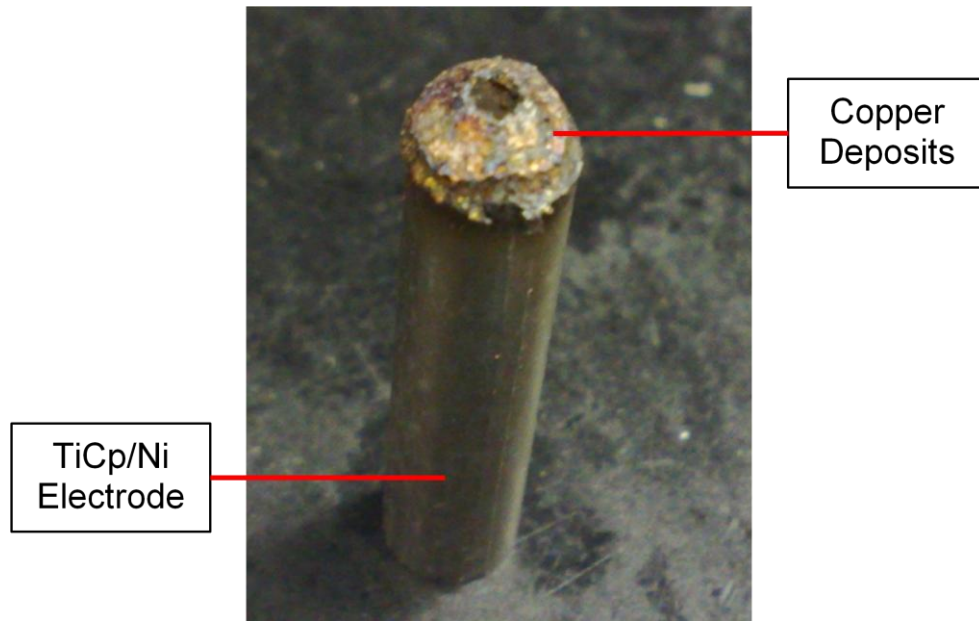**Figure 5.17: Time Duration Between Multiple Contacts**

Figure 5.18: Copper Accumulation and Material Pushing on TiC$_p$/Ni Electrode

Some results from the coatings produced by the Actively Controlled Rotating and Reciprocating setup can be seen in Figure 5.19. It was observed that the very little TiC$_p$/Ni deposition occurred during the process with small spots of TiC$_p$/Ni sparingly applied over the surface of the RSW Copper electrodes. Furthermore it was noted that the RSW Copper electrodes were left with very rough surfaces where the coating should have been applied. This result is further indication that the force generated by the Actively Controlled Rotating and Reciprocating was too large and was physically damaging the surface of the RSW Copper electrodes along with the surface of the TiC$_p$/Ni electrode. As the TiC$_p$/Ni electrode was struck against the surface of the RSW Copper electrode the melted portion of the TiC$_p$/Ni electrode was being pushed out of the melt pool entirely and leaving a crater in the contact area without any deposition. This also explains why copper deposits were noticed on the TiC$_p$/Ni electrodes from this setup. The soft surface of the RSW Copper electrode was being forced onto the harder TiC$_p$/Ni electrode as a result of the physical damage caused by this process. Also, any deposition which may have successfully been applied during the process was being torn away in successive contacts rendering the overall process useless.

Figure 5.19: Coating Results of Actively Controlled Rotating and Reciprocating Setup

The Actively Controlled Rotating and Reciprocating mechanism was able to eliminate the uneven TiC_p/Ni electrode wearing problem of the Manual-Automated Hybrid setup with the use of a rotating mechanism and was able to generate an even and predictable wearing pattern. However, due to the generation of large forces by this mechanism, the RSW Copper electrodes could not be coated with TiC_p/Ni. The large forces caused both the TiC_p/Ni electrode and the RSW Copper electrodes to be damaged during the process and a softer mechanism is required to overcome this issue.

5.3 Actively Controlled Rotating and Vibrating Setup Results

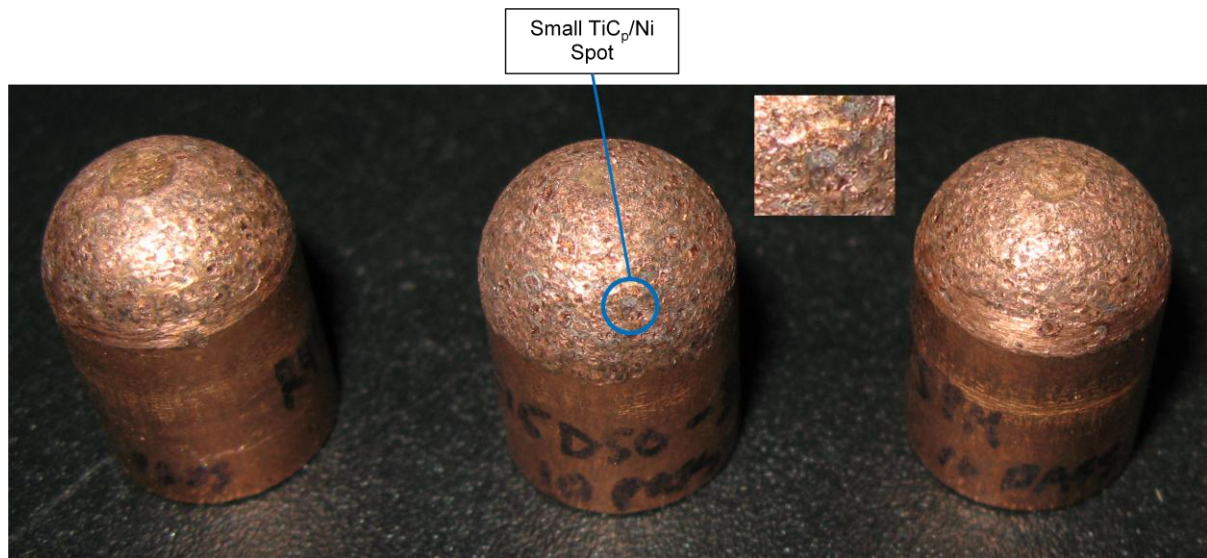Since the rotating mechanism in the Actively Controlled Rotating and Reciprocating setup produced successful results for even and predictable wearing of the TiC_p/Ni electrode it was reused for the Actively Controlled Rotating and Vibrating setup. The Actively Controlled Rotating and Reciprocating mechanism was modified by replacing the solenoid reciprocating mechanism with a vibrating mechanism as described in section 3.2.4. The main problem with the Actively Controlled Rotating and Reciprocating setup was that the contact force was too large and was causing both the TiC_p/Ni electrode and the RSW Copper electrode to be damaged during the process. By replacing the reciprocating mechanism with a vibrating the contact force was significantly reduced as can be seen from the test results in Figure 5.20 and Figure 5.21. Different tests were conducted at varying forward biases with the output varying between 2V and 2.5V, and generally averaging around 2.5V. This corresponds to a force of about 10N based on the graph in Figure 4.9, much closer to the results observed by the manual operators.
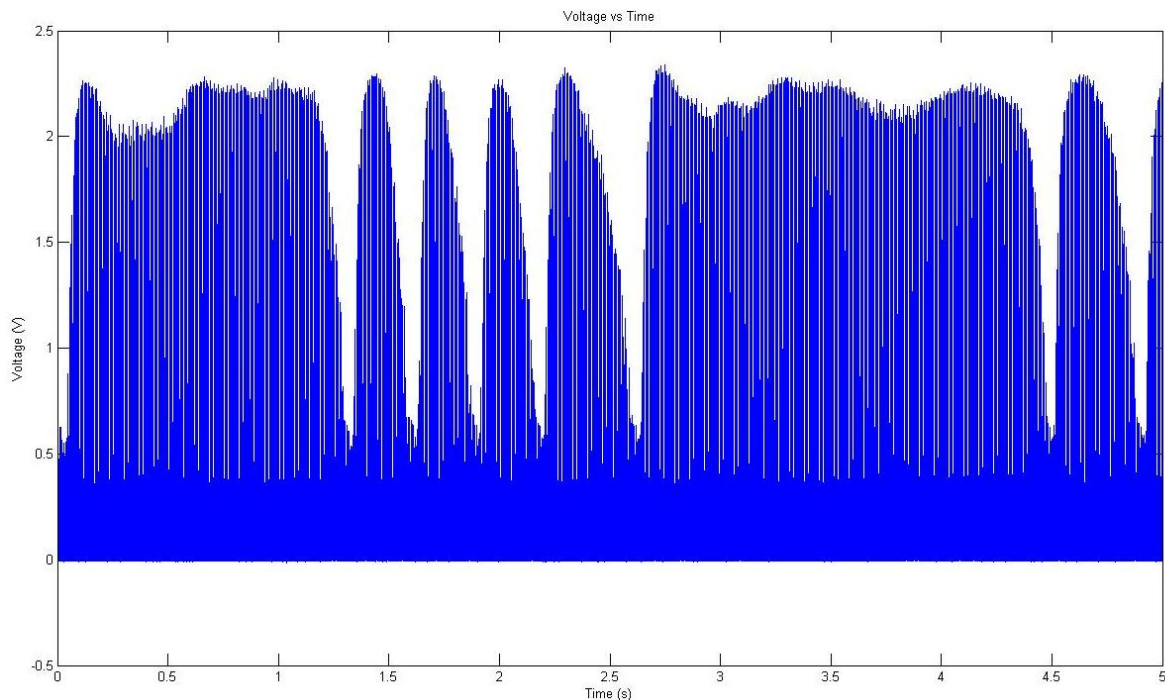

Figure 5.20: Force Measurement at ~200Hz, 20 thou Forward Bias
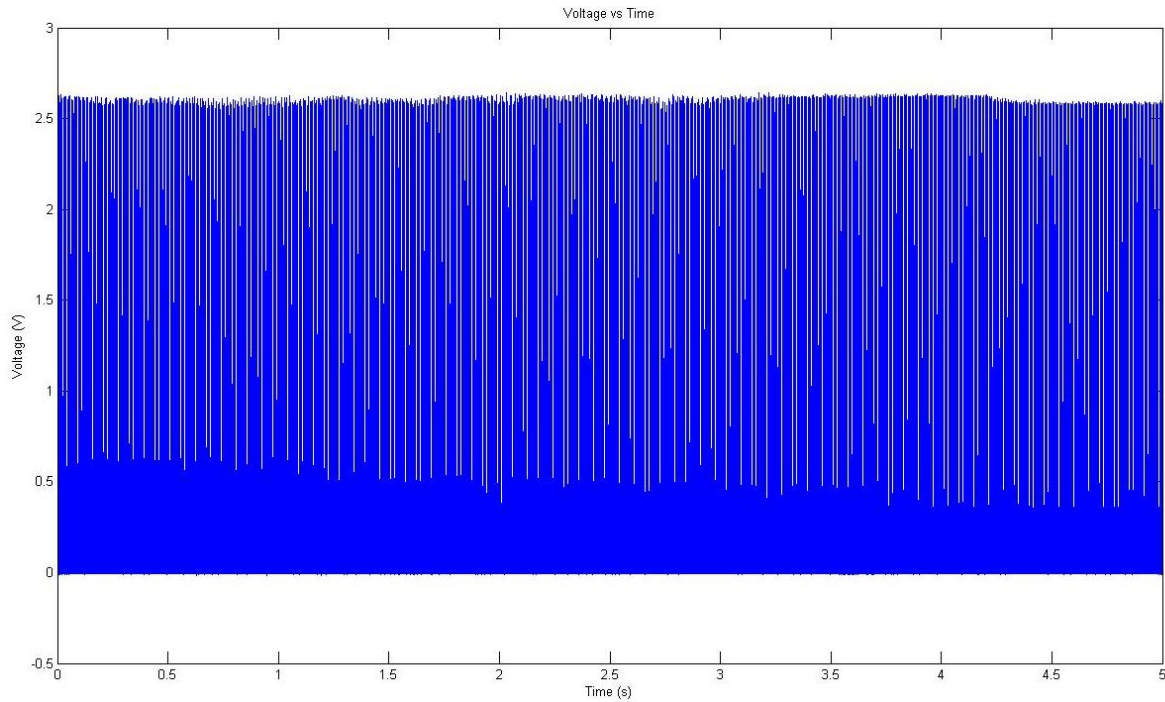
Figure 5.21: Force Measurement at ~200Hz, 50 thou Forward Bias

Close-ups of the force measurements can be seen in Figure 5.22 and Figure 5.23 and they show that the process is very consistent and produces the same force repeatedly for a given forward bias. It can also be seen that small forces are generated on either side of the main contact peak. This outcome is not representative of the process or the result of process parameters but rather a consequence of the physical design of the mechanism. Due to the simple nature of the mechanism the vibrations are not perfectly clean and experience mechanical resistance which generate these smaller forces around the main contact peaks. It is also notable that the contact duration is ~0.001s which is much smaller than the 0.008s charge cycle of the new power supply, based on a 60 Hz full wave rectifier. This ensures that the TiC_p/Ni electrode does not remain in contact with the RSW Copper electrode between charges of the power supply as was observed with the Actively Controlled Rotating and Reciprocating setup.
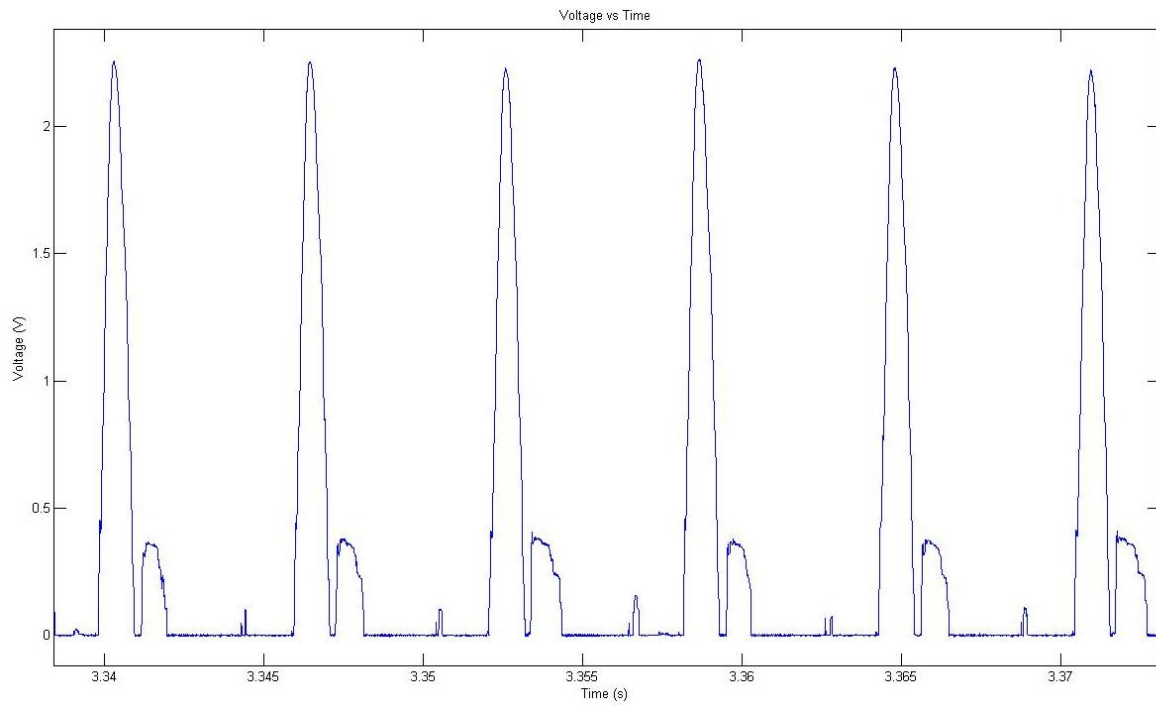
Figure 5.22: Close-up of Force Measurement at ~200Hz, 20 thou Forward Bias
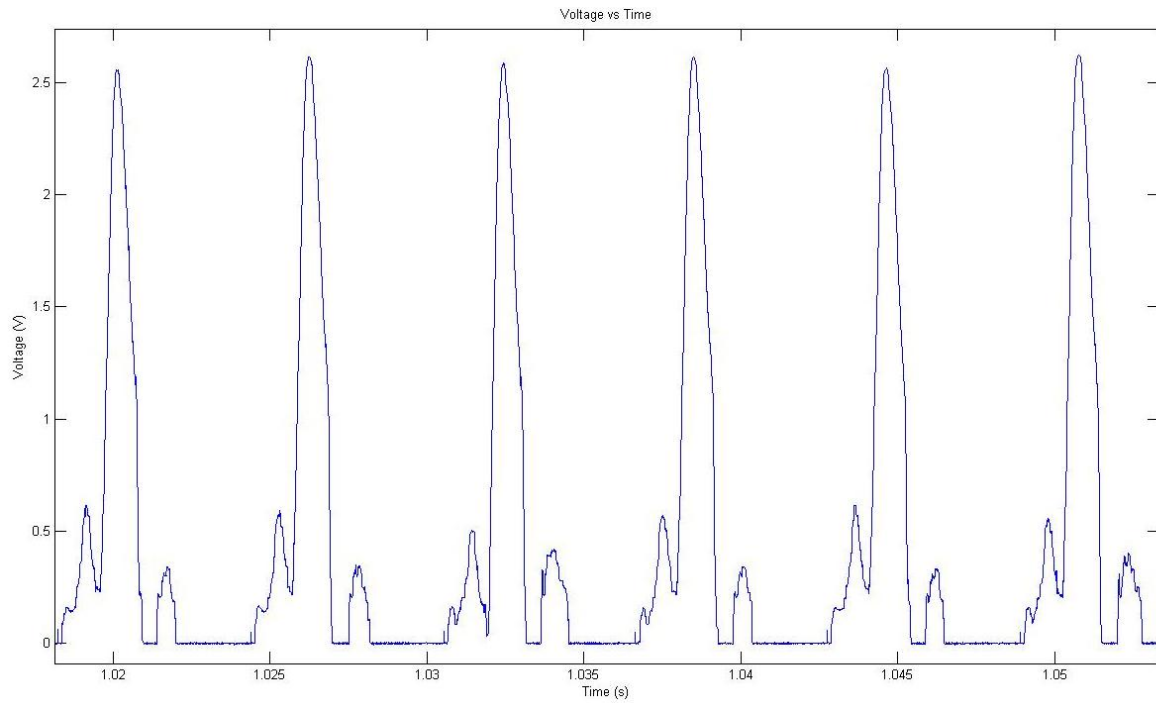
Figure 5.23: Close-up of Force Measurement at ~200Hz, 50 thou Forward Bias

67

The reduction of the contact force also aided in better wearing of the TiC_p/Ni electrode during the process as can be seen in Figure 5.24. The copper deposits which were previously observed on the TiC_p/Ni electrode were significantly reduced with the Actively Controlled Rotating and Vibrating setup to the point where it was nearly eliminated. Furthermore the material spreading which was seen with the Actively Controlled Rotating and Reciprocating setup was no longer observed and the TiC_p/Ni wearing was not only even and predictable but also clean and uniform. This supports the conclusion made previously which stated that excessive contact force during the ESD process causes damage to the TiC_p/Ni electrode and the RSW Copper electrode.

Figure 5.24: TiC_p/Ni Electrode Wear with Actively Controlled Rotating and Vibrating Setup

The power supply which was used for the Actively Controlled Rotating and Vibrating setup was the new advanced variable power supply. It can be seen in Figure 5.25 that the charge voltage is generally steady and consistent at 35V. This is despite the fact the vibrational frequency of the Actively Controlled Rotating and Vibrating mechanism is much faster than the charge cycle of the power supply which means that the TiC_p/Ni electrode will come in contact with the RSW Copper electrode multiple times between charges. Therefore the power supply has indeed aided the process by ensuring that discharges only occur after the capacitors have been charged to the desired voltage. The current can be seen to fluctuate a great deal which is inconsistent with what is expected. Such a variation would be seen if the resistance of the system were fluctuating, however the electrical system is fixed and there is no variability in the system's resistance. Another factor which could contribute to a change in the resistance would be the contact force between the TiC_p/Ni electrode and the RSW Copper electrode. Different contact forces would either increase or decrease the surface area of the contact point thereby changing the resistance. The forces generated by the mechanism have been shown to be consistent throughout the process so it seems that this possibility would be ruled out as well. However, one factor has not been considered yet. The force measurements were taken on a flat surface with 100% of the force acting normally to the surface, but the force exerted by the TiC_p/Ni electrode on the RSW Copper electrode during the process has both a normal and a lateral component to it as depicted in Figure 5.26. The normal force of the mechanism is generated by a combination of the spring loaded mechanism and the vibrational motion of the TiC_p/Ni electrode and was measured in the force test setup. The lateral motion of the TiC_p/Ni electrode is controlled with the lathe and does not have any compliance which makes it rigid and susceptible to large forces. This added force may increase the overall contact force of the system as well as vary the force between individual depositions. Due to the mechanical setup of this system it was not possible to take lateral force measurements.
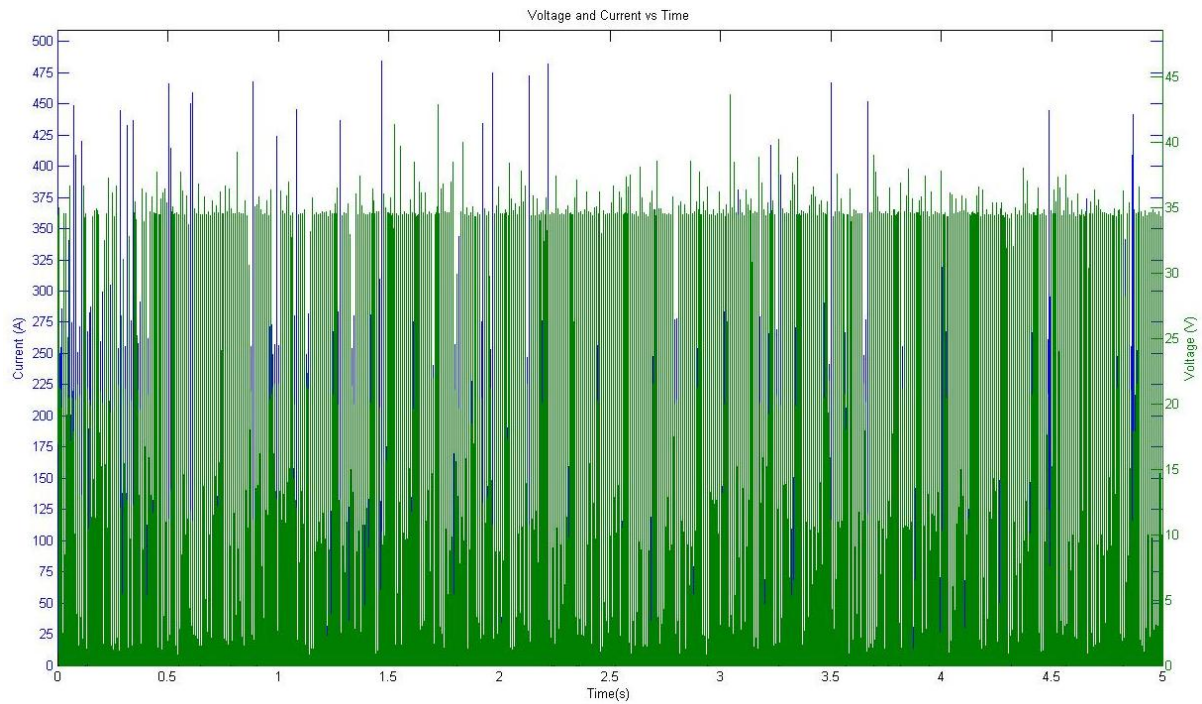
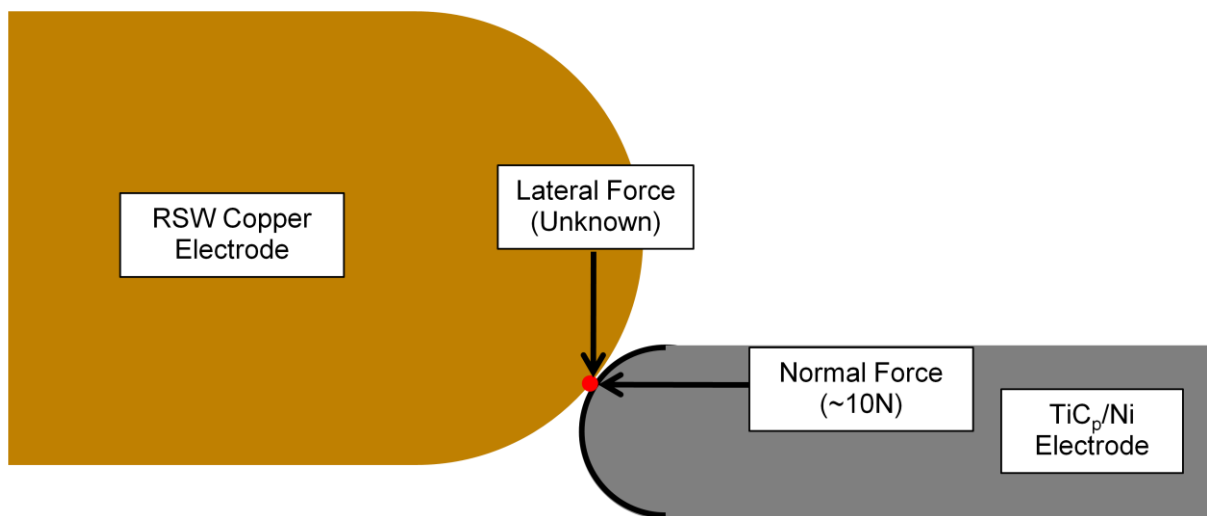**Figure 5.25: Electrical Waveform of Actively Controlled Rotating and Vibrating setup at ~150Hz**

Figure 5.26: Normal and Lateral Forces

A close-up of the electrical waveform shows that the power supply charges at 120Hz and only permits discharges after the capacitors have charged up to 35V. It can also be noted that the current waveform is as expected with double peaks.
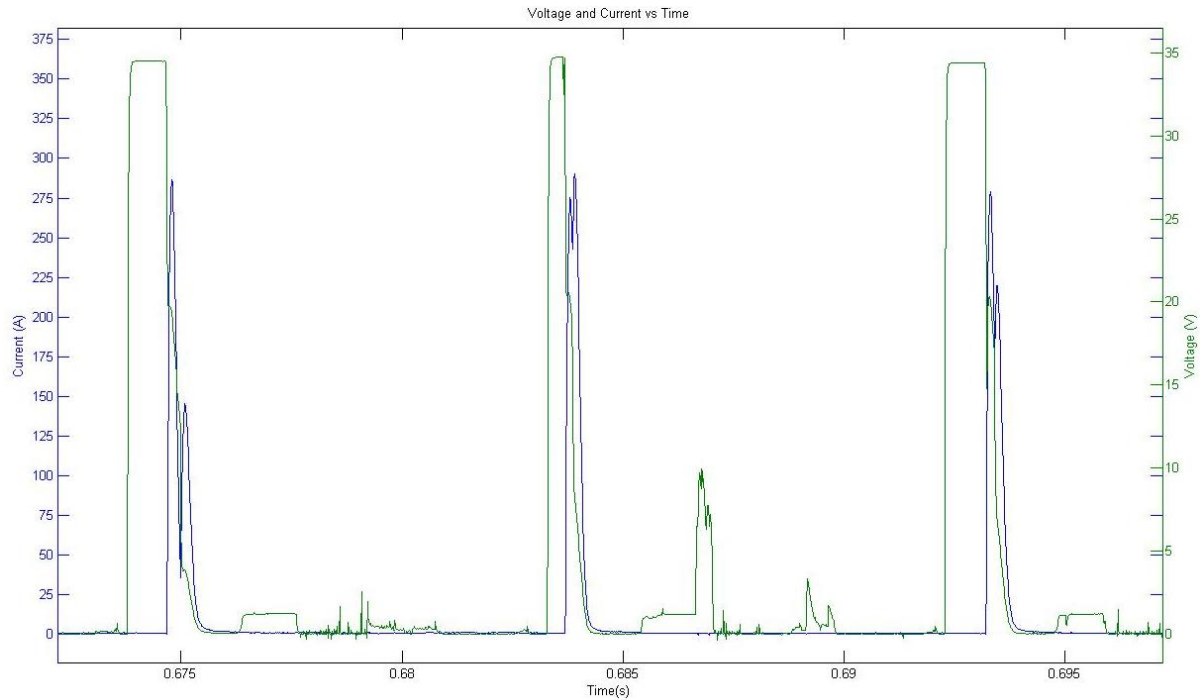
Figure 5.27: Electrical Waveform Between Individual Depositions at ~150Hz

A simple static test was first conducted with the TiC$_p$/Ni fixed in one position to coat a ring around the RSW Copper electrode. The result of the test showed that a layer of TiC$_p$/Ni was applied to the RSW Copper electrode as desired; however black rings were produced along the edge of the TiC$_p$/Ni coating. This effect can be seen in Figure 5.28. These black rings are believed to be the result of burning impurities on the surface of the TiC$_p$/Ni electrode or the RSW Copper electrode which since special surface preparations are not made before coating. The black rings are believed to exist on the outer edge because the impurities are pushed outwardly as the TiC$_p$/Ni electrode strikes the surface of the RSW Copper electrode. Although this effect is undesired it was assumed that when the full G-Code would be run then the black rings would be removed by the process as the TiC$_p$/Ni continued to coat the RSW Copper electrode.
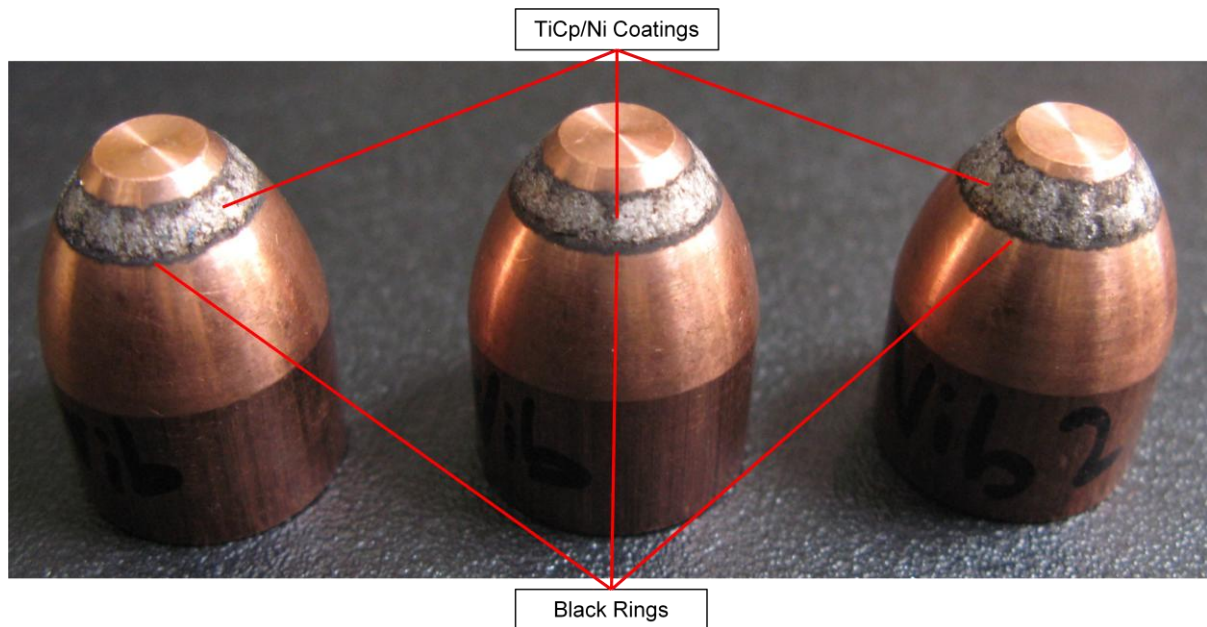
Figure 5.28: Black Rings Around Edge of TiC$_p$/Ni Coatings

The full G-Code was then run between 1 and 5 IPM to test the coating process and some of the results can be seen in Figure 5.29. It can be seen that the TiC$_p$/Ni coating has covered the top surface of the RSW Copper electrode as desired but the black rings which were observed in Figure 5.28 appear to have become uniformly distributed along with the TiC$_p$/Ni coating. This is believed to have occurred because the black rings were produced continuously as the TiC$_p$/Ni electrode passed along the surface of the RSW Copper electrode. As the TiC$_p$/Ni electrode moved from one position to the next the TiC$_p$/Ni coating which was created in the previous position was covered with the black impurities in the current position. Once the TiC$_p$/Ni electrode completed coating the RSW Copper electrode the surface was left with a combination of the TiC$_p$/Ni coating and the black impurities. This resulted in an unclean, impure, inconsistent, and partially rough coating surface.

72

Figure 5.29: Black Deposit Throughout TiC$_p$/Ni Coatings with G-Code Between 1 and 5 IPM

Since the impurities seen in Figure 5.28 were observed to exist as rings on the outer edge of the coatings as a result of being pushed outwardly it was hypothesized that by moving the TiC$_p$/Ni electrode across the RSW surface faster the impurities would be pushed away from the RSW surface before they could settle. By doing this it was also believed that the TiC$_p$/Ni coating would have more time to cool and solidify in any one position thereby creating a stronger coating. The G-Code was run again at 15 IPM. It was necessary to run the G-Code multiple times to produce full coverage of the RSW Copper electrode surface since running the G-Code at this speed left too many gaps. The tests were run with 5, 10, 15, 20, and 25 passes and the results can be seen in Figure 5.30 with the number of passes increasing from left to right. As can be seen from the results 5 passes left many gaps between individual depositions and resulted in an incomplete coating. Increasing the number of passes increased the deposition density and at 25 passes full coverage of the RSW Copper electrode was accomplished. It is also evident that the impurities have been significantly reduced by increasing the travel speed of the TiC$_p$/Ni electrode and it appears that the aforementioned hypothesis was correct. If a thicker and denser coating is desired then the number of passes may be increased.

Figure 5.30: Final Coating Results with G-Code at 15 IPM

The Actively Controlled Rotating and Vibrating mechanism has reduced the contact force between the TiC_p/Ni electrode and the RSW Copper electrode and has eliminated the copper deposits which were observed on the TiC_p/Ni electrode with the use of the Actively Controlled Rotating and Reciprocating mechanism. The wearing of the TiC_p/Ni electrode is also more consistent and smoother without the damage which was caused by larger forces. Lastly, by running the G-Code at a much higher travel rate with multiple passes permitted full, smooth, consistent, and impurity free coatings.

Chapter 6
Conclusions

During this study three automation solutions were tested to identify key parameters for the purpose of automating ESD of TiC_p/Ni on RSW Copper electrode. The first solution to be attempted was a Manual-Automated Hybrid setup which used an existing TiC_p/Ni applicator on a CNC lathe. The manual applicator provided vibration of the TiC_p/Ni electrode while the CNC lathe provided motion of the TiC_p/Ni electrode in the X and Z axes. It was found that this setup was able to produce TiC_p/Ni coatings on the RSW Copper electrodes but only while the TiC_p/Ni electrode was new and unconsumed. The TiC_p/Ni electrode wore unevenly with this setup and this caused the process to change from one coating to the next, degrading the quality of the applied coatings over time resulting in incomplete coatings with many gaps of uncoated areas on the RSW Copper electrode. This problem rendered the setup useless and necessitated a mechanism which would ensure even wearing of the TiC_p/Ni electrode.

The second solution was to develop a novel mechanism, the Actively Controlled Rotating and Reciprocating mechanism, which would replace the vibration of the manual applicator with a reciprocating mechanism and add the ability to rotate the TiC_p/Ni electrode simultaneously while using the CNC lathe for positioning. The use of a rotating mechanism for the TiC_p/Ni electrode solved the uneven wearing problem observed with the Manual-Automated Hybrid setup. The TiC_p/Ni electrode wore with a semi-spherical pattern which was uniform and predictable which makes the process less dynamic and simplifies the automation process. This leads to the conclusion that a rotating TiC_p/Ni electrode is necessary for automation to ensure predictable wear patterns which can be accounted for in the programming of the TiC_p/Ni electrode motion.

The use of a simple fixed voltage power supply showed that the charge level of the capacitors varied between individual deposition pulses which added more variability to the process. To increase the consistency of the capacitor charging a new variable voltage power supply was used which ensured that the capacitors were charged to a user set voltage before current discharge was allowed.

Tests from the Actively Controlled Rotating and Reciprocating mechanism showed that at relatively low reciprocation frequencies (10Hz) the deposition pulses would be followed by a number of short circuits. This occurred because the contact duration between the TiC_p/Ni electrode and the RSW Copper electrode was longer than the charge cycle of the power supply. This continuous contact increases the risk of heating the RSW copper electrode to undesired levels due to the high current short circuit. It also causes the TiC_p/Ni electrode to scratch the surface of the RSW Copper electrode and tear away deposited coatings from previous deposition pulses. In order to avoid this problem the contact duration must be shorter than a single charge cycle of the power supply; less than 0.017s for the fixed voltage power supply and less than 0.008s for the variable voltage power supply.

The reciprocating mechanism in the Actively Controlled Rotating and Reciprocating setup was seen to generate excessively large forces (>40N) compared to those observed by manual operators (4-7N). Such large forces cause the TiC_p/Ni electrode and the RSW Copper electrode to be physically damaged. Deposits of copper were transferred onto the TiC_p/Ni electrode and the material on the surface of the TiC_p/Ni electrode was pushed outwardly indicating that proper deposition was not occurring. The excessive force causes the surface of the RSW Copper electrode to become rough and tears away any coatings which may have been applied ultimately leaving an uncoated RSW Copper electrode. The contact force must be reduced significantly to ensure that damage free coatings can be produced with this process.

The third mechanism to be tested was the Actively Controlled Rotating and Vibrating mechanism. The same rotating mechanism that was used in the Actively Controlled Rotating and Reciprocating mechanism was used but the reciprocating mechanism was replaced with a vibrating mechanism. The use of vibrations instead of reciprocation reduced the force considerably and prevented damage to the TiC_p/Ni electrode and the RSW Copper electrode. It was found that forces of 10N or less are needed to ensure damage free coatings.

When using slow travel speeds (<5 IPM) for the TiC_p/Ni electrode the Actively Controlled Rotating and Vibrating mechanism generated black impurities which prevented clean

coatings on the RSW Copper electrode. These impurities can easily be pushed aside before they can settle by using faster travel speeds (>15 IPM), however at such fast travel speeds multiple passes must be made with the TiC_p/Ni electrode to ensure full gapless coatings. A minimum of 25 passes is recommended for complete coverage and more passes may be used if denser and thicker coatings are desired. The resulting coatings with this setup are complete and smooth.

Chapter 7
Recommendations and Future Work

The Actively Controlled Rotating and Vibrating mechanism provided relatively decent results at higher travel speeds with multiple passes but was still partially restricted due to mechanical design issues. As discussed in section 5.3, the lateral force between the TiC_p/Ni electrode and the RSW Copper electrode was unaccounted for and immeasurable with this setup. It is recommended that a test setup be created to measure the lateral force of the mechanism to ensure that it remains within the recommended 10N of force stated in this study. In addition, a dual spring system should be tested with one spring in the normal direction as was used in the current design and another in the lateral direction to add compliance in this direction as well.

Further tests should also be conducted to identify an optimal setting for the travel speed and the number of passes to maximize the process throughput while maintaining acceptable impurity free coatings. The addition of a cleaning mechanism such as a brush may also be considered to remove impurities from the process as the coating is applied.

The vibrational frequency of the Actively Controlled Rotating and Vibrating mechanism (~200Hz) was well above the charge cycle of the new power supply (120Hz). This indicates that the TiC_p/Ni electrode strikes the RSW Copper electrode more frequently than depositions can occur. A study should be conducted to identify the effects of varying vibrational frequencies on the coating quality and characteristics. It is hypothesized that the maximum vibrational frequency required or desired should be less than the charge frequency of the power supply so that ever contact between the TiC_p/Ni electrode and the RSW Copper electrode results in a deposition.

Appendix A
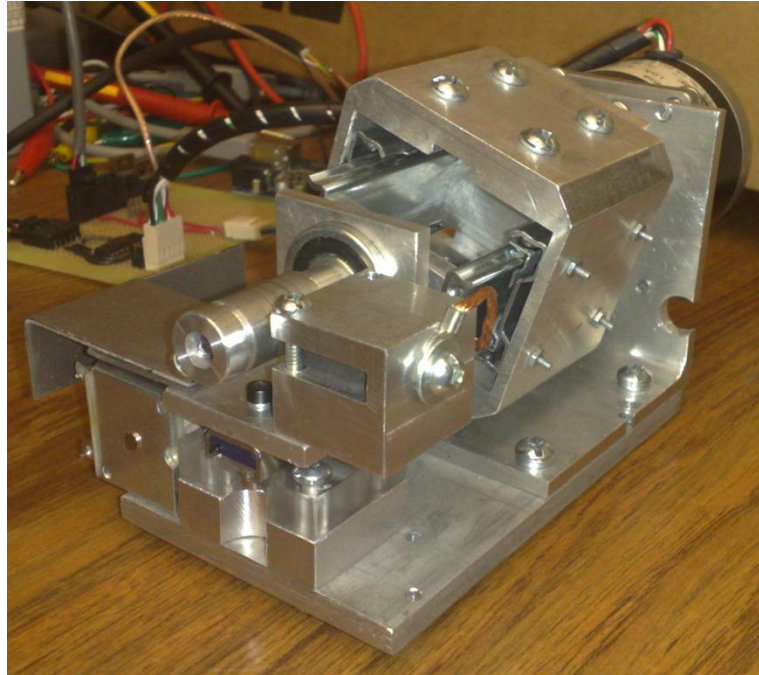## More Pictures of Actively Controlled Rotational and Reciprocating Mechanism

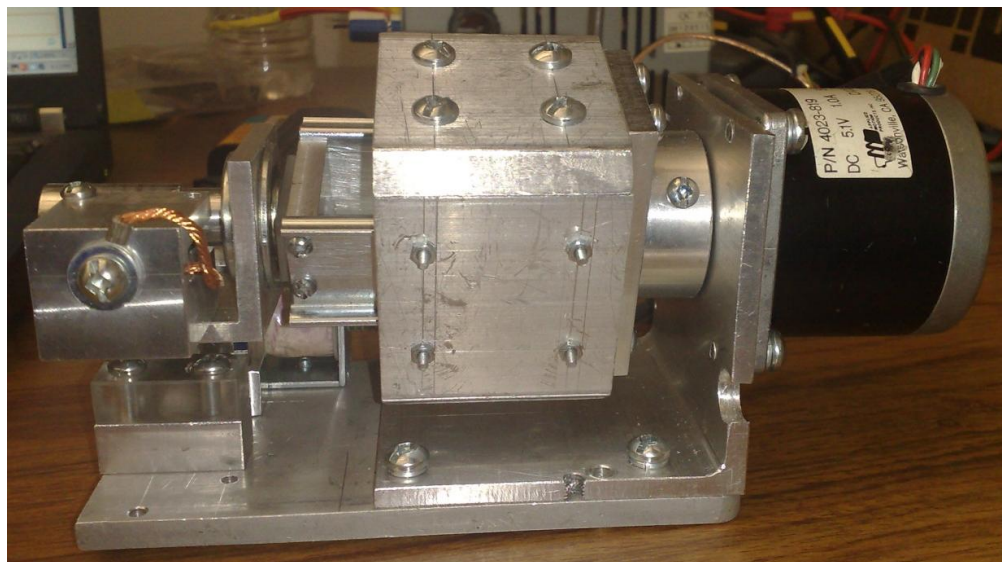**Figure A.1: Isometric View of Actively Controlled Rotating and Reciprocating Mechanism**

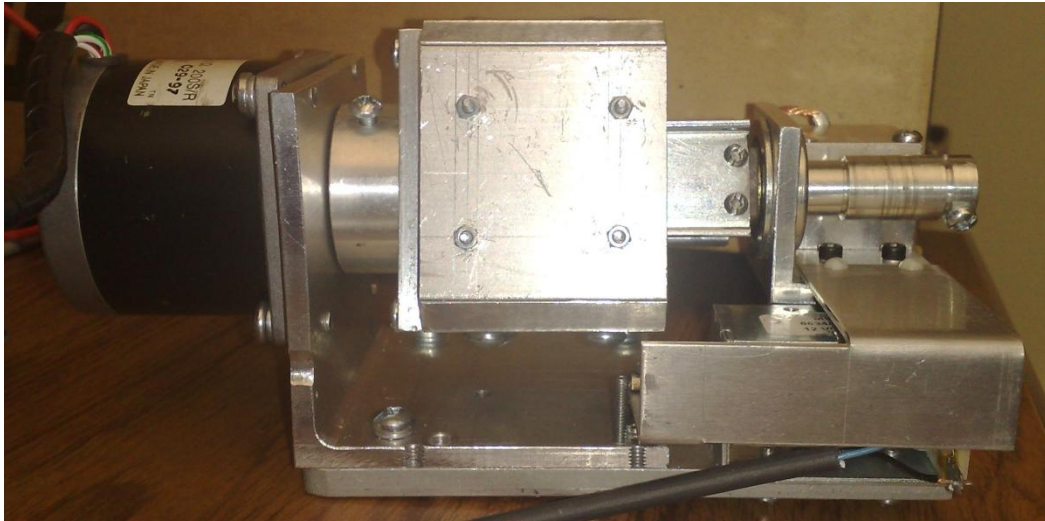**Figure A.2: Left Side View of Actively Controlled Rotating and Reciprocating Mechanism**

Figure A.3: Right Side View of Actively Controlled Rotating and Reciprocating Mechanism
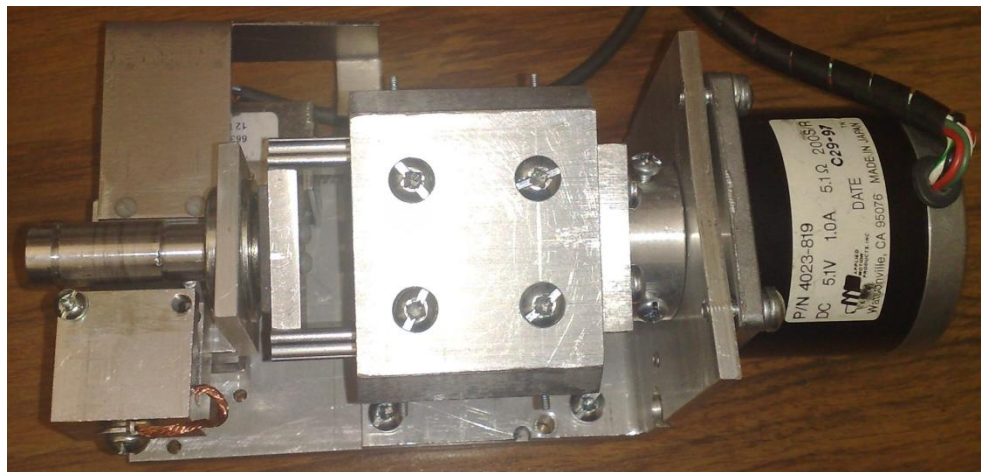

Figure A.4: Top View of Actively Controlled Rotating and Reciprocating Mechanism
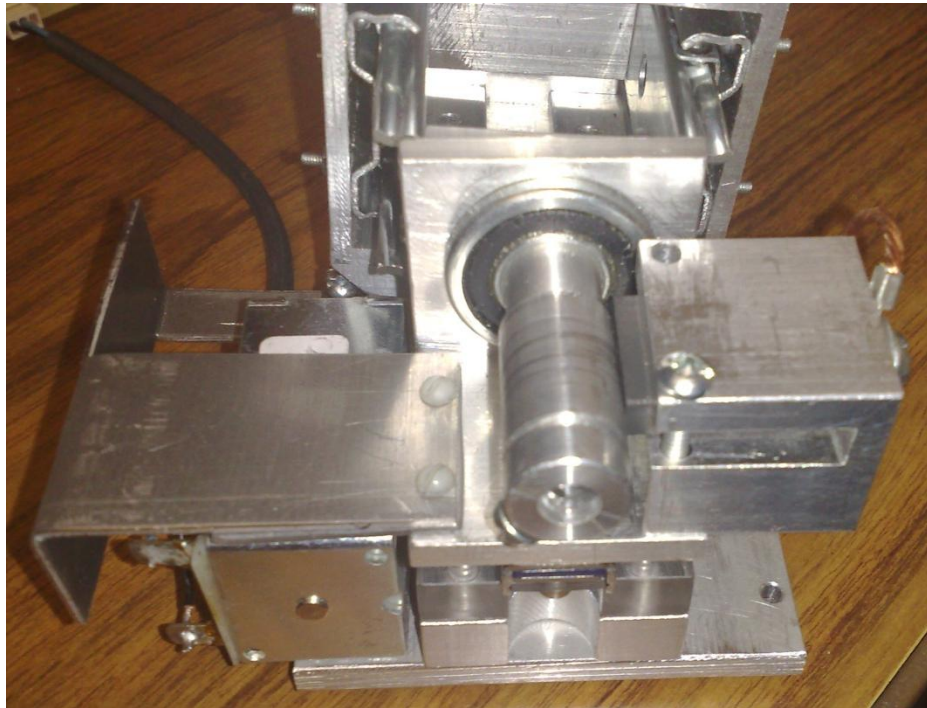
Figure A.5: Front View of Actively Controlled Rotating and Reciprocating Mechanism

Appendix B
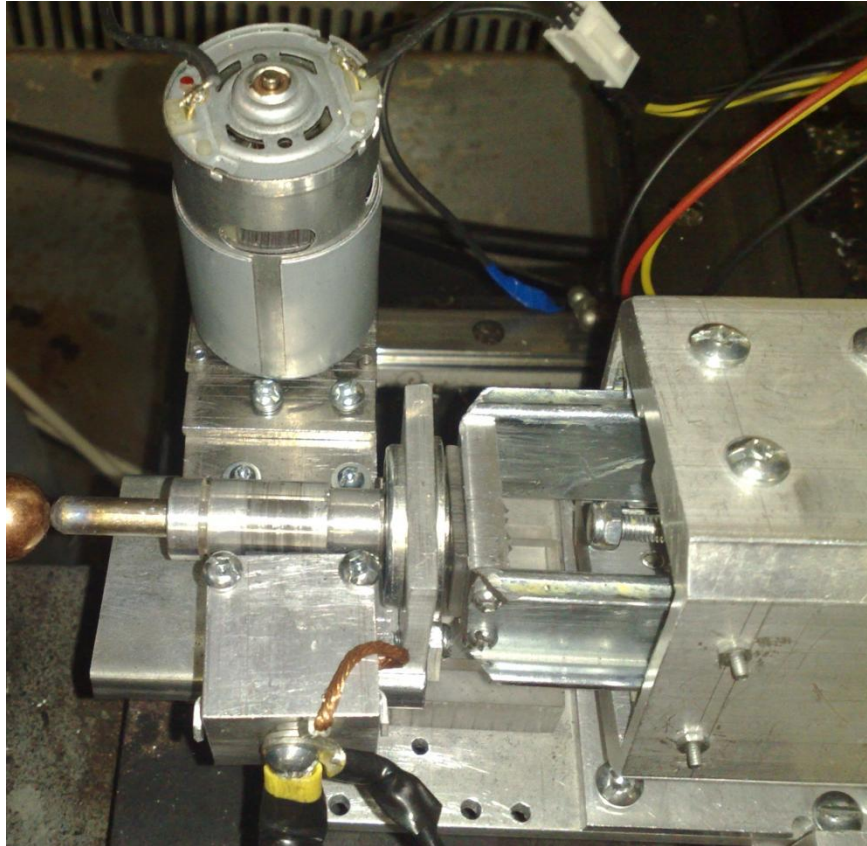# More Pictures of Actively Controlled Rotational and Reciprocating Mechanism

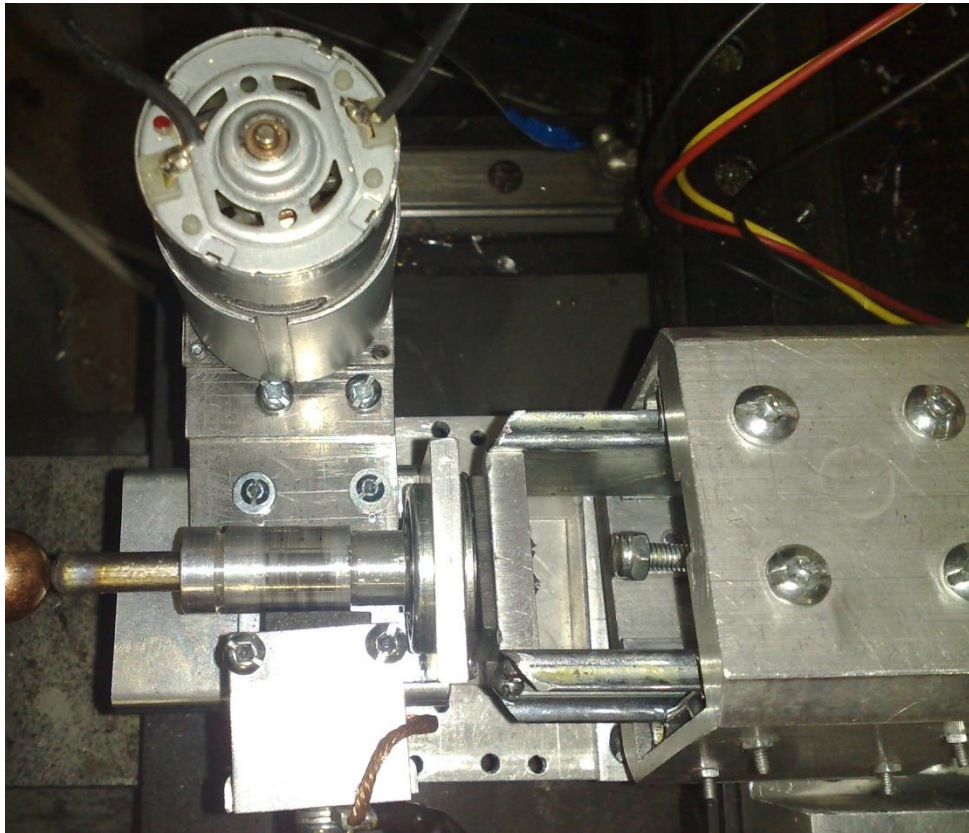**Figure B.1: Close-Up of Vibrating Mechanism**

Figure B.2: Top View of Vibrating Mechanism

Appendix C

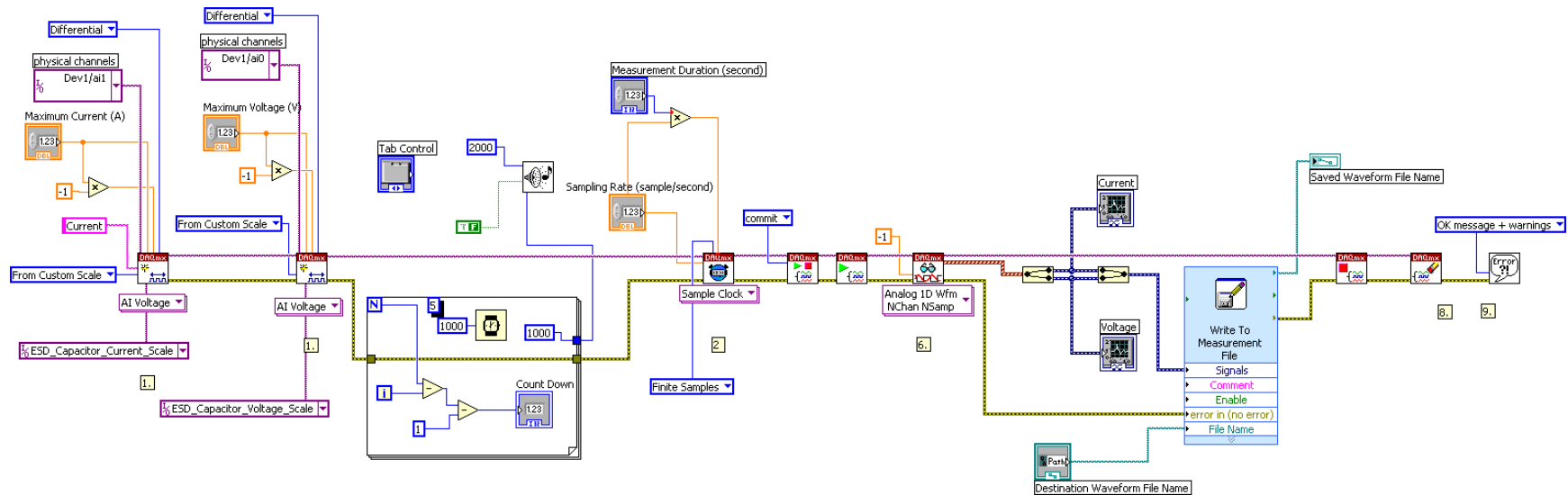# LabVIEW Program for Voltage and Current Measurements

Figure C.1: LabVIEW Program for Voltage and Current Measurements

Appendix D

MATLAB Script for Graphing Voltage and Current Measurements

```matlab
clc;
clear;
%close all;

testNumber = 1;
fileLocation = 'Test Results\';
fileName = ['2010-07-07_ESD_Automation_Results_' num2str(testNumber)];

    %   Use this code segment for .txt files
        %   open the file in read mode ('r')
        %   'w' would be used for write mode (file will be created if it
doesn't
        %   already exist)
        %fid = fopen([fileLocation fileName '.txt'], 'r');

        %   creat an array with all the values in the text file using
floating
        %   point numbers
        %data = fscanf(fid,'%e', [3,inf]);

        %   close the file
        %fclose(fid);

        %   creat variables for each parameter
        % time = data(1,:);
        % current = data(2,:);
        % voltage = data(3,:);
        % power = voltage.*current;

%   Use this code segment for .lvm files
%   creat an array with all the values in the lvm file
data = lvm_import([fileLocation fileName '.lvm']);

%   creat variables for each parameter
time = data.Segment1.data(:,1);
current = data.Segment1.data(:,2);
voltage = data.Segment1.data(:,3);
power = voltage.*current;

%   apply conversions for voltage and current measurements
%data = [data(1,:); data(2,:)*10; data(3,:)/0.008];

%   update data array with power
data = [time; current; voltage; power];

%   plot voltage and current vs time
%subplot(2,1,1);
```

```matlab
figure();
plotyy(time, current, time, voltage);

%   label title and x-axis
title('Time vs Voltage and Current');
xlabel('Time(s)');

%   create special labels for 2 y-axes
%   Voltage on right and current on left
[AX,H1,H2] = plotyy(time, current, time, voltage);
set(get(AX(1),'Ylabel'),'String','Current (A)');
set(get(AX(2),'Ylabel'),'String','Voltage (V)');
set(AX(1),'YLim',[0 max(current)+25]);
set(AX(1),'YTick',(0:25:max(current)+25));
set(AX(2),'YLim',[0 max(voltage)+5]);
set(AX(2),'YTick',(0:5:max(voltage)+5));


saveas(gcf, [fileLocation fileName '.fig']);

%   Use this code to plot the Power vs Time curve
%
% %   plot power vs time
% subplot(2,1,2);
% plot(time, power);
%
% %   label axes
% title('Time vs Voltage and Current');
% xlabel('Time(s)');
% ylabel('Power (W)');
%
% %   integrate power to get energy using Trapezoidal numerical
integration
% energy = trapz(time, power);
```

Appendix E

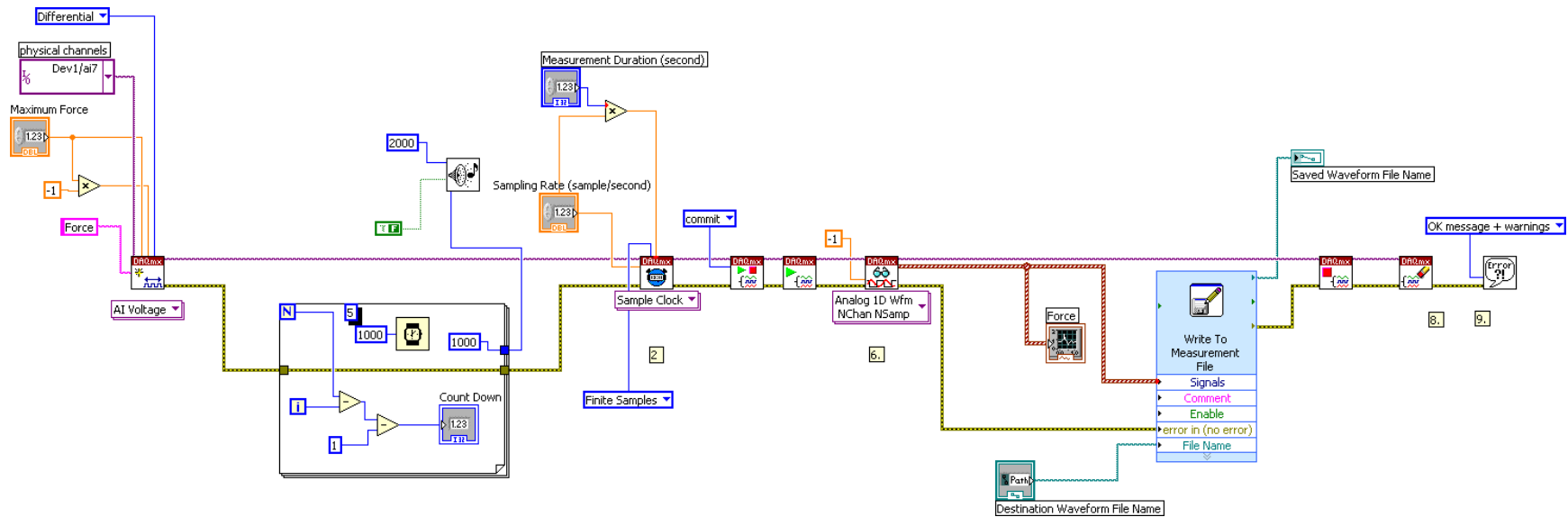## LabVIEW Program for Force Measurements

Figure E.1: LabVIEW Program for Force Measurements

Appendix F

MATLAB Script for Graphing Force Measurements

```matlab
clc;
clear;
%close all;

%testNumber = 9;
fileLocation = 'Force Results\';
%fileName = ['ESD_Automation_Results_' num2str(testNumber)];
%fileName = '20Thou_12H_50D_95F_1';
fileName = 'Manual_Huys_Operator_Slow0';

    %   Use this code segment for .txt files
        %   open the file in read mode ('r')
        %   'w' would be used for write mode (file will be created if it
doesn't
        %   already exist)
        %fid = fopen([fileLocation fileName '.txt'], 'r');

        %   creat an array with all the values in the text file using
floating
        %   point numbers
        %data = fscanf(fid,'%e', [3,inf]);

        %   close the file
        %fclose(fid);

        %   creat variables for each parameter
        % time = data(1,:);
        % current = data(2,:);
        % voltage = data(3,:);
        % power = voltage.*current;

%   Use this code segment for .lvm files
%   creat an array with all the values in the lvm file
data = lvm_import([fileLocation fileName '.lvm']);

%   creat variables for each parameter
time = data.Segment1.data(:,1);
voltage = data.Segment1.data(:,2);

%   calculate the average force of weight
%   Used for calibrating the FSR (Force Sensing Resistor)
average_voltage = mean(voltage);

%   plot voltage and current vs time
%subplot(2,1,1);
figure();
%fullscreen = get(0,'ScreenSize');
```

88

```matlab
%figure('Position',[0 -50 fullscreen(3) fullscreen(4)]);
plot(time, voltage);
title('Voltage vs Time');
xlabel('Time (s)');
ylabel('Voltage (V)');

saveas(gcf, [fileLocation fileName '.fig']);
%saveas(gcf, [fileLocation fileName '.jpg'])
```

Appendix G

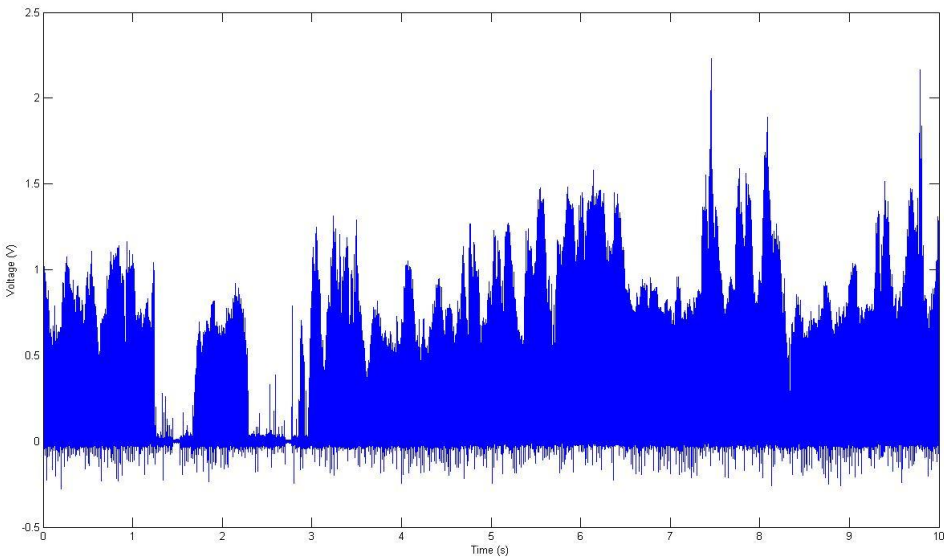## More Force Measurements of Manual Operators at Huys Industries

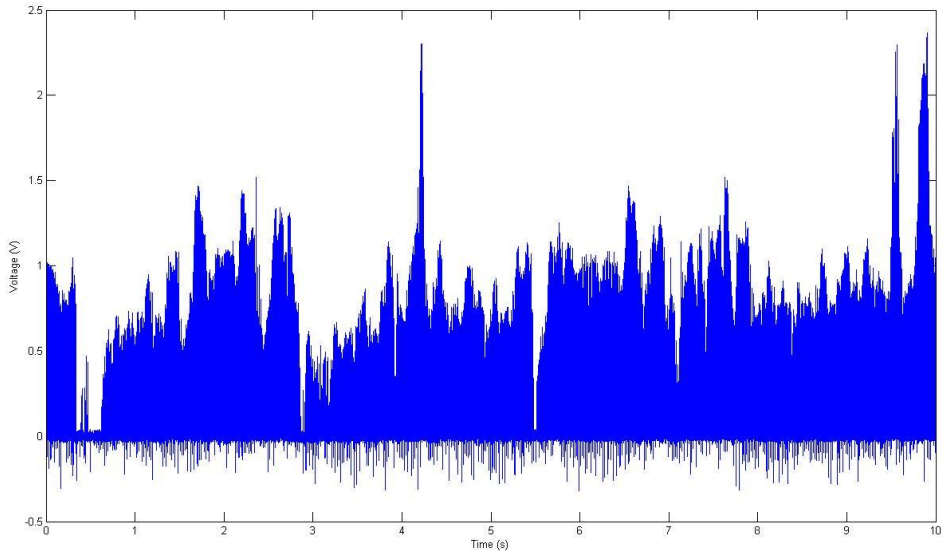

Figure G.1: Force Measurement of Operator 1
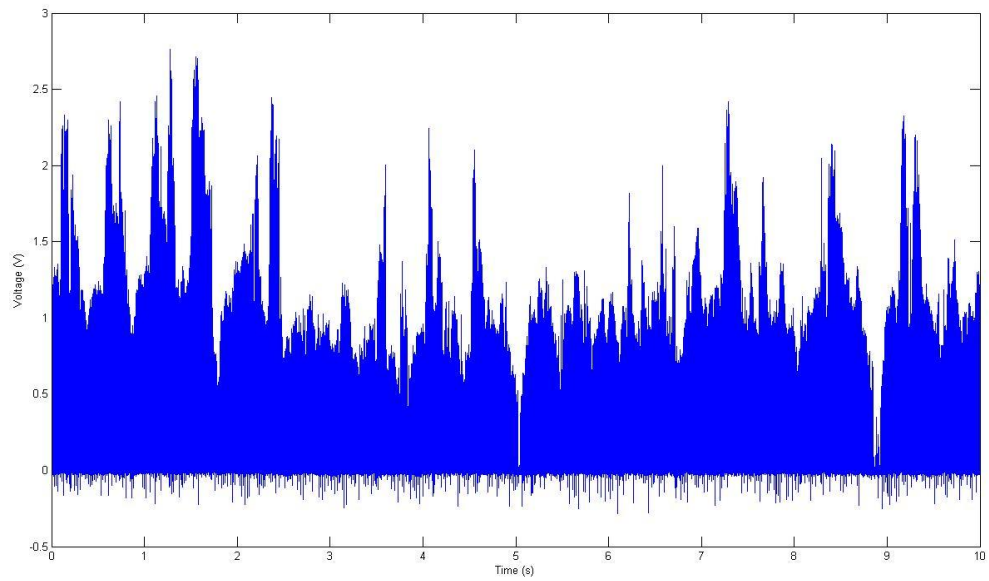

Figure G.2: Force Measurement of Operator 2
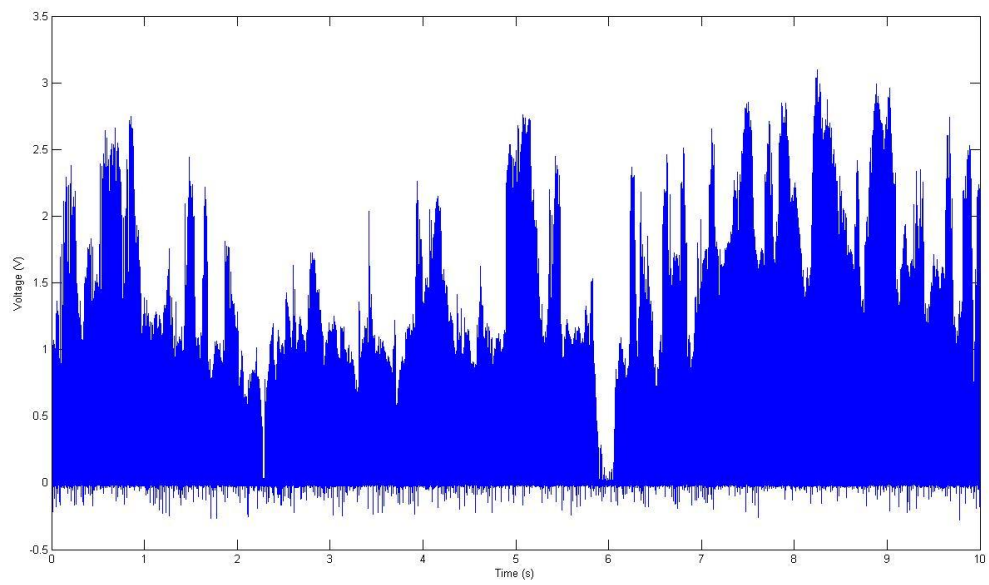
Figure G.3: Force Measurement of Operator 3

Figure G.4: Force Measurement of Operator 4
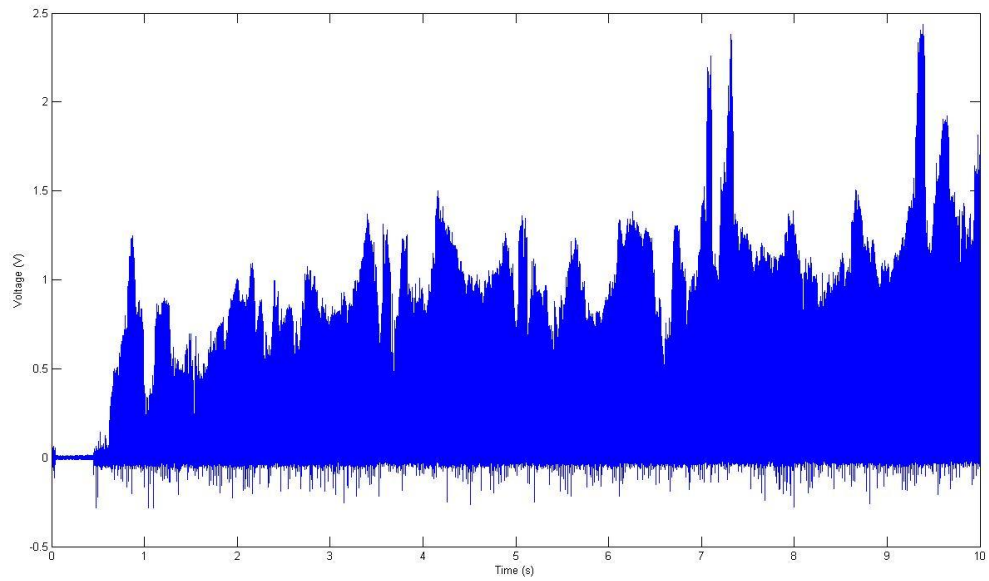
91

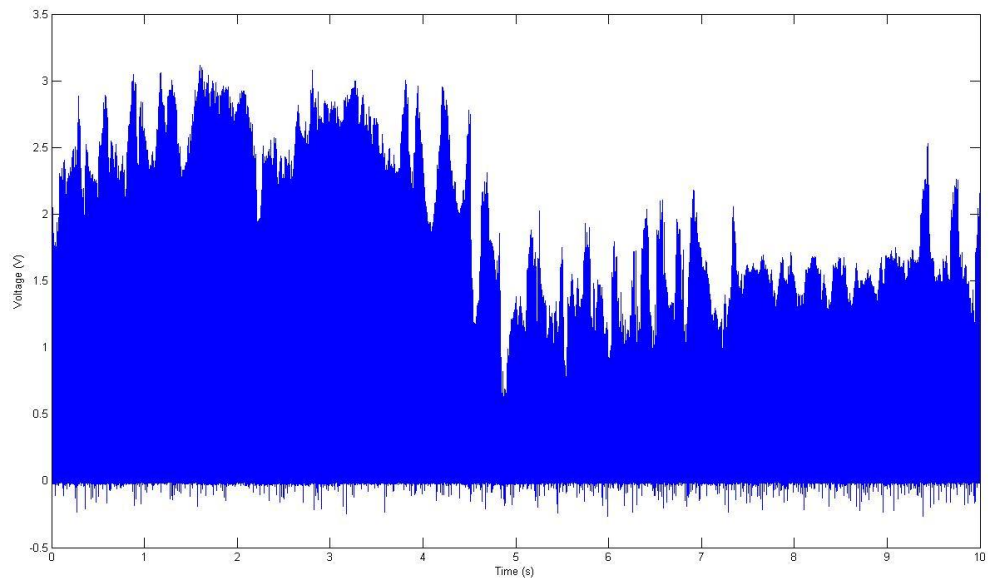**Figure G.5: Force Measurement of Operator 5**

Figure G.6: Force Measurement of Operator 6

Bibliography

[1] Brown, E. A., Sheldon, G. L., & Bayoumi, A. E. (1990). A parametric study of improving tool life by electrospark deposition. *Wear , 138* (1-2), 137-151.

[2] Agarwal, A., & Dahotre, N. B. (1998). Pulse electrode deposition of superhard boride coatings on ferrous alloy. *Surface and Coatings Technology , 106*, 242-250.

[3] Lesnjak, A., & Tusek, J. (2002). Processes and properties of deposits in electrospark deposition. *Science and Technology of Welding and Joining , 7* (6), 391-396.

[4] Johnson, R. N. (2002). ElectroSpark Deposition: Principles and Applications. *Society of Vacuum Coaters 45th Annual Technical Conference*, (pp. 87-92).

[5] Tang, S. K. (2009). *The Process Fundamentals and Process Parameters of Electro-Spark Deposition.* Waterloo, Ontario, Canada: University of Waterloo.

[6] Reynolds, J. L., Holdren, R. L., & Brown, L. E. (2003). Electro-Spark Deposition. *Advanced Materials and Processes , 161* (3).

[7] Johnson, R. N., & Sheldon, G. L. (1986). Advances in the electrospark deposition coating process. *Journal of Vacuum Science and Technology , 4* (6), 2740-2746.

[8] Jou, M. (2003). Real time monitoring weld quality of resistance spot welding. *Journal of Materials Processing Technology , 132*, 102-113.

[9] Connor, L. P. (Ed.). (1987). *Welding Handbook* (8th ed., Vol. 1). Miami, FL: American Welding Society.

[10] Dong, S. J., & Zhou, Y. (2003). Effects of TiC Composite Coating on Electrode Degradation in Microresistance Welding of Nickel-Plated Steel. *METALLURGICAL AND MATERIALS TRANSACTIONS A , 34A*, 1501-1511.

[11] Chan, K. R., Scotchmer, N., Zhao, J., & Zhou, Y. (2006). Weldability Improvement Using Coated Electrodes for RSW of HDG Steel.

[12] Chen, Z., & Zhou, Y. (2006). Surface modification of resistance welding electrode by electro-spark deposited composite coatings: Part I Coating characterization. *Surface & Coatings Technology , 201*, 1503–1510.

[13] *Welding Handbook* (9 ed., Vol. 3). (2007). Miami, FL: American Welding Society.

[14] Wang, P. Z., Pan, G. S., Zhou, Y., Qu, J. X., & Shao, H. S. (1997). Accelerated Electrospark Deposition and the Wear Behavior of Coatings. *Journal of Materials Engineering and Performance , 6* (6), 780-784.

[15] Banovic, S. W., DuPont, J. N., & Marder, A. R. (1997). Iron Aluminide Weld Overlay Coatings for Boiler Tube Protection in Coal-Fried Low Nox Boilers. *Proc. 11th Ann. Conf. on Fossil Energy Materials*, (p. 297).

[16] Johnson, R. N. (1995). Electrospark Deposited Coatings for Protection. *Proc. 9th Ann. Conf. on Fossil Energy Materials*, (p. 407).

[17] Brouwer Metaal. (n.d.). *Brouwer Metaal - products electrode caps*. (Brouwer Metaal) Retrieved August 2010, from www.brouwermetaal.com:

http://www.brouwermetaal.com/?page=products&product=electrode_caps

[18] ASM. (2002). *Volume 2, Properties and Selection: Nonferrous Alloys and Special-Purpose Materials* (Vol. 2). ASM International.

[19] ASM. (1995). *Engineered Materials Handbook: Engineering Tables: Ceramics and Glasses.* ASM International.

[20] ASM. (2002). *Volume 18, Friction, Lubrication, and Wear Technology* (Vol. 18). ASM International.

[21] ASM. (2002). *Volume 20, Materials Selection and Design* (Vol. 20). ASM International.

[22] Chen, Z., Zhou, Y., & Scotchmer, N. (2005). Coatings on Resistance Welding Electrodes to extend life. 1-4.

[23] Agarwal, A., & Dahotre, N. B. (1999). Pulsed Electrode Surfacing of Steel with TiC Coating: Microstructure and Wear Properties. *Journal of Materials Engineering and Performance , 8* (4), 479-486.

[24] Liu, J., Wang, R., & Qian, Y. (2005). The formation of a single-pulse electrospark deposition spot. *Surface & Coatings Technology , 200*, 2433– 2437.

[25] Frangini, S., & Masci, A. (2010). A study on the effect of a dynamic contact force control for improving electrospark coating properties. *Surface & Coatings Technology , 204*, 2613–2623.

[26] Advanced Surfaces and Processes, Inc. (2002). Retrieved from http://www.advanced-surfaces.com/